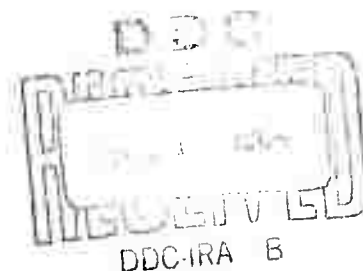# OCEANICS
INC.

AN EXPERIMENTAL STUDY OF THE DYNAMIC AND STEADY STATE FLOW

DISTURBANCES ENCOUNTERED BY AIRCRAFT DURING

A CARRIER LANDING APPROACH

by

August F. Lehman

Prepared For:

Office of Naval Research
Department of the Navy
Washington, D. C.   20360

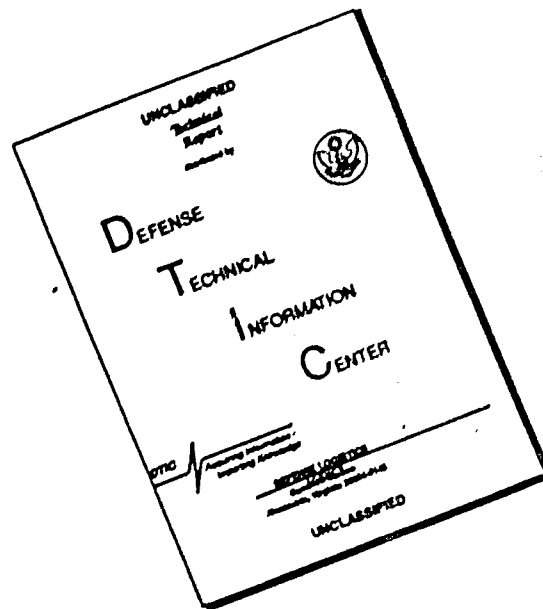DDC-IRA B

COPY ⬚ ⬚ OF ⬚ ⬚

hARL COPY $. 5 ⬚ ⬚

MICROFICHE $. /. ⬚⬚

Report No. 64-16   September 1964

Technical Industrial Park / Plainview, N.Y.

DISCLAIMER NOTICE

THIS DOCUMENT IS BEST
QUALITY AVAILABLE. THE COPY
FURNISHED TO DTIC CONTAINED
A SIGNIFICANT NUMBER OF
PAGES WHICH DO NOT
REPRODUCE LEGIBLY.

AN EXPERIMENTAL STUDY OF THE DYNAMIC AND STEADY STATE FLOW

DISTURBANCES ENCOUNTERED BY AIRCRAFT DURING

A CARRIER LANDING APPROACH

by

August F. Lehman

Prepared For:

Office of Naval Research
Department of the Navy
Washington, D. C.   20360

Under Contract No. Nonr-4186(00)

Report No. 64-16   September 1964

OCEANICS INC.

TABLE OF CONTENTS

ABSTRACT

A series of investigations were undertaken in a water tunnel to obtain greater insight into the disturbances encountered by aircraft engaged in the process of landing on a carrier. Water tunnel tests were selected because the use of water as the test medium permitted the disturbed flow areas to be identified by the cavitation phenomenon. In addition, these studies were undertaken at Reynolds numbers higher than those normally achieved in wind tunnel investigations.

The real situation is dynamic and, in view of this, these studies included observations of the dynamic disturbed flow patterns due to carrier motions induced by waves, using the cavitation technique and high speed movies. Steady flow observations were also made wherein both the velocity magnitude and direction were determined in the flow field downstream of the model up to equivalent full scale distances of 1875 feet. Key conclusions are that dynamic conditions produce flow regimes significantly different from those produced with steady state conditions; that the downstream wake is periodic, with the periodicity having a direct relationship with the pitching and heaving motions of the ship; that the overhang of the deck is the principal cause of the flow disturbances (far outweighing the disturbances caused by the island); and that steady state measurements are of considerable value and do permit some quantitative estimation of the velocity fluctuations occurring in a wake resulting from carrier motions.

LIST OF ILLUSTRATIONS

Page No.

APPENDIX MATERIAL

Note:
  Distances are given in equivalent full scale values.

Note:
  Distances are given in equivalent full scale values.

OCEANICS INC.

INTRODUCTION

The processes involved in landing an aircraft on a
carrier are exceedingly complex. One must consider an aircraft
approaching at speeds in excess of 100 knots with a touchdown
length in the neighborhood of several aircraft lengths. Add to
this the fact that the carrier will be undergoing various degrees
of pitching, heaving, and rolling motions, thus constantly chang-
ing the orientation of the landing deck in space. Include also
in these considerations the fact that the response of the aircraft
tends to be somewhat slow or sluggish during the process of land-
ing and that disturbances affecting the aircraft in the glide path
are of considerable concern to the pilot. This is true since a
short landing is extremely hazardous to the aircraft and the pilot
while an overshoot of the arresting cables requires the aircraft
to become airborne again within a dozen or so aircraft lengths.

It is the cause and nature of the disturbances affecting
the aircraft in the glide path which have been investigated and
which will be described in this report. But, before doing so,
perhaps a paragraph or two of additional background material appli-
cable to the aircraft landing problem might be helpful.

At the present time, one of the landing signal systems
employed to indicate to the pilot of an aircraft whether or not his
approach to a carrier in the landing process is proper is the
Fresnel Lens Optical Landing System. With this system or with a
similar signal system three major elements are involved:

1- ship dynamics,

2- aircraft dynamics, and

3- pilot response.

Of these three, two (aircraft dynamics and pilot response) will be affected by disturbances in the glide path.

A major disturbance does exist in the glide path and is identified by pilots as a "burble." The burble encounter time before touchdown, based on discussions with pilots and from records of thirty three landing approaches in an instrumented F4B aircraft [1], is predominantly within the last ten seconds of an approach. The most common encounter time is about five or six seconds before touchdown. The significance of the burble is that after emergence from the burble, the pilot has between one and two seconds to commit himself to a landing or to an abort. There can be little doubt that such decision-making creates considerable strain on the pilot in view of the possible consequences resulting from an error in this decision.

PROGRAM OBJECTIVES

The primary purpose of this program concerned an investigation of the flow conditions existing in the glide path of aircraft approaching a carrier for a landing. To achieve this purpose, two basic objectives, both involving model studies, were established:

1- to observe both visually and photographically the vortex formation representing and comprising the major characteristics

of the air-wake existing downstream of a carrier, and

2- measure the velocity flow field at a number of axial positions downstream of the carrier model extending far enough aft to include all reported burble encounters.

The contractual program calls for the above investigations to be made in a steady state condition; that is, the model would be positioned at various pitch, heave, and yaw orientations and standard testing techniques then employed to obtain information satisfying the basic objectives. However, it was most strongly believed that the dynamic wake conditions which exist behind a carrier undergoing heaving, pitching, and rolling motions would be significantly different in character than the wake existing with the carrier stationary. Because of this belief and with the approval of the ONR Project Officer, basic objective (1) was achieved in the dynamic condition (a change from the original contractual undertaking), and objective (2) was obtained in a steady state condition as originally requested.

It was (and is) believed that dynamic test conditions will also be required before objective (2) can be satisfied in terms of obtaining information that can be used in simulator studies such as those undertaken by Systems Technology, Inc., involving the entire Fresnel Lens system [4]. However, steady state test conditions were undertaken for several valid reasons. One is that such testing will afford a rather good indication of changes in the gross wake field orientation associated with changes in ship orientation. Also, similar information has been obtained by other investigators using techniques different from

those employed here. Therefore, these tests will afford a good comparison of data-----something all serious investigators welcome. In addition, the techniques enabling such dynamic measurements had, for the most part, not been developed or proved to the stage where successful studies seemed probable*. Therefore, the information presented here (applicable to objective (2)) does supply certain data which is of some value at the earliest possible time.

GENERAL APPROACH EMPLOYED TO SATISFY PROGRAM OBJECTIVES

It was recognized that the burble disturbances encountered by landing aircraft must originate from some portion(s) of the ship hull, deck, or island. All of these major components will produce flow disturbances either having well established vorticity patterns or with vorticity tendencies. For example, depending upon the relative wind direction, the leading edges of the bow and landing deck can act much as the leading edges of wings. Thus, the "tips" (or corner edges) would shed the well-known tip vortices commonly observed from aircraft wing tips. This type of vorticity can be extremely strong and for the problem under consideration the cores of the vortices would travel essentially parallel to the wind direction. The leading edges of the bow and landing deck can also shed Karman type vorticity; that is, vorticity in which the core of the vertex

*It should be noted that a program for developing such instrumentation and test techniques is now being considered under a separate ONR Contract Amendment

is essentially parallel to the leading edge of the shedding
structure. It is easy to postulate that such shedding would be
intermittent due to the cross flow of the wind along the edge
due to the pitch and heave motions of the carrier. How correct
this postulation is will be discussed later.

The island is located on the deck parallel to the
longitudinal center line of the ship's hull and therefore at an
angle to the landing deck. Since the wind or the relative wind,
which is that composed of the natural wind and that generated by
the carrier's forward motion, is oriented along the landing deck,
the island is at an attack angle. Because of this orientation,
the island will produce disturbances associated with such a blunt
structure at an attack angle. The hull itself, projecting as it
does from the water, will also create an air-wake aft of it.

To what degree each of the above components of a carrier
shed disturbed flow and to what degree the induced disturbances
might tend to combine was not known prior to under-taking this
investigation, but it was believed that a technique should be em-
ployed that would permit ready visual observation of the disturbed
flow emanating from all portions of the carrier together with
concurrent observations of the entire downstream wake field. This
belief led to the conclusion that the experiment should be under-
taken in a water tunnel.

In the real case the aircraft carrier creates disturbances
in the medium identified as air. At the velocities involved, air
can be considered and treated as an incompressible medium.

Flow disturbances (vortex formations) can exist in any fluid and such disturbances can be observed in water tunnel investigations through the phenomenon known as cavitation.

Cavitation is defined as the formation, growth, and collapse of vapor or gas filled voids in a liquid resulting from local pressure reductions in a dynamic flow field. It is the presence of the vapor or gas filled voids (bubbles) which makes the observation of disturbed flow and vorticity patterns visible. Tip vortex formations have an exceptionally long life, a quality evidenced in Figure -1-, a photograph showing tip vortex formations on a propeller, and Figure -2-, a photograph showing the tip vortex from a hydrofoil.

In addition to the capability of visualizing the flow, the use of a water tunnel is quite reasonable from scaling considerations also. Reynolds number is the normal scaling parameter involved in the study of flows of this nature and because of the difference in the kinematic viscosity in the two fluids (air and water), water investigations have an inherent advantage in their favor by a factor of about 20. Thus, in comparing water tunnel investigations with similar air tunnel investigations, water tunnel models can be considerably smaller than those employed in air tunnels yet the water tunnel test data will be obtained at higher Reynolds number values.

TEST FACILITIES AND EQUIPMENT

In the following section, the facilities and equipment
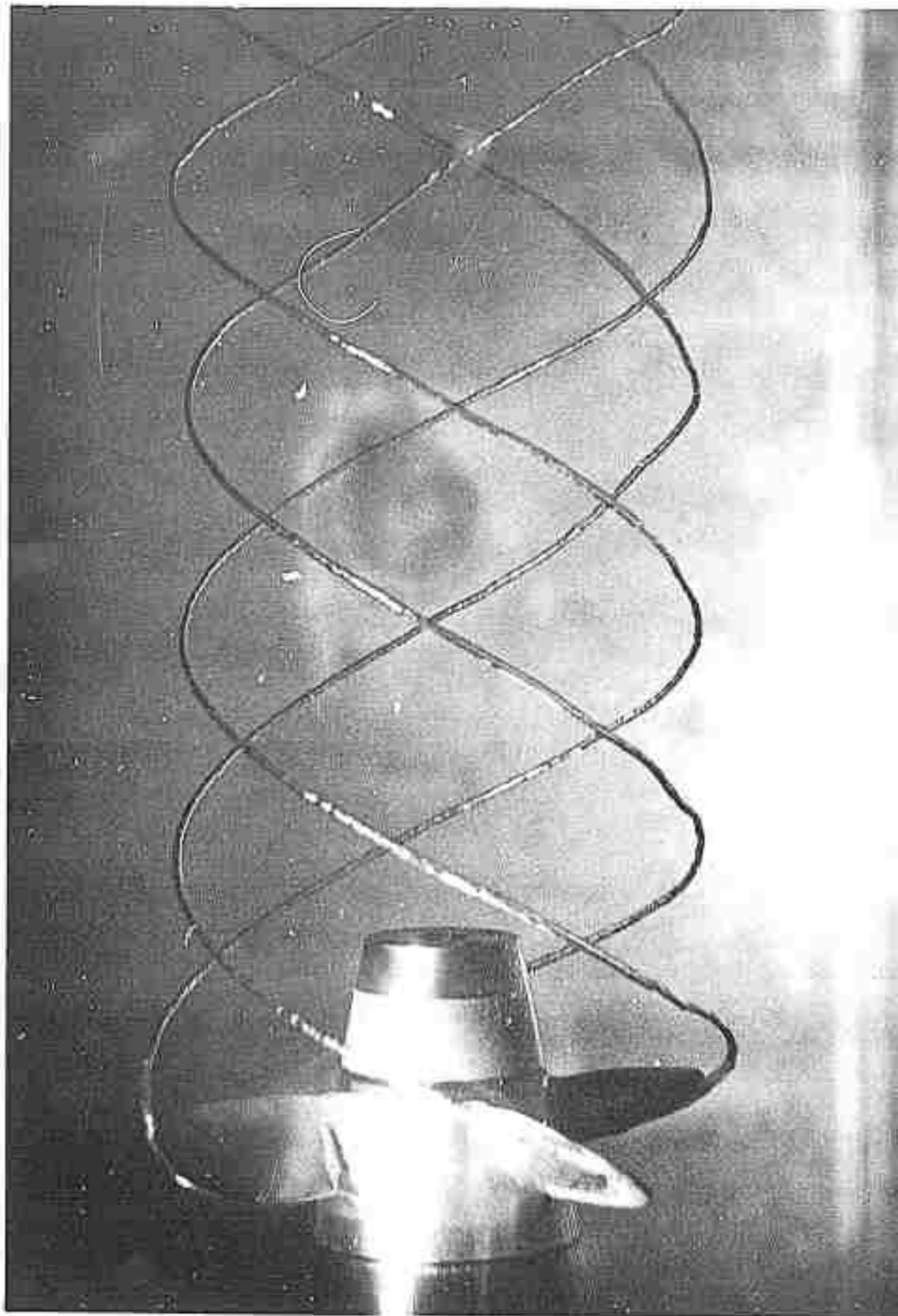
FIGURE 1 TIP VORTEX FORMATION FROM A PROPELLER (FROM REFERENCE [2])
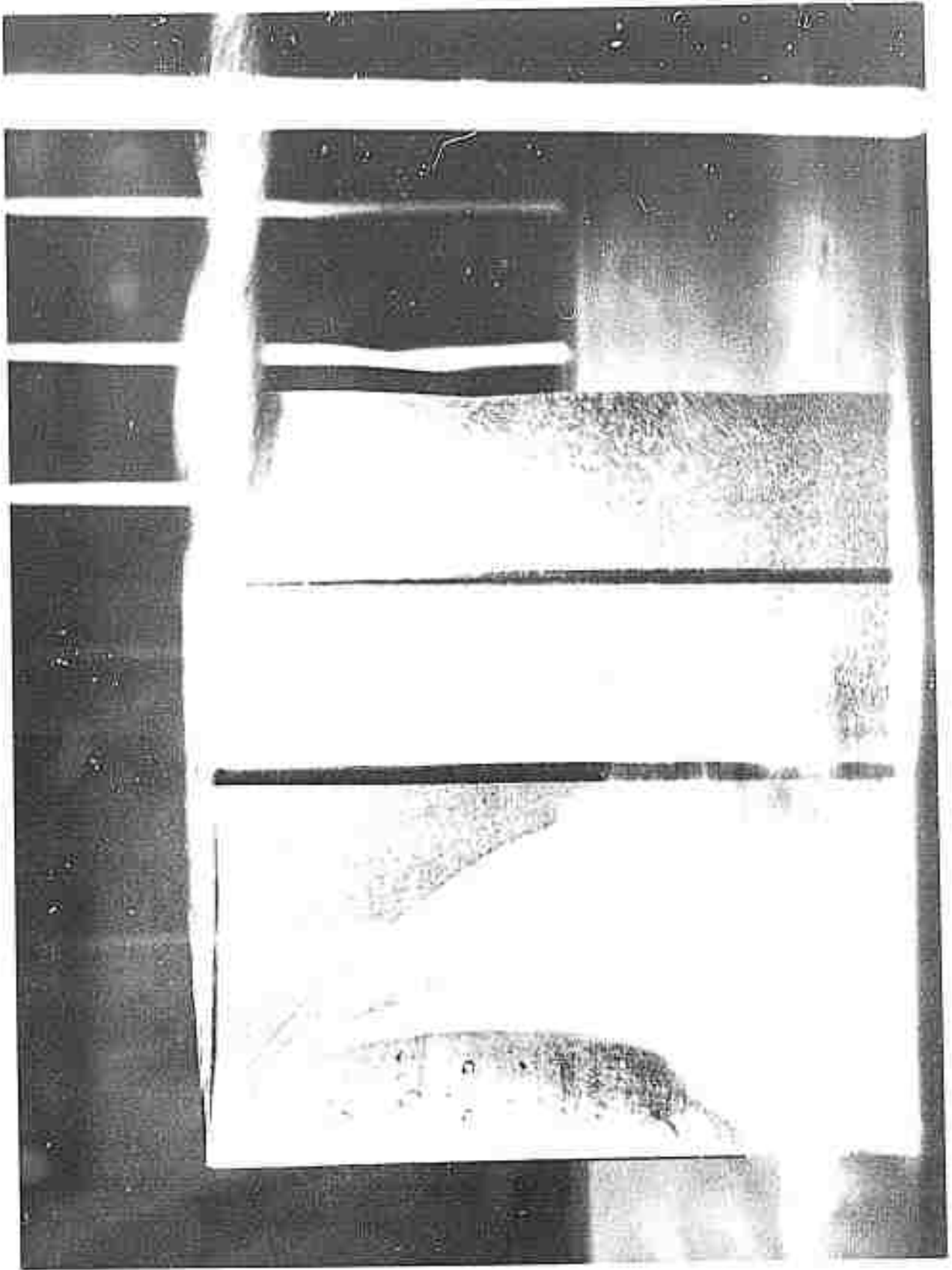
FIGURE 2 TIP VORTEX FORMATION FROM A HYDROFOIL

employed in the test program will be discussed.

Oceanics Water Tunnel

The major item of test equipment is the Oceanics water tunnel. This tunnel is a closed jet, recirculating type of tunnel having both the velocity and pressure variable. The maximum test section velocity is about 40 feet per second, while the test section pressure, which can be controlled independently of the test section velocity, covers a range from about -0.9 atmospheres to +1.0 atmospheres using atmospheric reference. The test section itself is about 20-inches on a side, having rounded corners. The overall length of the test section is 7-feet. There are eight viewing windows; two on each of the four sides, with each window having a viewing area of 10x30-inches. A propeller dynamometer having the capability of driving a propeller with thrust values to 300 pounds in either direction and torque values to 40 lb.-ft. in either direction can be mounted at either end of the upper leg of the tunnel, thus permitting the propeller to be driven from either its upstream or downstream side. At the beginning of the test section, provisions are incorporated for the insertion of screens permitting the establishment of wakes having a desired axial velocity variation.

Models

The models employed in this test investigation were of two sizes; one had a deck length of 20.75-inches, the other a deck length of 33-inches. The models were fabricated from aluminum, with the hulls cast and the flight deck and island machined. Extreme detail is not required in the models as only major components or parts will

produce disturbance of a magnitude large enough to affect air-craft of the size and weight under consideration. Figure -3- is a photograph showing the two models.

The hulls were machined to permit their attachment to an actuation mechanism. The deck and island were separate components fastened to the hull. Small openings were drilled in various portions of the deck and island. The purpose of these holes, which were connected to the outside of the tunnel by plastic lines running from the bottom of the hull to the tunnel wall, was to permit air or dye to be emitted into the test stream enabling an indication of how the flow from a particular area progressed as it moved downstream of the model. A sketch of the hole locations is shown in Figure -4-.

Actuation Mechanism

The mechanism used to actuate the models in heaving, pitching, and rolling motions was designed especially for this program. It has the capability of varying the roll period in-dependently of pitching and heaving motion periods. Besides the pure heave and pure pitch motions, combinations of pitch and heave can also be introduced to the model.

The main portion of the mechanism controlled the heave and pitch motions and was powered by a variable speed three horse-power motor. This motor drove a gear box which, in turn, powered two "crank shaft" units. To the crank shaft units were attached two push rods. After passing through support and alignment bearings in the tunnel wall, these rods supported the model in
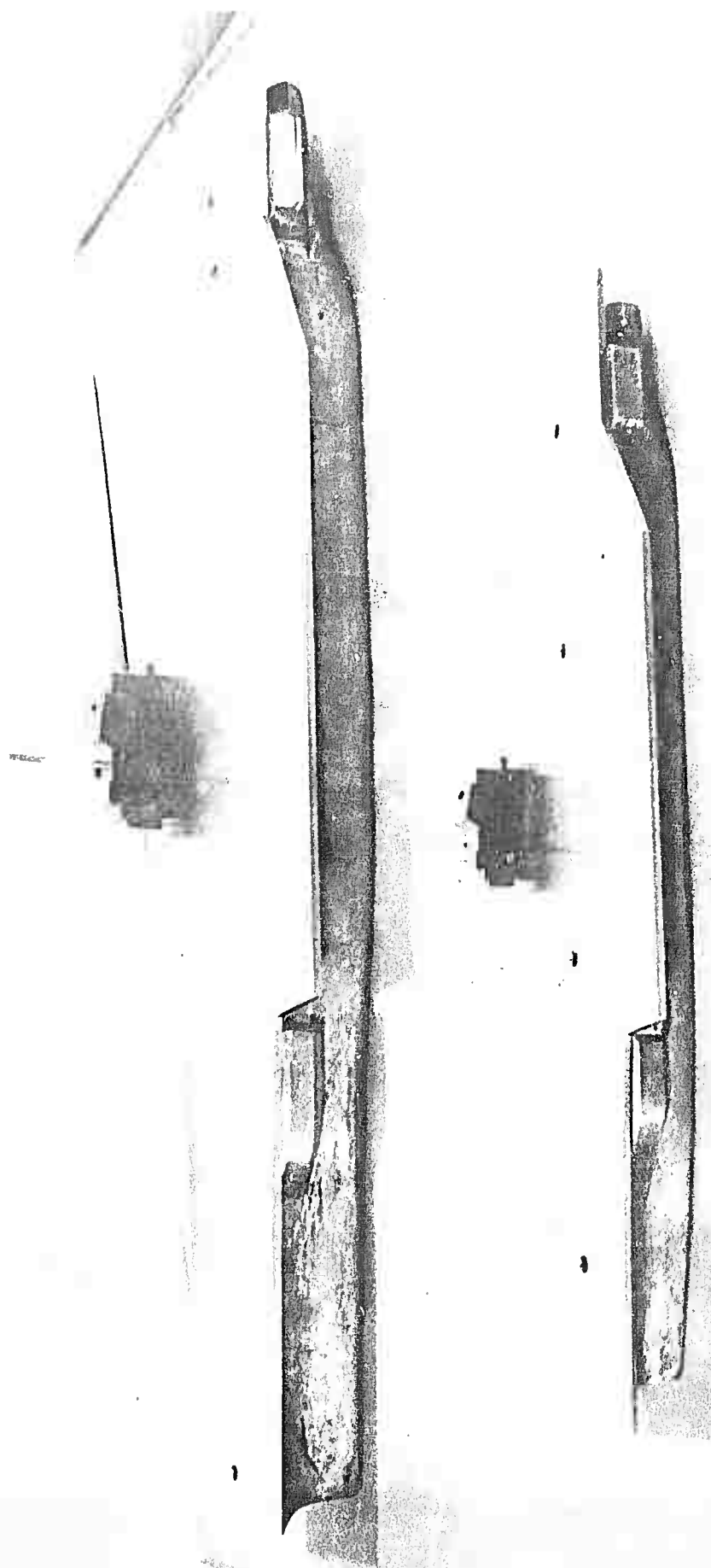
FIGURE 3   MODELS USED IN TESTS (LARGER MODEL 33 INCHES
LONG, SMALLER 21 INCHES LONG)
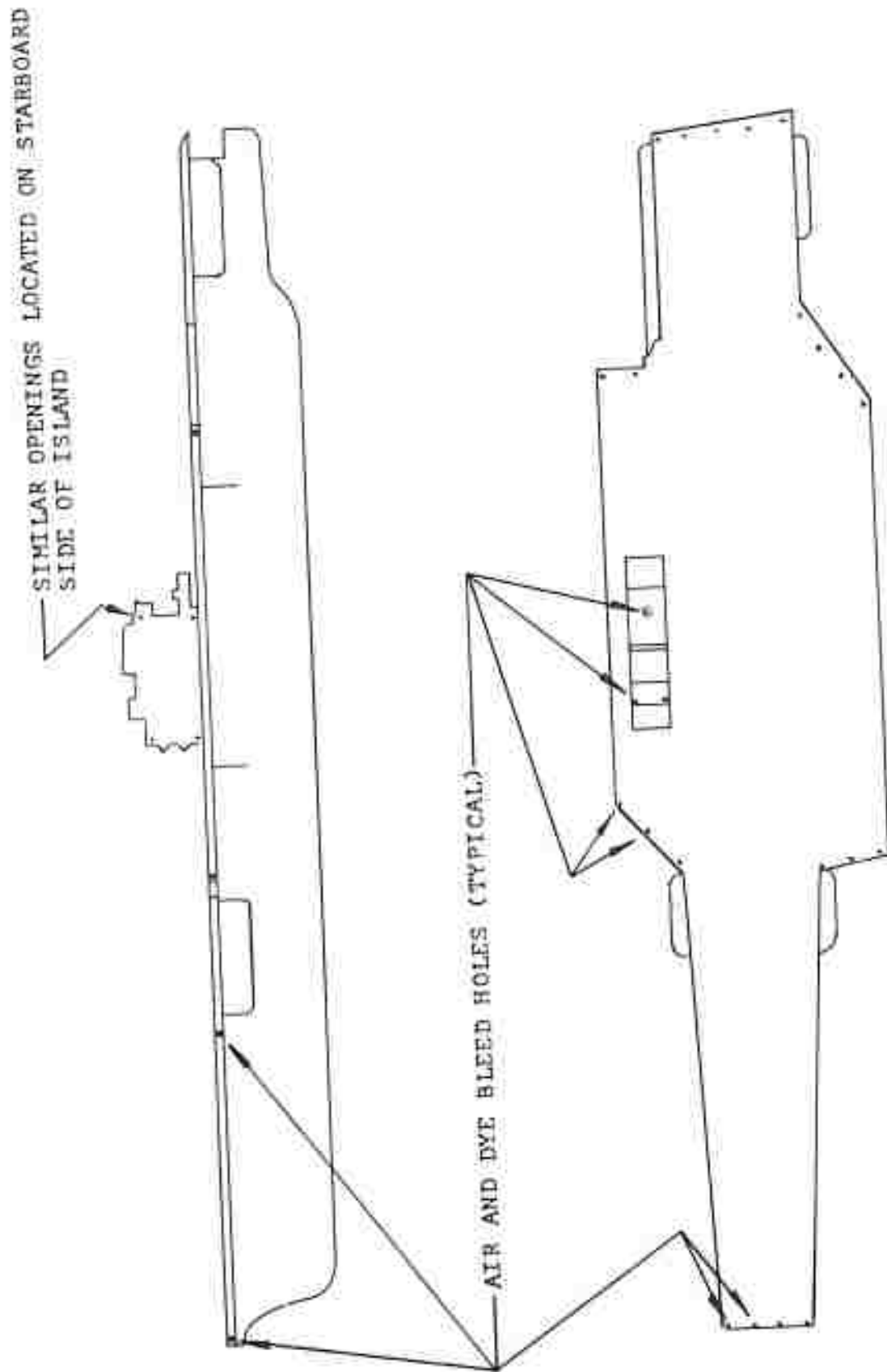
FIGURE 4   SKETCH SHOWING LOCATION OF AIR AND DYE BLEED HOLES

the tunnel test section. The crank shaft units had the capability of adjusting the amount of crank "throw," this throw controlling the amount of pitch or heave introduced to the model. In addition, one crank unit could be rotated relative to the other so that the crank orientation was changed. In other words, if both cranks were aligned with each other the push rods would translate together thus resulting in a pure heaving motion of the model. If the "throw" of one crank was oriented 180° out of phase with the other (one crank up, one crank down) the resulting action was a pure pitching motion of the model. In between these orientations combinations of pitch and heave are produced.

The model is attached to the upper ends of the push rods. At the top of the rods are self-aligning rod ends which are mated to a longitudinal shaft forming a part of the model mounting system. Because the actuation rods pass through bearing and sealing units in the tunnel wall, the distance between the push rods is fixed. With the introduction of pitching motions to the model, the distance between the ends of the rods, where they are attached to the model, will vary. In order to permit this distance variation, one rod bearing is fixed against axial motion at the model attachment end, the other rod end can slide in a longitudinal direction thereby permitting the desired pitching motion. A photograph of the push rods and carrier mounting method is shown in Figure -5-.

Roll motions of the carrier are introduced independently of the pitch and heave motions by a push-pull cable arrangement.
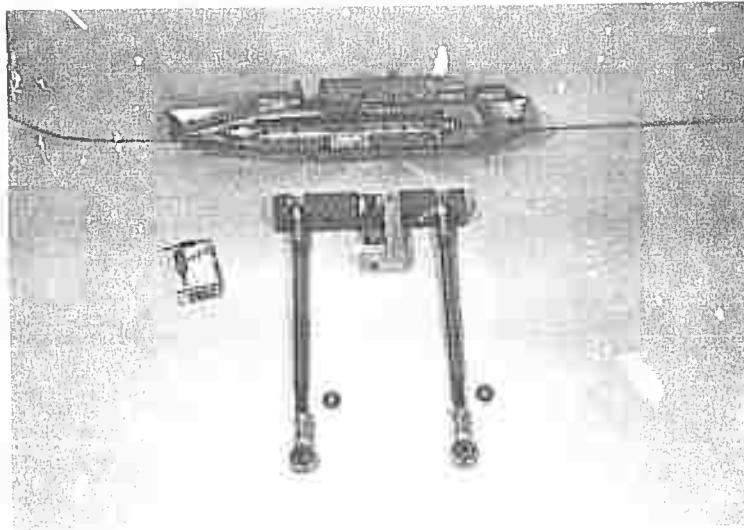
FIGURE 5   PUSH RODS AND MOUNTING SYSTEM
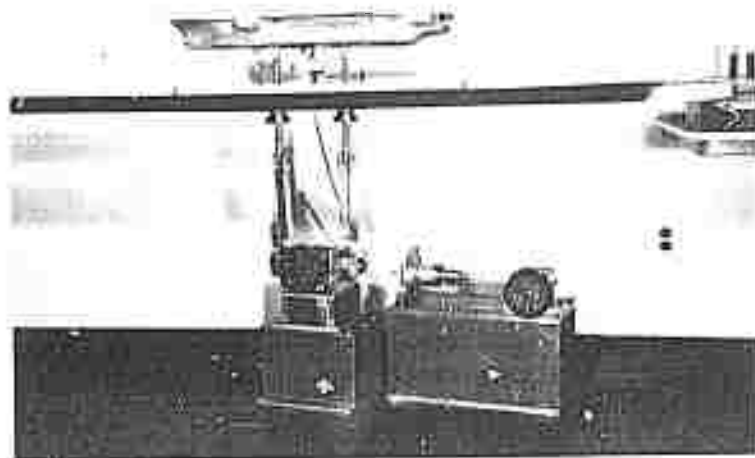
FIGURE 6   MODEL MOUNTING AND ACTUATING SYSTEM

One end of the cable is attached to a yoke which is pivoted to rotate about the longitudinal axis of the ship. The other end of the cable is attached to a separately driven crank shaft mechanism. The drive for this mechanism is a separate one horse-power variable speed motor. The throw of the crank is adjustable and, in this manner, the degree of roll introduced to the model can be varied. The adjustable speed drive motor permits the roll time period to be varied.

An overall view showing both drive mechanisms and the carrier mounted on the push rods is shown in Figure -6-. This photograph also shows the tunnel bottom mounting plate (inserted in a normal window opening) and some of the plastic lines attached to the forward bleed holes in the carrier. The manifolds to which the bleed lines are connected are also visible. Not shown in this photograph is the streamlined strut which surrounds the entire actuation mechanism covering the distance from the bottom of the tunnel to the underside of the plate which simulates the sea surface. The plate representing the sea surface is not shown in the photograph either.

Photographic Equipment

The camera used for the high speed photography was a Fastex WF-3. Figure -7- is a photograph showing the camera in the position used when movies were made through the forward side window of the tunnel.

Wake Measuring Instrumentation

The measurement of the velocity flow field downstream of the carrier was undertaken with the aide of two instruments.
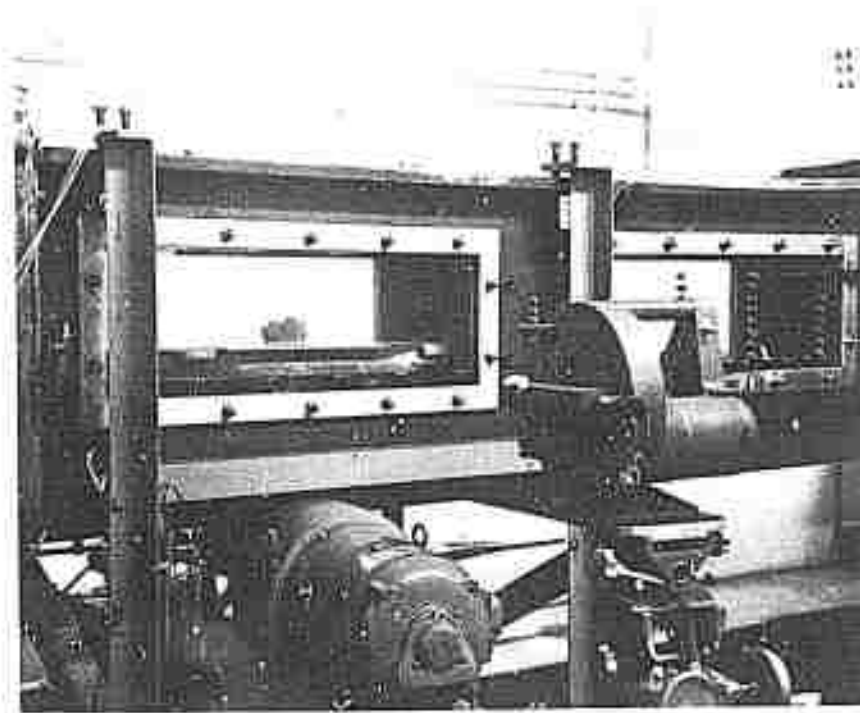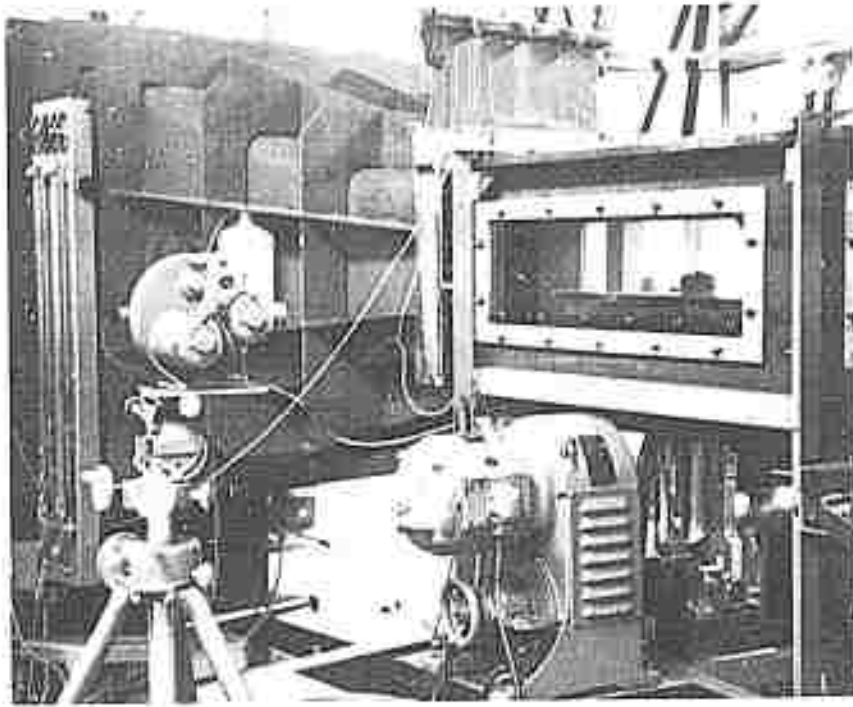
FIGURE 7   CAMERA IN POSITION FOR HIGH SPEED MOVIES

OCEANICS INC.

One instrument was a United Sensor and Control Corporation Type
DA three dimensional probe. This is a five hole unit with a
prism shaped measuring section. This unit measures the total
and static pressures, the yaw angle and the pitch angle. It is
calibrated by the manufacturing firm. The diameter of the
sensing portion of the unit is 0.120-inch.

The other probe had a sensing element of the Prandtl
pitot tube type. This pitot had a 0.060-inch diameter. The
pitot tube was mounted on a specially designed head which per-
mitted the pitot to be remotely positioned at any desired yaw
or pitch orientation. In this manner the smaller diameter Prandtl
type tube could be oriented at any point in space at the same
yaw and pitch angle as determined by the United Sensor unit.
This permitted a comparison of the information obtained using
the smaller probe with the larger diameter United Sensor unit.
The purpose of the two probe sizes was to see if a change in
probe size resulted in a change in the measured local velocity
vector. A close-up of the measuring portions of both probes
is shown in Figure -8-, while Figure -9- is an overall view of
both probes.

TEST ARRANGEMENT

The basic test arrangement consisted of having the
model positioned on a flat plate which represented the surface
of the sea. This plate extended across the entire width of
the tunnel test section and also extended the length of the

FIGURE 8   CLOSE-UP VIEW OF MEASURING PORTION
OF VELOCITY SENSING PROBES

FIGURE 9   OVERALL VIEW OF MEASURING PROBES

test section. Thus, the plate divided the flow passing through the test section. The flow which passed over the upper portion of the plate represented air flow in the real case. This was the portion of flow which was of interest in this program. The portion of flow below the plate could be considered as sea flow (without surface effects) but was of no interest in this study.

The hull of the model actually passed through an opening in the plate and was fastened to the actuation mechanism. This opening was just large enough to permit the model to undergo heaving, pitching, and rolling motions without hitting the sides of the opening. A sketch of the tunnel installation is shown in Figure -10-.

For the studies involving the measurement of the downstream flow field the model was not actuated, but statically positioned in the desired pitch and yaw orientations. The velocity field information was obtained using the probes discussed in the section on instrumentation. Velocity field information was obtained at five axial positions downstream of the model. For the large model, the farthest downstream position was equivalent to 1310 feet (full scale) while for the small model the distance was equivalent to 1875 feet. The element of space examined with the large model had an approximate width and height of 620 feet by 230 feet (above the sea surface). With the small carrier the corresponding dimensions were 950 feet and 345 feet. The entire area was not investigated at each downstream station, but that checked was considerably more than the area immediately about the glide path.
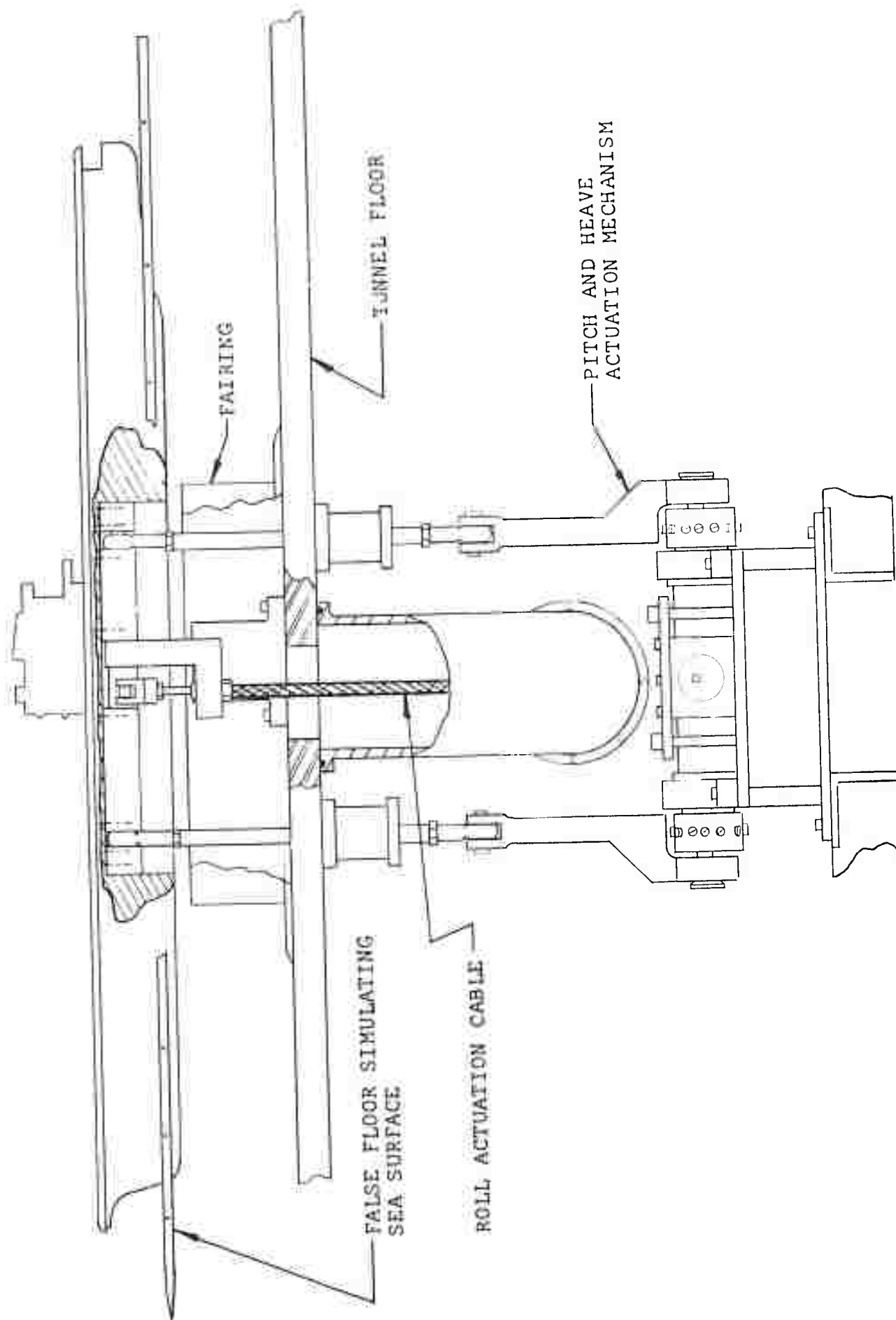
FIGURE 10 SKETCH OF TUNNEL INSTALLATION

In each of the planes in space examined, a matrix of points was investigated. It was possible to investigate eight stations above the surface of the sea at each position with any number of positions across this element. This held for the last four planes of investigation. For the measuring plane nearest the carrier only five vertical positions could be investigated. Figure -11- is a sketch of the test arrangement showing the model, plate, probe mounting positions and probe installation.

TEST PROCEDURES

The test program involved two major phases. One phase involved the flow visualization studies, the other involved the measurement of the velocities in the flow field downstream of the carrier. The procedures employed in obtaining information for each of these major phases will be presented separately.

Flow Visualization Studies

These studies involved the visual observation and high speed movies of the carrier while undergoing dynamic pitching, heaving and rolling motions. To permit the dynamic motion of the model, it was mounted on the actuation mechanism and the drive motors set at speeds which would introduce the proper time periods (scaled) of pitching, heaving and rolling. The desired tunnel velocity was then obtained and the tunnel static pressure slowly reduced until various portions of the disturbed flow about the carrier became visible through the phenomenon of cavitation.

MEASURING PLANES

FLOW
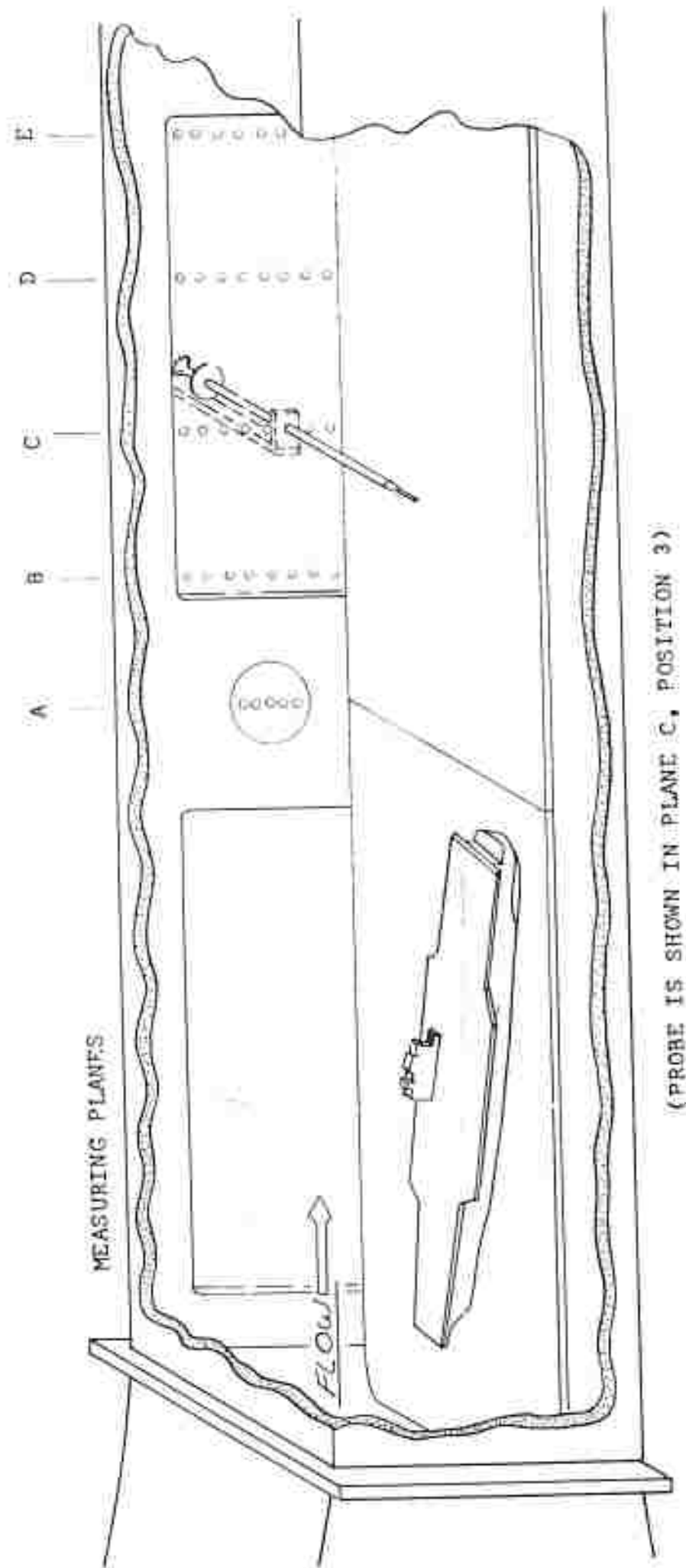
(PROBE IS SHOWN IN PLANE C, POSITION 3)

FIGURE 11 SKETCH OF TEST ARRANGEMENT FOR WAKE MEASUREMENTS

OCEANICS INC.

This phenomenon was described in the earlier section on General Approach Employed to Satisfy Program Objectives.

Several days were spent visually observing the disturbed flow patterns with the carrier in different fixed orientations and also with varying rates of pitch, heave and roll. Observations were made with varying degrees of cavitation and the disturbed flow patterns were checked with both normal illumination and with the aide of a strobotac. Using the strobotac, attempts were made to "stop" individual disturbed flow formations. From these observations a good general understanding of the causes of the flow disturbances and the flow field downstream of the carrier was obtained. The marked differences in the disturbed flow formations when the model was stationary and when it was undergoing dynamic motion was noted. Air and dye were emitted from the various openings in the carrier deck and island to see how the flow associated with a particular area behaved using an observation technique other than cavitation. Air and dye were also exhausted from the smoke stack to note the behavior of the stack gases and its mingling with the downstream flow patterns.

When it was believed that the flow field was examined in adequate detail by visual observations, high speed movies of the carrier undergoing dynamic pitch, heave, and roll motions were exposed. During these movies, scaling with the actual carrier was undertaken using the following dimensionless parameter;

$$\frac{L\omega}{V} \ \text{full scale} \ = \ \frac{L\omega}{V} \ \text{model}$$

where   L = ship length

V = wind velocity over landing deck

ω = cyclic rate of carrier motion.

Through the above relationship, the flow conditions between the actual case and the model studies were properly scaled. The Reynolds number consideration was previously discussed.

The camera was positioned so as to take separate movies through four of the viewing windows, two windows on one side and two windows on the top of the tunnel test section. In this manner rather good observation was possible about the carrier model and in the flow field existing downstream. Because the cyclic rate of the model was quite high in order to maintain the scaling parameter described above*, film speeds up to 4,000 frames per second were employed to stop the action. Both black and white and color film were exposed. In a number of instances dye was emitted from the carrier for high speed photography observation in the same manner as it was during the visual observations. Dye simulating smoke was also exhausted from the stack for stack gas records.

During actual testing, the camera and lights were properly positioned for the desired view and the actuation mechanism speeds adjusted to produce the desired ship motion time periods
_____
*For example, a full scale wind velocity of 35 kts and a pitch period of 10 seconds required a water velocity of 20 fps and a cyclic rate of 20 cps for the small model while the large model values were 15 fps and 9.6 cps respectively. The same tunnel velocities were used in the steady state test.

for the tunnel velocity to be employed. The tunnel speed and the cavitation pressures were then established. The camera was checked for focus and loaded with film. The lights were turned on and model actuation started. If dye or air was to be emitted this was also started. The camera switch was then thrown and in less than one second a fifty foot roll of film was then exposed.

Steady State Flow Field Measurements

In determining the velocity flow field downstream of the carrier, the carrier was initially oriented in the required pitch and yaw setting. The tunnel was started and the desired tunnel velocity obtained. The static pressure in the test section was maintained slightly above atmospheric during these runs. For each carrier orientation, the downstream flow was examined at the various axial planar positions discussed earlier. The probes which were used were connected to a water-mercury manometer.

Two tubes on the manometer board indicated the tunnel nozzle pressure drop and thus the velocity head of the water entering the test section. When using the three-dimensional probe, the next five tubes on the manometer board were connected to the probe. With this unit, the first step in determining the velocity vector at a specific point in the flow field was to adjust the probe by rotating it about its longitudinal axis until the holes on the opposite sides of the prism were experiencing the same pressure as indicated by identical levels on the manometer board tubes to which these two holes were connected. This meant that the flow was now properly oriented in one plane and the angle was read directly off a vernier protractor to 0.02°. The

difference in the pressure values read on the manometer board by two additional holes on the probe permitted the calculation of the other angle by referring to the calibration chart for this unit. The absolute velocity was determined from a total head opening (now properly oriented with the flow) and the values of the pressure read by the holes on the sides of the prism (again corrected for calibration). Thus for each point in space the true velocity vector could be obtained with its proper yaw and pitch angle orientation. In processing the data, the raw data from the manometer board was fed into a computer program such that the computer presented the true velocity vector, the yaw and pitch angle orientation, the reference* tunnel velocity, an adjustment of this velocity to the axial plane under investigation, the nondimensionalized velocity vector's X(axial), Y(transverse), and Z(vertical)axis components and the vector's projection in three orthographic planes.

For conditions in which the relative wind was along the landing deck and the carrier pitch orientations were 0°, +1.5°, and -1.5°, a rather complete examination of the entire flow field as contained in the tunnel boundaries was undertaken. For the conditions in which the flow was along the hull centerline and when the wind was crossing the landing deck from the port side, the examination of the flow field was reduced somewhat so that the area consisted of that encompassing glide paths from about 1.5° to 5°.

After the data was obtained with the three dimensional probe, the adjustable Prandtl type pitot was employed as the sensing unit.

* The reference velocity was measured at the start of the test section.

A calibration of this unit was first obtained in the free stream using the United Sensor unit as the calibrating device. After the calibration value was established, a run of check points directly behind the carrier was made. This location was chosen as the flow was most violently disturbed here and the local vector velocity angles had the greatest deviation from the average flow. The agreement between the two instruments was excellent and, therefore, data obtained with the United Sensor unit is used as the basis for all information reported.

DATA EVALUATION, PRESENTATION AND DISCUSSION

Up to now this report has attempted to present the reasons for and the concepts entertained in undertaking this program. The test equipment and instrumentation have been described, and the test techniques and procedures employed presented. In this section, the results of this planning and the data obtained during this under-taking will be reviewed. The material will be presented in two sub-sections corresponding to the basic objectives of the program.

Flow Visualization

This section should present enough details and description to satisfy the majority of those interested in the results of this investigation. However for those individuals working directly on the problem who feel a detailed viewing of the dynamic flow field would be worthwhile, a 16mm sound movie has been made using some of the high speed film exposed during these studies. This movie affords an

opportunity to actually see this most interesting dynamic presentation of the disturbed flow occurring about a carrier. Several prints of this movie have been sent to the Office of Naval Research, Code 461.

The one most outstanding observation made during the visual and photographic studies of the disturbed flow field about the carrier was the marked difference between the conditions observed with the model in a fixed position (steady state) and when the carrier was actually undergoing dynamic heaving, pitching and rolling motions. While the same areas of the carrier were involved in creating the flow disturbances, the formation and resulting nature of the flow was markedly different for the two cases.

Perhaps it would be advantageous in the process of presenting the information applicable to the flow observation phase to first discuss each of the major areas or portions of the carrier which disturb the flow and then follow that line of presentation with a discussion of the differences noted between the dynamic and the "steady" flow regimes. Before doing so, however, it might be well to point out that in observing the disturbed flow field through the phenomenon of cavitation, a qualitative comparison of the "life" or "dissipative time" between different types of disturbed flow or between similar types of disturbed flow formation is possible provided these observations are undertaken with identical conditions of reference velocity and pressure. If, for example, two tip vortices are observed and one is larger in diameter and extends further downstream than the other, it is correct to conclude

that the larger and longer one is the "stronger" vortex. Similarly
any visible disturbed flow pattern which exists for a longer period
of time than another can be said to be stronger or conversely it can
be said that one dissipates more rapidly than the other. It should
be emphasized, however, that one should not fall into the fallacious
belief that the vorticity dies with the disappearance of cavitation.
This is not the case at all. The only thing which the cavitation
did was to make visible portions of the disturbed flow field where
the local pressure was reduced to the condition where vaporization
or gaseous diffusion took place. If a disturbed flow field exists,
the process of raising or lowering the reference static pressure
level of the flow field only permits more or less of the disturbed
flow to reach the stage where cavitation occurs and thus portions
of the flow field become visible. It is also not correct to assume
that the extent of a given disturbance in a liquid flow field can
be revealed by continuously reducing the reference static pressure
of the flow field thus having more and more of the disturbance
regime become visible. This doesn't hold as profuse cavitation will
affect the normal flow field. In these conditions what is observed
can no longer be considered as that which exists without the in-
fluence of the profuse cavitation. Therefore, this technique, as
many experimental techniques, must be employed with a full under-
standing of its strengths and its limitations. With that concept
in mind, a description of the flow will now be given.

The island is a rather blunt body and as such produces a
rather violent and disturbed wake. This was the most severe (for

the conditions tested) when the relative wind direction was parallel to the landing deck as this placed the island at the greatest attack angle. The flow about the island was quite complex but it can perhaps be described as being formed from three basic disturbed* flow regimes. One of the disturbances observed was the forming and shedding of vorticity from the vertical "corner" of the island. For the case with the wind parallel to the landing deck this became the forward starboard vertical corner. The flow from this corner or edge acted much as the flow from the leading edge of a flat plate placed at a similar attack angle. In general the flow separates from the surface aft of the leading edge, but, after a certain degree of separation occurs downstream, flow re-enters the separated region moving along the surface and under the separated portion towards the leading edge. This in a sense "fills" the separated region but almost immediately the flow starts to separate again only to repeat the cycle again and again. It should be noted that each cycle exists for an extremely short time period with many cycles occurring each second.

Moving to the aft end of the island the flow from the blunt end is very periodic in nature and suggests flow of a Karman vortex street nature. In general, the flow sheds alternately from one side and then the other of the body with the center of the shed vortices having their cores parallel to the sides of the island.

* Disturbed is used here to identify flows which deviate from the normal steady flow conditions. Steady is defined here as nonchanging with time.

A rather good illustration of shedding of this nature is shown in Figure -12- wherein a series of photographs shows the alternate shedding of the flow from one side of a sphere to the other. In this photograph the shed flow is made visible by the phenomenon of cavitation.

Superimposed on the above flows, but primarily influencing the flow from the aft end of the island, is a rotation of the flow resulting from the circulation introduced about the island because it is at an attack angle. An earlier photograph, Figure -2-, illustrated a tip vortex from a hydrofoil at an attack angle but because the island has such a short "span" and is so blunt the vortex formed by the circulation about the island tends to cause the entire disturbed flow field aft of the island to rotate about an axis parallel to the direction of travel.

With the carrier under fixed orientations the disturbances mentioned above could be considered as generally "continuous" in nature, but containing unsteady components. These unsteady components had a rather high rate of frequency of occurence. With carrier motions, the disturbances appeared in the downstream wake as discrete, well-defined pulses or groupings of disturbed flow with one mass or grouping of disturbed flow associated with each pitch or heave cycle. Pure pitching created larger masses of disturbed flow than equivalent heaving motions but both conditions introduced a pronounced periodicity in the wake. Pitching and heaving motions actually increased the magnitude of the disturbance when comparing it to the disturbances originating
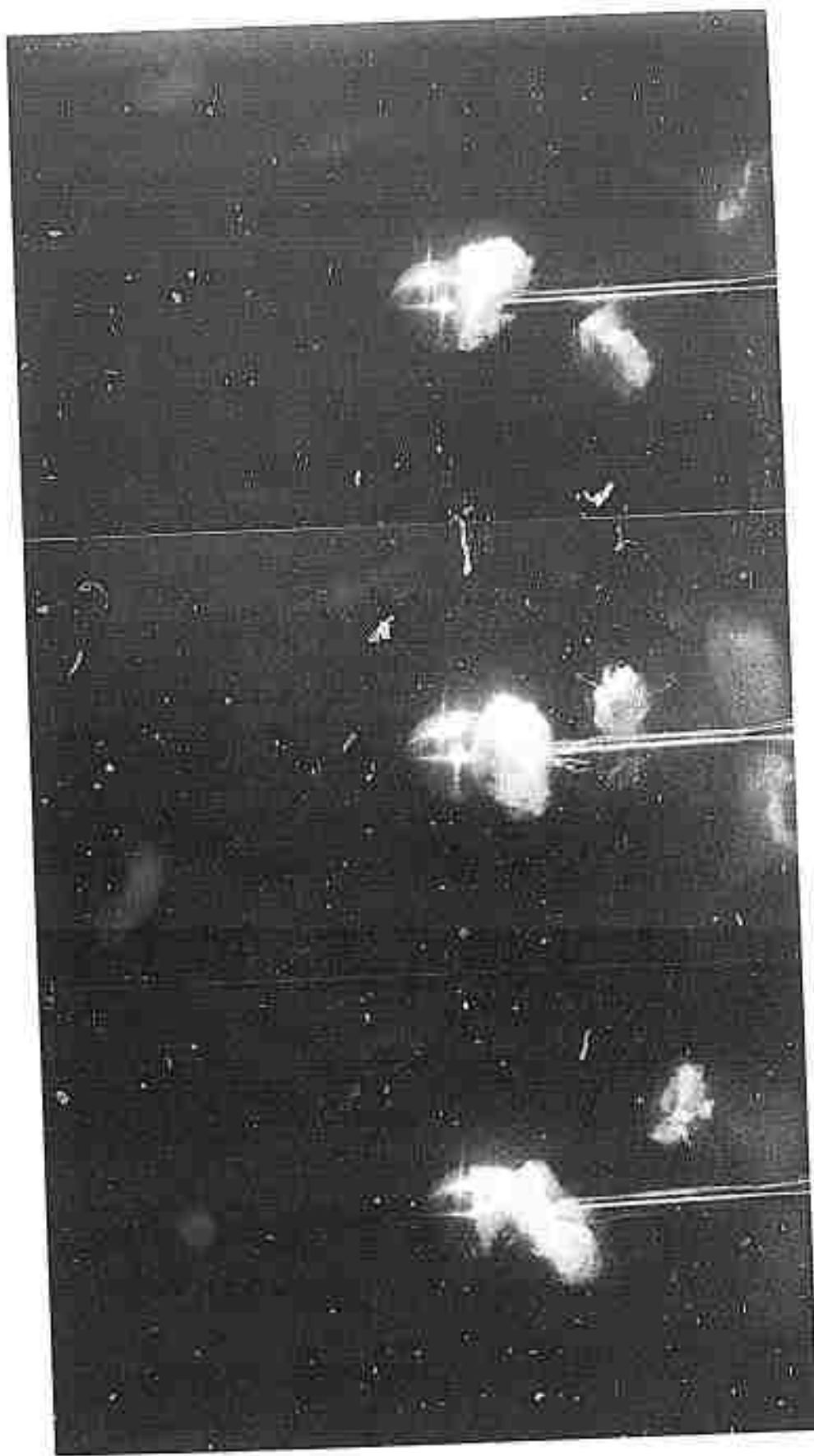
FIGURE 12   ALTERNATE SHEDDING OF FLOW FROM ONE SIDE OF A
SPHERE TO THE OTHER (FROM REFERENCE [2])

with the carrier in a fixed orientation. By this it is meant
that pitching and heaving motions did not merely segment the
disturbed flow field occurring with the model under fixed condi-
tions, but actually increased the amount of disturbance as well
as introducing the periodicity. For sketches of the disturbed
flow patterns see Figures 13 and 14. Roll motions of the carrier
did not seem to affect the flow patterns to a noti. . degree.

The leading edges of the bow and angled deck act much
as the leading edges of wings. With the model stationary and
with a zero or +1.5° pitch angle, the flow from the leading edges
of the bow deck and the angled deck tended to shed vortices of a
nature very similar to that of a Karman vortex street, although
only one half of the street was formed. At a -1.5° pitch angle
of the carrier this separation did not take place. It did occur
at the zero and higher pitch angles, however, because the leading
edges of these structures were at an effective attack angle due to
the up wash of air caused by the presence of the hull and the tend-
ency of the displaced air to be trapped between the surface of the
sea and the overhang of the carrier deck.

Examination of the formation and shedding of this flow
disturbance under both strobotac and high intensity illumination
indicated that a separated region was created from the leading
edge and extended downstream. After extending to some point down-
stream it appeared as if the separated flow region could no longer
retain its identity as a unit and the trailing edge or downstream
portion of the separated zone "broke off," separating first near

FIGURE 13   SKETCH OF MAXIMUM DISTURBED FLOW PATTERN ORIGINATING
FROM THE ISLAND WITH NO CARRIER MOTION (MAXIMUM
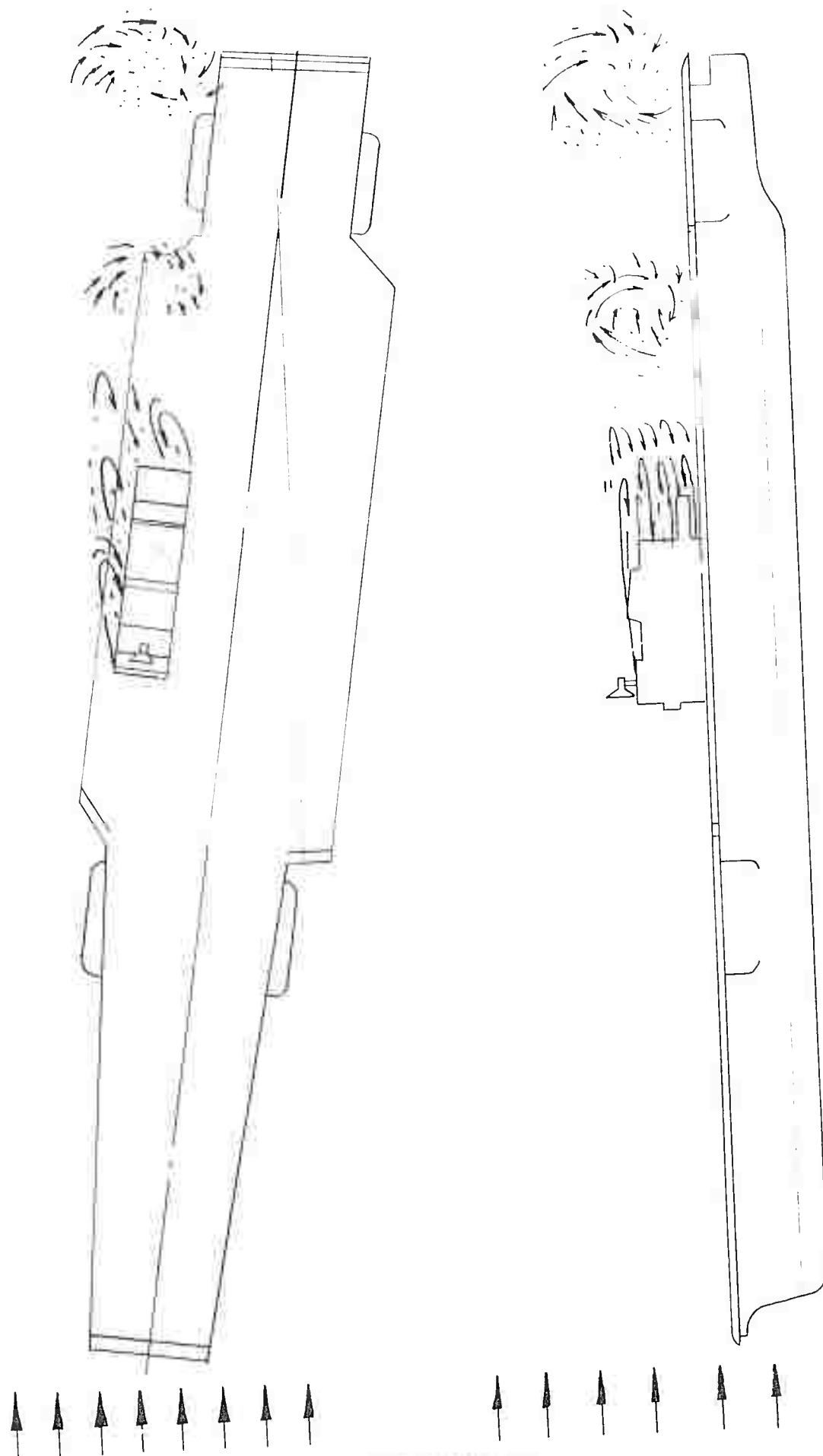DISTURBANCE AT POSITIVE ATTACK ANGLES OF THE DECK)

FIGURE 14   SKETCH OF MAXIMUM DISTURBED FLOW PATTERN ORIGINATING
FROM THE ISLAND WITH CARRIER MOTION (COMPARE WITH
FIGURE 13)

the center of the zone and lastly near the ends of the separated region. Since the separated region extending from the leading edge had a parabolic shape, the portions of the disturbed flow that separated themselves from the parent disturbed region had the shape somewhat similar to a horseshoe. See Figure -15- for a sketch of this flow phenomenon.

Under dynamic conditions of pitch and heave the vertical motions of the carrier introduce cross flow velocities at the leading edges of the bow and angled deck and this increased the extent of the separated regions. More important, however, is the fact that the shedding now occurred only when the motion of the forward part of the model was in a downward direction. As a result, flow disturbances were created and shed with a periodicity directly associated with carrier pitch and heave motions. In moving downstream, the patches of disturbed flow shed from the bow collided with the island and passed about it. After passing about the island, the disturbed mass tended to be more tightly grouped. This observation was made both using the cavitation technique and through that of emitting dye and air bubbles from small holes along the leading edge of the bow deck. The visual observation was reinforced by a study of the high speed movies. The shedding of the disturbed flow from the leading edge of the angled deck just progressed downstream. A sketch of this type of disturbance under dynamic conditions is shown in Figure -16-. Roll motions of the model did not appear to affect the disturbed flow pattern.
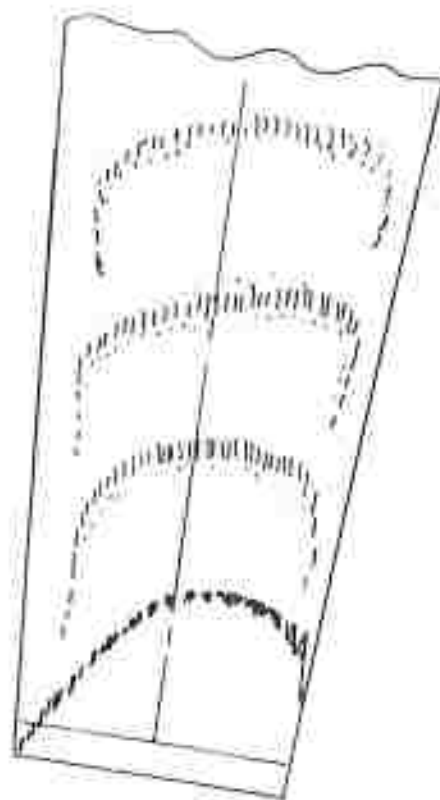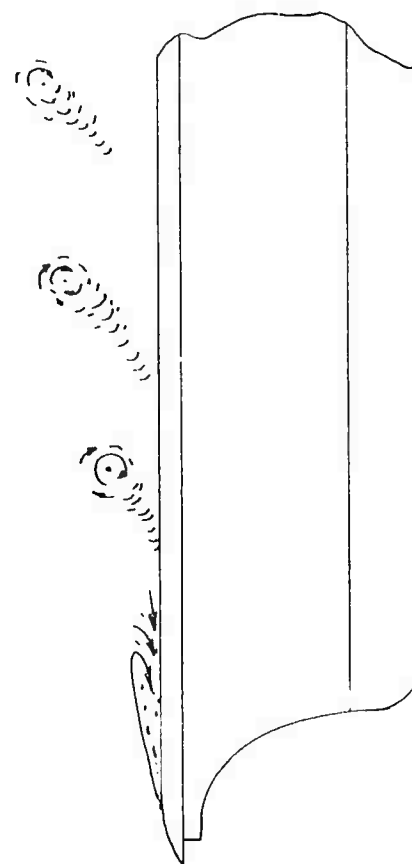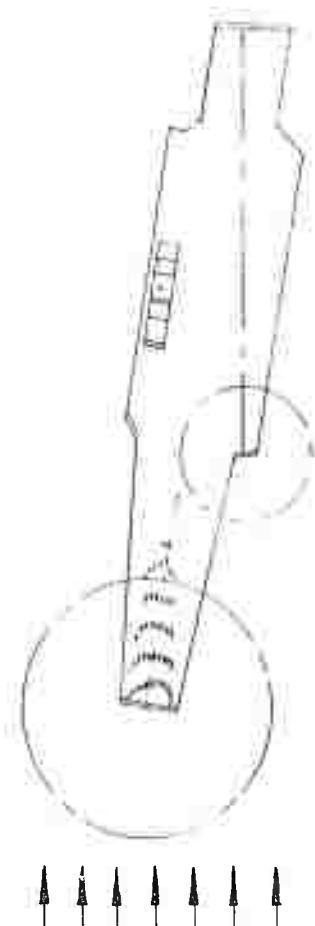
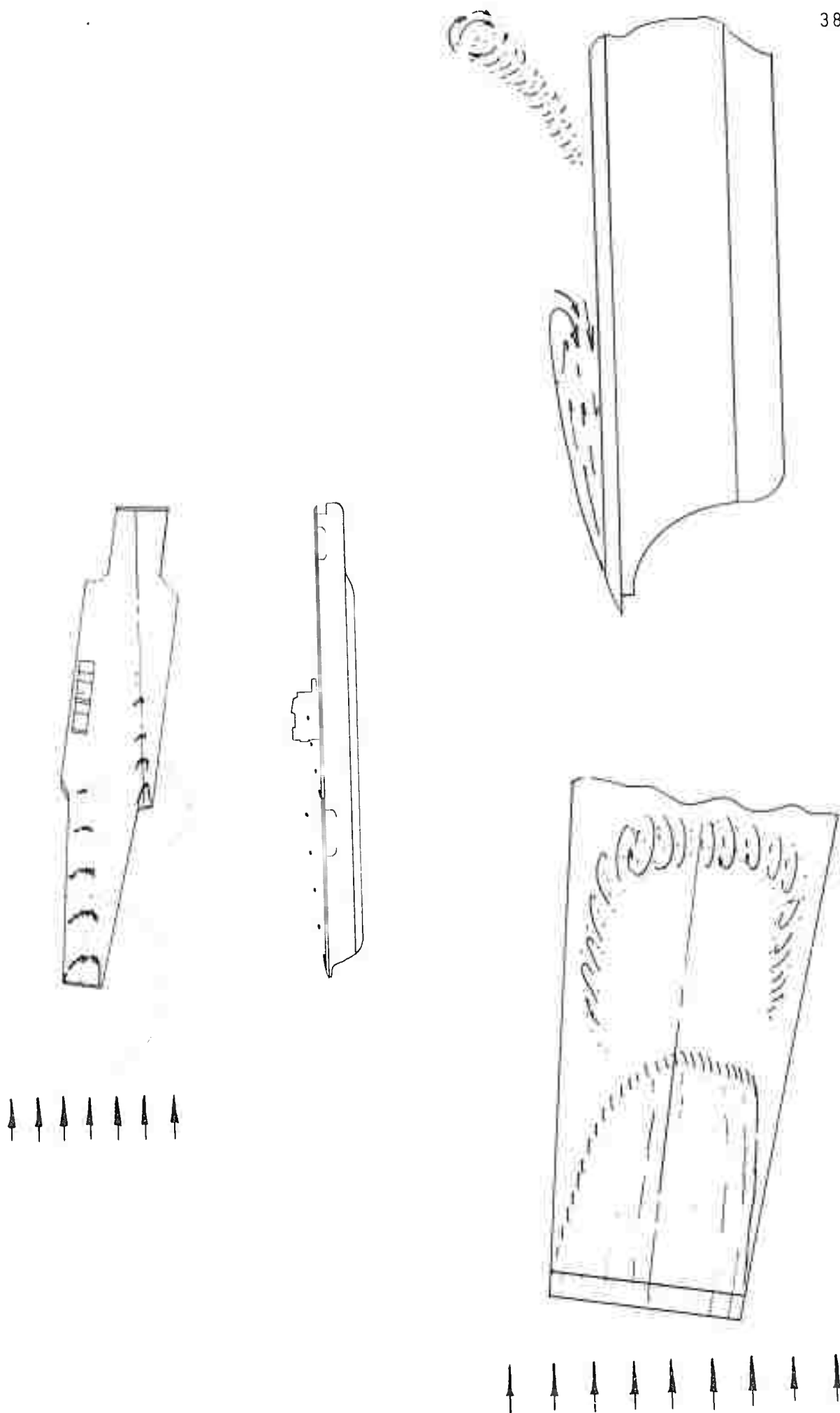FIGURE 15   SKETCH OF FLOW SHEDDING FROM BOW AND ANGLED DECK WITH
NO CARRIER MOTION

FIGURE 16 SKETCH OF FLOW SHEDDING FROM BOW AND ANGLED DECK WITH
CARRIER MOTION (COMPARE WITH FIGURE 15)

OCEANICS INC.

Tip vortices were formed from the edges of the bow and angled deck and from the upwash created by the forward port sponson (this is for conditions with the flow parallel to the angled landing deck). Under steady conditions, the formation of the vortices could be observed at zero and greater pitch angles with negative pitch angles of the carrier rapidly diminishing the tendency to create vorticity. The tip vortex from the bow joined with that formed by the forward port sponson. As a result there were two major vortex trails moving downstream; one composed of the tip vortex formed from the bow and forward port sponson, the other from the edge of the angled landing deck. The vortex composed of that originating from the bow and from the forward port sponson had the larger core.

Under dynamic conditions of pitch and heave the formation of the tip vortices occurred only with downward motions of the forward portion of the ship. The motion of the ship, in addition to limiting the shedding times of the vorticity to that corresponding to times equivalent to one half of the pitch or heave cycle, also increased the strength of the vortices as they were being shed. This was particularly true of the vortex trail originating from the bow and forward port sponson. On a downward motion of the carrier the upwash of fluid about the entire length of the deck edge extending from the forward port sponson to the bow tended to form a large sheet vortex co-mingling with the vortex from the bow and then subsequently joining with the vortex from the forward port sponson. A photograph of

the carrier in fixed orientation illustrating the vortex formations quite clearly is shown in Figure -17- while Figure -18- is a sketch of the vortex formations under dynamic conditions.

The carrier areas described above tended to produce the major disturbed flow patterns, and the dynamic formations described above apply when the relative wind was 9° port of the ship center-line. Minor flow disturbances were observed from other portions of the carrier, but it is believed that those detailed above are responsible for nearly all of the flow disturbances affecting aircraft in the process of landing.

The portions of the carrier causing the flow disturbances have been described. If one now considers the entire flow field consisting of the carrier and a distance of some three carrier lengths aft, the following characteristics can be enumerated. Under conditions wherein the model was fixed in orientation, a wake existed downstream which was disturbed, but one which could be considered as fairly homogenous at any particular point in the wake with time. The height of the disturbance above the sea surface reached a level of some 150 feet about 600 feet downstream of the carrier, and thereafter did not tend to go appreciably higher although some patches reached a level of 200 feet.

Under dynamic conditions all disturbances joined or merged just downstream of the fantail and formed a wake extremely periodic in nature. This periodicity was associated with the pitch and heave motions of the model - one mass of disturbed flow for each pitch or heave cycle. The pitch motions produced a
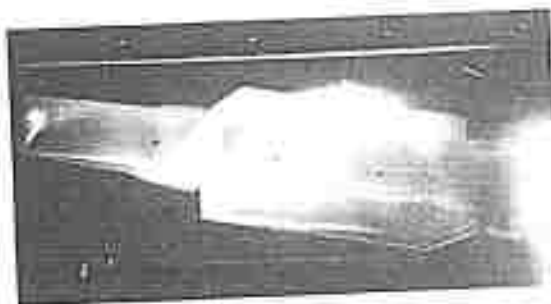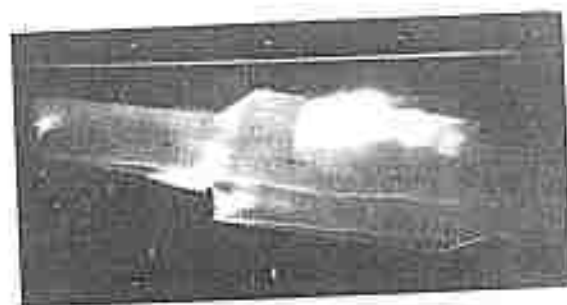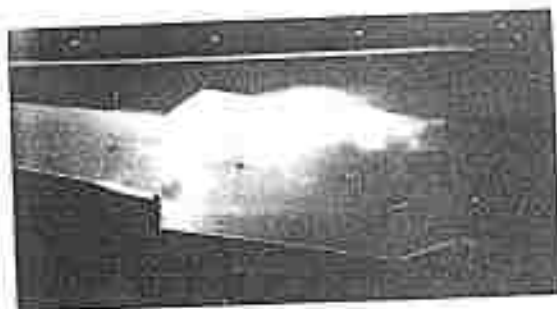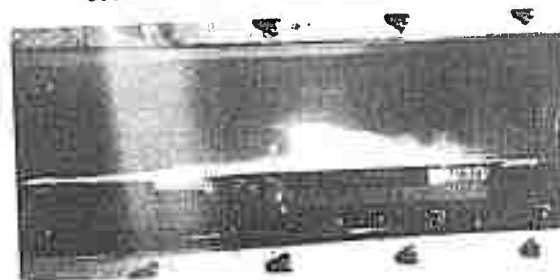
CARRIER PITCH ANGLE +1.5°

CARRIER PITCH ANGLE 0°

CARRIER PITCH ANGLE -1.5°

FIGURE 17   PHOTOGRAPHS OF VORTEX FORMATIONS WITH
FIXED CARRIER ORIENTATION
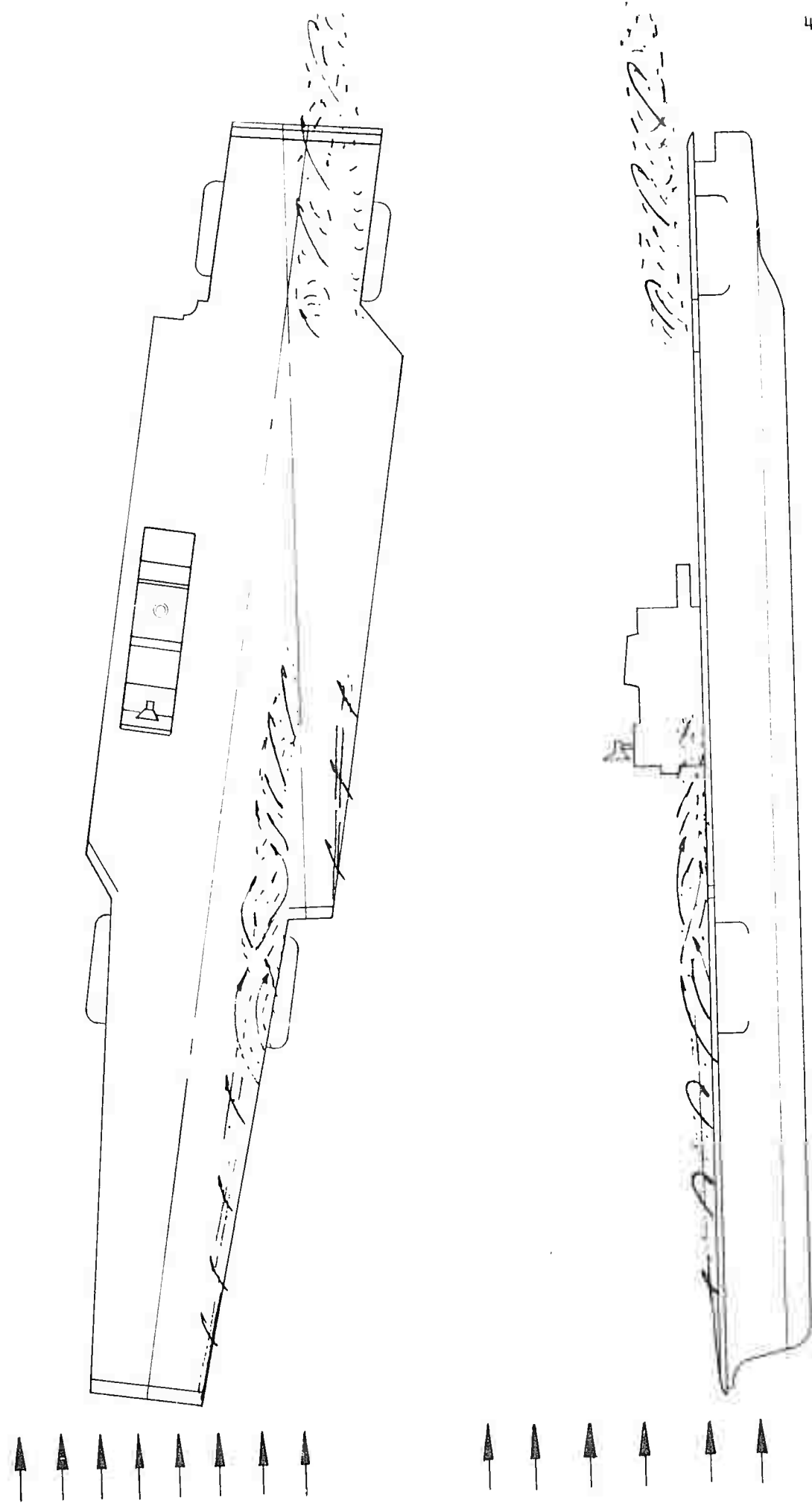
FIGURE 18 SKETCH OF VORTEX FORMATION FROM DECK EDGES WITH CARRIER MOTION

significantly more discrete periodicity in the wake and appeared
to produce masses or patches of disturbed flow which were more
violent in nature than those occurring from pure heave motions.
In examining individual masses of disturbed flow in the downstream
wake, very often elements of vorticity, most probably tip vortex
elements, could be noted (see Figure -19-).

In an effort to better understand the flow, it has been
mentioned that both dye streams and air bubbles were emitted from
the stack to study stack gas effects, and from holes on various
portions of the carrier to observe the flow trail from these
portions of the carrier (see Figure -4-). From observing both
air and dye trails, studying the high speed motion picture film,
and augmenting this information by full scale observations on the
FORRESTAL, it is believed that the stack gases are injected into
the existing disturbed flow field about the island. These gases
do very little more than make visible the path of the wake from
the island (and further aft portions of the overall wake) provided
the carrier is subjected to a relative wind of the magnitude
required for aircraft operations. Under these conditions, the
stack gas velocity is not high enough to "blow" the gas through
the surrounding island flow field and into the undisturbed
atmosphere above. While the stack gas itself does not appear to
affect the flight characteristics of the aircraft except from
minor thermal effects, the psychological effect on the pilot of
being more or less temporarily blinded while going through the
stack gases (mixed with the existing turbulent flow) cannot be

FIGURE 19 SKETCH OF MANNER IN WHICH DISTURBED FLOW MASSES ARE FORMED

INDIVIDUAL MASSES — ONE PER PITCH OR HEAVE CYCLE

FORMING AREAS
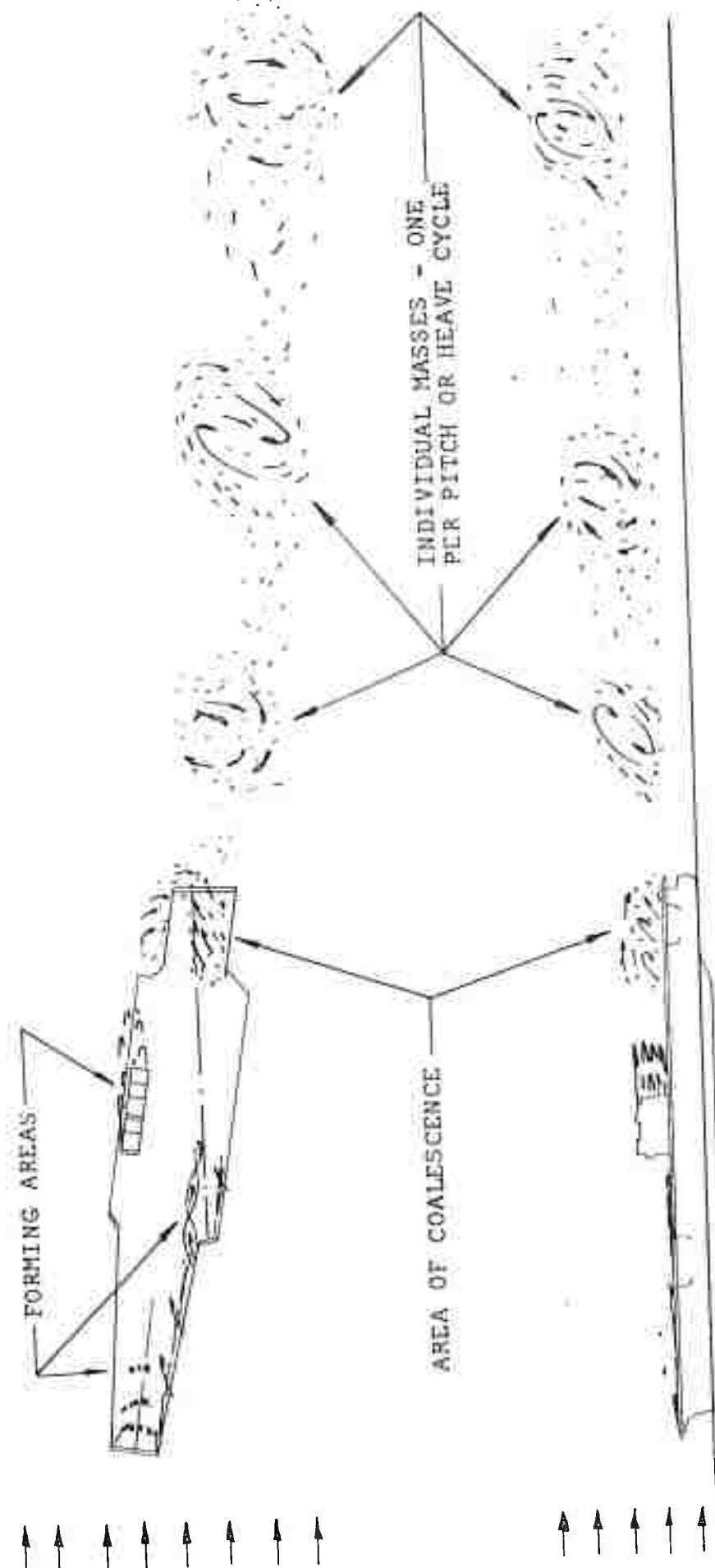
AREA OF COALESCENCE

~OCEANICS~ inc.

ignored.   Therefore, the temporary loss of visual orientation in space tends to make the pilot believe any encountered flow disturbances are actually more violent than they really are.

So far discussion of the flow disturbances has been limited to the downstream and the vertical directions.   The flow pattern in the yaw plane was also quite interesting.   With the simulated wind velocity along the **hull** centerline, the flow disturbances moved downstream with the flow and parallel to the hull centerline.   While there was some dispersion of the disturbances it did not appear to be quite as wide as in the vertical direction.   The dispersion was, however, symmetrical about an extension of the hull centerline.

With the flow over and parallel to the landing deck, the disturbances tended to be influenced by the orientation of the carrier in that the disturbances did not move directly downstream with the simulated wind field, but rather progressed parallel to the hull centerline for some distance and then gradually veered into a direction which was parallel to the entire simulated wind field.   While this latter comment was particularly true of the tip vortex disturbances, the entire flow field was affected and the entire mass of disturbed flow was port of a projection of the center line of the angled deck at a distance approximately one-quarter carrier length aft.

As there was considerable interest in the contribution various portions of the carrier made to the overall downstream flow disturbances, the island was completely removed for one series of runs.   With the island removed, the magnitude of the

downstream disturbed flow pattern decreased somewhat, but the amount of decrease bordered on the marginally insignificant. It is believed that the deck, due to the extreme overhang, is the major cause of the downstream flow disturbances, as this acts much as a wing element undergoing changes in attack angle as the carrier undergoes pitching and heaving motions.

In certain past investigations a rough estimate of the turbulence level of a liquid stream was made by tracing the path of a single bubble or dye stream with multiple photographs and noting the deviation from the main flow direction. It was hoped that this technique could be used in this series of investigations but the number of bubbles, and/or the rapid dispersion of the dye stream, because of the intense disturbance in the flow field, did not permit it*.

From the observations made employing the various flow visualization techniques described, the following major conclusions can be drawn.

1. The use of the cavitation technique for visualizing and qualitatively interpreting the flow disturbances appears to be superior to either the use of dye or air bubble streams in that greater detail of the flow disturbance is possible.

2. The cavitation technique affords a full three dimensional visualization of the object and the surrounding flow field

_____

* A measure of the velocity "gustiness" is to be directly made in a new series of investigations planned for the later part of 1964, thus affording some insight in this area of interest.

whereas dye or air streams are limited to discrete positions in space, but the latter technique does contribute to an understanding of the path of flow from a particular area of the carrier.

3. The form and nature of the originating disturbances and the downstream wake field are markedly different in cases when the carrier is fixed in orientation and when the model is undergoing pitching and heaving motions.

4. Without motions of the model, the downstream wake appears as if it would be fairly steady at any point with time.

5. Pitching and/or heaving motions not only introduce a pronounced periodicity in the shedding action, but also in the downstream wake. Each pitch or heave motion produces one mass or grouping of disturbed flow and the motion appears to significantly increase the violence of the downstream disturbances in addition to introducing the periodicity. Each mass has a general clockwise motion (resulting from the tip vorticies) when looking in the direction of travel.

6. It is believed that each mass of disturbed flow associated with each pitch or heaving motion of the carrier is a burble. However, the combination of aircraft glide path angle, carrier orientation, relative wind velocity, and carrier pitch or heave periods is such that an aircraft will only encounter one such burble in a typical approach. It is possible, depending upon the parameters involved, that the aircraft will not encounter any burble and the possibility of encountering two is much less than not

encountering any.

7.   It is not believed that stack gases by themselves influence the flight characteristics of an aircraft. The stack gases mingle with the disturbed flow field originating from the island with this disturbance later combining with the disturbed flow field from the entire carrier. Thus, the gases make the existing flow disturbances visible and, in addition, add the psychological effect of interfering with the pilot's process of visual orientation.

8.   Roll motions of the carrier do not appear to significantly influence the pattern of flow disturbances.

9.   Disturbances originate from the island, the deck, and the hull but the complete elimination of the island only reduced the downstream disturbed flow pattern to a minor degree.

10.   It is believed the deck is the major contributor to the downstream disturbances. This results from the extreme overhang of the deck in relation to the hull.

11.   The orientation of the carrier with respect to the existing natural wind has an important influence on the path of the disturbed flow field after it leaves the near vicinity of the carrier as the disturbances then become a part of the atmospheric flow field.

12.   Model size did not appear to affect the formation of the flow disturbances or the nature of the downstream flow field.

13.   Direct similitude of the carrier's motion periods with relation to the relative wind is possible, and rather high

Reynolds numbers can be achieved using a water tunnel for this type of investigation.

14. High speed motion picture studies of the flow disturbances, coupled with the scaling possible in water tunnel tests, afford an excellent means of detailed study of flow disturbances of the nature described here.

Steady State Flow Field Measurements

This section deals with the second basic objective; i.e., the measurement of the velocity flow field downstream of the carrier with fixed carrier orientation. As was pointed out earlier, the introduction of dynamic motions to the carrier causes significant changes in the flow field, but these steady state measurements with various carrier orientations do afford some insight into the probable nature of the flow field with carrier motions.

All measurements were taken with the directional pitot tube described in the section on Wake Measuring Instrumentation and shown in Figures -8- and -9-. With the large carrier, flow measurements were made at five (5) axial planes located the equivalent of 222, 480, 760, 1030 and 1310 feet aft of the touchdown point on the carrier. The touchdown point was assumed to be 150 feet forward of the end of the deck. The following conditions were investigated:

wind velocity 35 kts., 9° from port, carrier pitch angle 0°

wind velocity 35 kts., 9° from port, carrier pitch angle +1.5°

wind velocity 35 kts., 9° from port, carrier pitch angle -1.5°

wind velocity 35 kts., from dead ahead, carrier pitch angle 0°

wind velocity 35 kts., 13° from port, carrier pitch angle 0°.

With the small carrier, studies were made at two (2) axial planes located the equivalent of 600 and 1875 feet aft of the touchdown point. The following conditions were investigated:

wind velocity 35 kts., 9° from port, carrier pitch angle 0°

wind velocity 35 kts., 9° from port, carrier pitch angle +1.5°

wind velocity 35 kts., 9° from port, carrier pitch angle -1.5°

Depending upon the axial plane under investigation, the number of individual points in space at which the flow direction and magnitude were determined varied with a maximum of 160 points per axial plane. At each point in space, the angle the flow made with a horizontal plane and the angle the flow made with a vertical plane were determined. The flow magnitude at this position was also determined and then compared to the average flow value at that axial plane. A nondimensionalized velocity vector value was determined by dividing the magnitude of the velocity vector by the value of the average flow in the section. This ratio can then be applied to the magnitude of the undisturbed oncoming wind velocity to obtain the actual velocities at these points, since this method includes the necessary corrections for the effects of tunnel wall interference, blockage, etc.

Understandably, these studies produced a mass of data and the question then arises as to the manner in which to present this information. For those individuals desiring to examine or

analyze the flow themselves, all of the data is presented in a series of thirty one (31) figures contained as an appendix to this report. Each of these figures represents one axial plane of velocity measurements for a particular carrier model size and orientation. Each point is physically determined in space by means of the distance scales along the sides and bottom of the sketches. The velocity vector at each point is described in terms of a dimensionless velocity ratio together with its orientation in the axial and vertical planes. These figures present a rather incomprehensible appearance at first glance, but with a slight amount of conscientious examination a rather descriptive pattern of the flow can be mentally visualized. In examining these figures it should be remembered that the values in close proximity to the walls of the tunnel and the plate simulating the sea surface are influenced by flow boundary layer growth along these surfaces.

For example, examine Figure A-7 which shows the flow conditions equivalent to 480 feet aft of the touchdown point for conditions of wind 9° port and a carrier pitch angle of +1.5°. Examining the figure permits identifying the location of the two major disturbed flow regimes. The center of the disturbed flow mass behind the island appears to be located about 60 feet starboard and 25 feet below the glide path. The center of the disturbed flow mass resulting from tip vortex shedding off of the bow, forward port sponson and angled landing deck

appears to be located perhaps 60 feet port and 25 feet below the glide path. The glide path is thus in the area where both disturbed flow regimes are mixing, but somewhat above the centers of the individual disturbed masses. The very disturbed flow behind the stern is also evident, but this does not appear to directly influence the flow conditions about the glide path.

In Figure A-8, which is equivalent to 760 feet aft of the touchdown point, evidence of both disturbed flow masses can still be noted, but the strength of the disturbed flow mass behind the island is somewhat reduced. On the other hand, the strength of the tip vortex type disturbance does not appear to have diminished much in strength which, of course, is typical of this type of disturbance. The center of the core of the disturbed flow mass originating from the bow deck, forward port sponson and angled landing deck remains at about the same elevation, but is now between 100 and 150 feet port of the glide path.

In Figure A-10, which shows conditions equivalent to 1310 feet aft of the touchdown point, slight evidence of the island disturbances still exist, but the major disturbed flow area still comes from the tip vortex type of disturbed flow regime. The center of the core appears to have approximately the same strength, but the area of the disturbed flow has grown larger as the rotation of the vortex has induced disturbances in the flow at increasing radial distances from the core. The

core position has changed slightly as it now is about 40 feet above the touchdown point and between 150 to 200 feet port of the glide path.

The principal interest is, however, in the area relatively close to the glide path and, recognizing that few readers of this report have the time to study all the figures in the Appendix, several other sketches have been prepared. These sketches portray in three dimensions the projections of the non-dimensionalized velocity vector in the axial (horizontal) and vertical (transverse) planes. They present in a somewhat more easily understandable manner the flow conditions an aircraft would encounter under certain conditions while traveling a 4° glide path to a carrier maintaining a fixed orientation in space. Both horizontal and vertical variations in the nondimensionalized vector quantities are shown. The area presented about the glide path was roughly selected so as to encompass the limits in space that an aircraft might operate in and still make an acceptable approach and landing. In other words, when the aircraft is 1800 feet aft of the touchdown point it can deviate from the idealized glide path more than it can when it is only 200 feet aft of the touchdown point.

Figure -20- is a sketch of the flow conditions about a 4° glide path with the carrier deck at a zero pitch angle and the wind 9° from port (or approximately along the angled landing deck). Here it can be noted that at the 222 foot station the disturbances
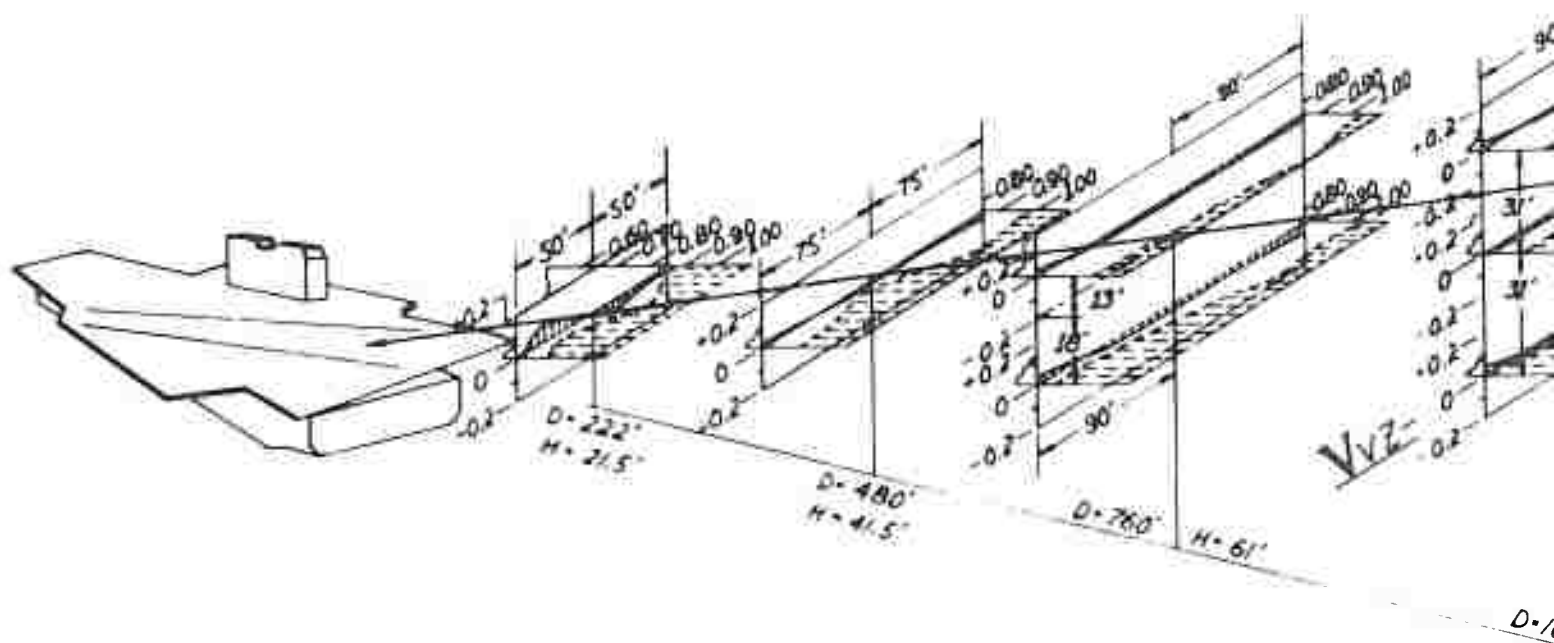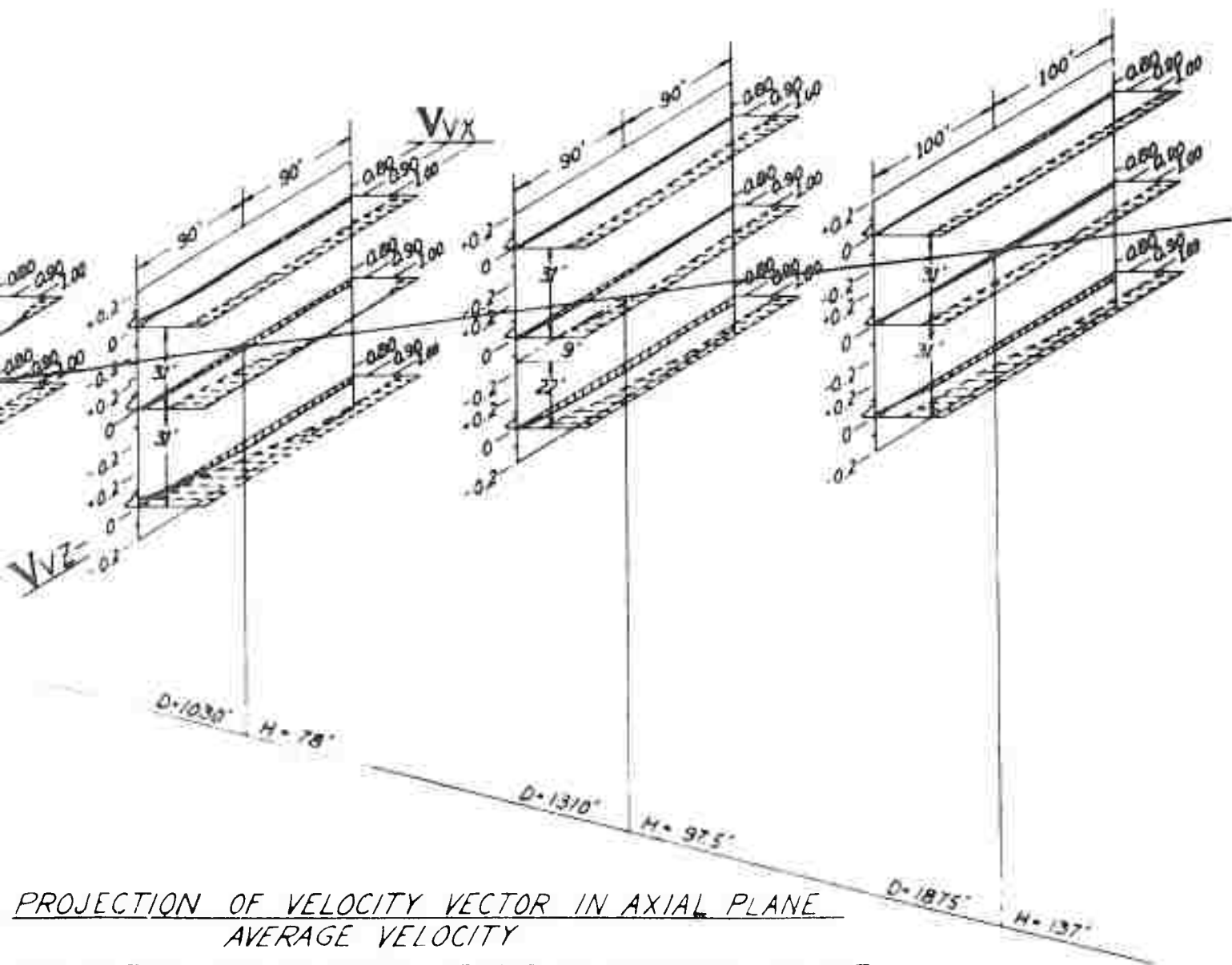
CONDITIONS

WIND 35 KTS; 9° PORT OF SHIP ₵
SHIP PITCH ANGLE 0° ROLL ANGLE 0°
GLIDE ANGLE 4°
TOUCHDOWN 150′ FWD OF DECK AFT EDGE
WING 6′ ABOVE DECK

V_{VX} = $\dfrac{PROJECTION}{}$

V_{VZ} = $\dfrac{PROJECTION}{}$

D - DISTANCE
H - DISTANCE

PROJECTION OF VELOCITY VECTOR IN AXIAL PLANE
                AVERAGE VELOCITY

PROJECTION OF VELOCITY VECTOR IN VERTICAL PLANE
   AVERAGE VELOCITY

D = DISTANCE AFT OF TOUCHDOWN POINT

H = DISTANCE ABOVE TOUCHDOWN POINT

FIGURE 20

caused by the island and those caused by the leading edges of
the deck and forward port sponson still retain their individual
identities. At the 760 foot station, the disturbances have tended
to combine in one single disturbed mass centered about the core
of the tip vortex type disturbance, although some evidence of
separate island disturbances remains. This conclusion is based
upon the material presented in the figures in the Appendix and
a study of the high speed movies, as well as the evidence
presented in this figure. This conclusion also follows the trend
of information presented in [3]. Of particular interest is the
variation in the magnitude of the nondimensionalized velocity
vector projections with a change in elevation. Examining any of
the stations beyond the 480 foot station, it can be seen that the
projection of the nondimensionalized velocity vectors in the
horizontal plane changes markedly. The vertical projections also
show considerable change. Both effects tend to die out as one
moves aft. In other words, at the 760 foot station the changes
in the projections of the velocity vectors about the glide path
are more pronounced than at the 1875 foot station.

Figures -21- and -22- are sketches illustrating flow
conditions for the same wind conditions except that the carrier
deck is at a pitch angle of +1.5° and -1.5° respectively. By
comparing these three figures (-20-, -21-, -22-) it is possible
to obtain an indication of how the flow conditions at a fixed
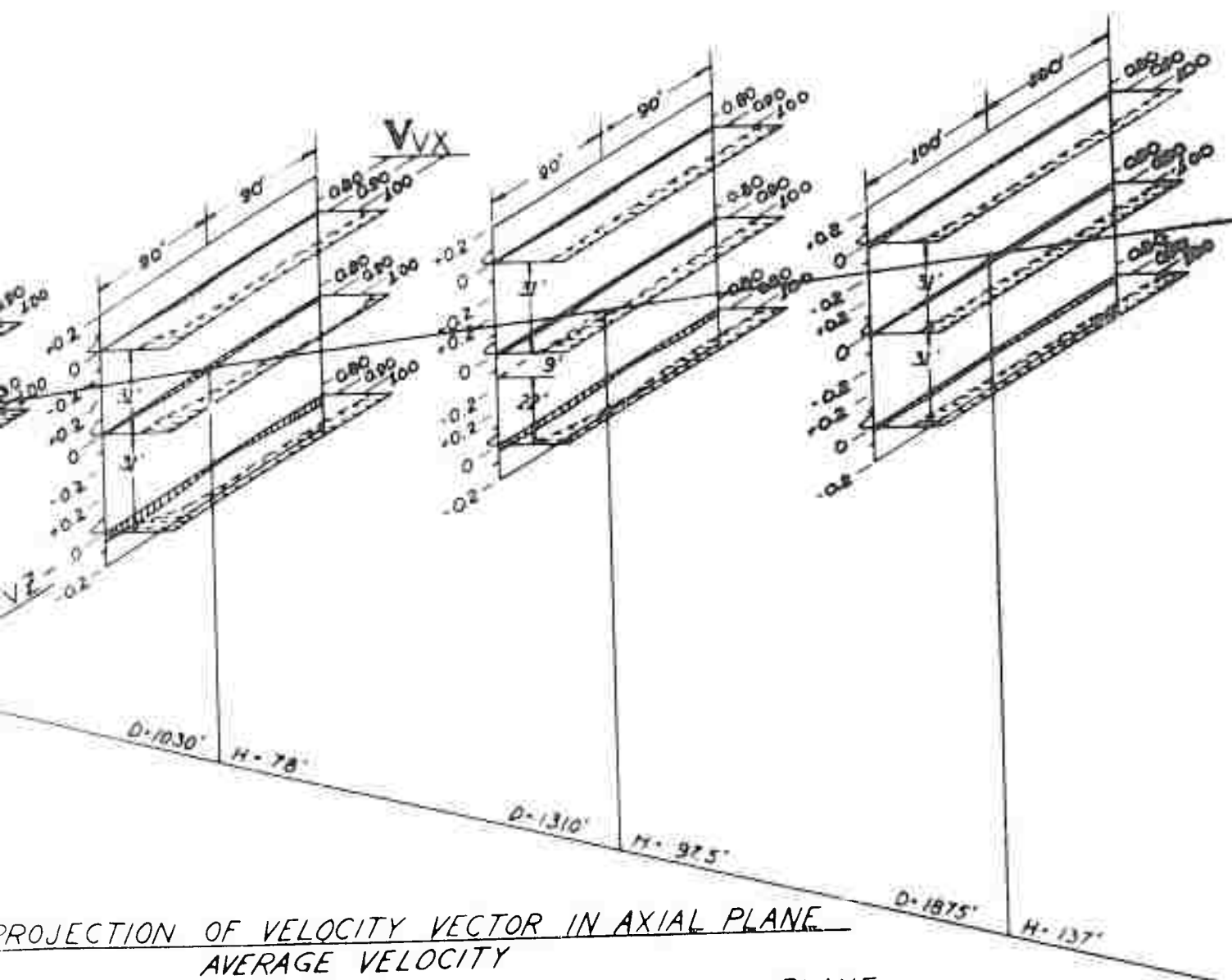distance downstream of the carrier change as the carrier deck
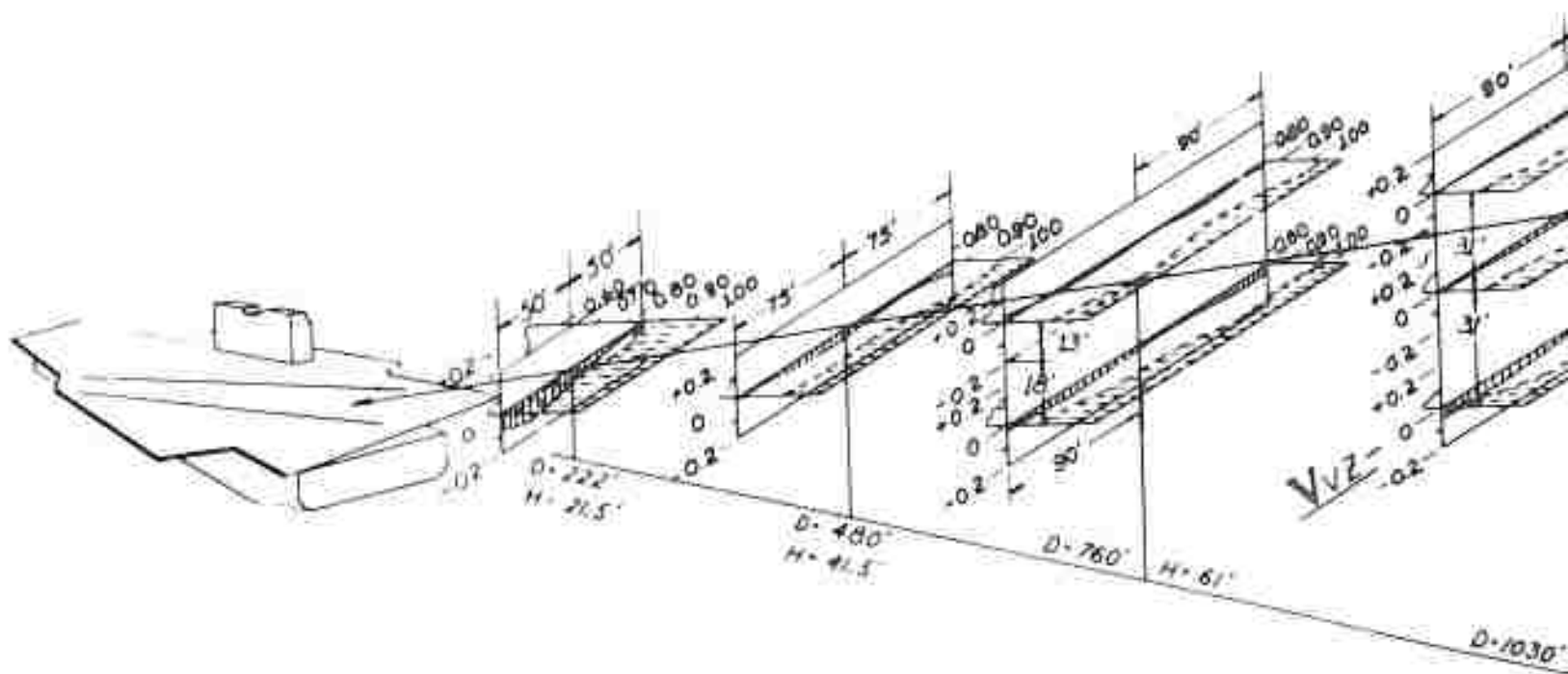
CONDITIONS
WIND 35 KTS; 9° PORT OF SHIP ₵
SHIP PITCH ANGLE +1.5° ROLL ANGLE 0°
GLIDE ANGLE 4°
TOUCHDOWN 150' FWD OF DECK AFT EDGE
WING 6' ABOVE DECK

$V_{VX} = \dfrac{PROJECTION}{}$

$V_{VZ} = \dfrac{PROJECTION}{}$

D = DISTANCE

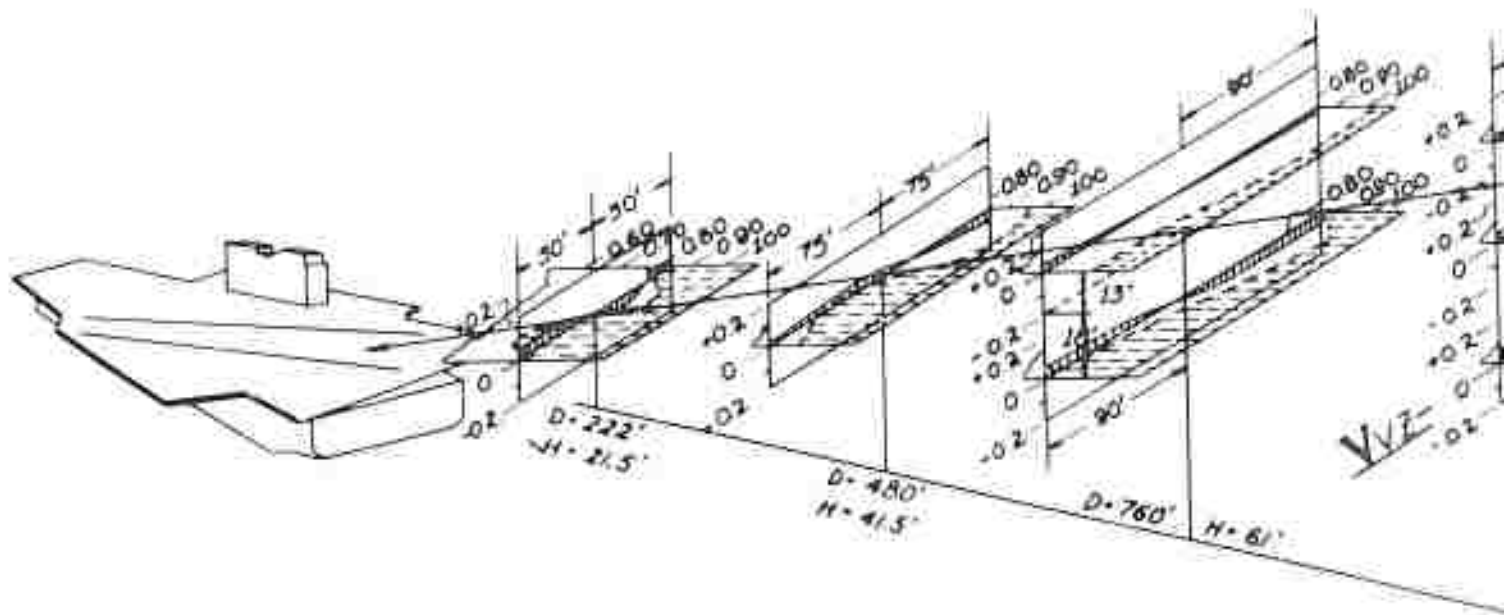H = DISTANCE

V_{VX}

PROJECTION OF VELOCITY VECTOR IN AXIAL PLANE
          AVERAGE VELOCITY

PROJECTION OF VELOCITY VECTOR IN VERTICAL PLANE
          AVERAGE VELOCITY

D = DISTANCE AFT OF TOUCHDOWN POINT

H = DISTANCE ABOVE TOUCHDOWN POINT
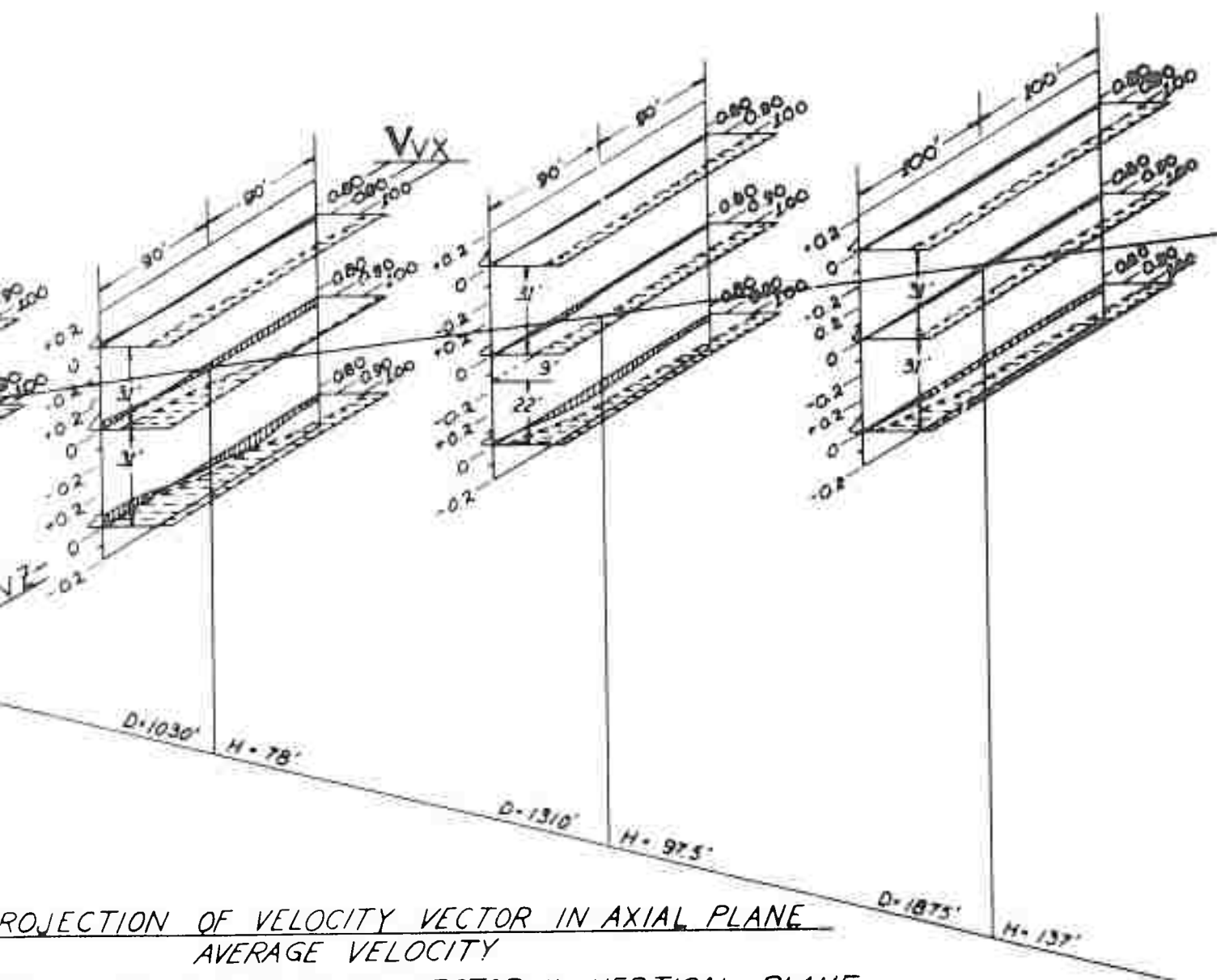
FIGURE 21

CONDITIONS
WIND 35 KTS; 9° PORT OF SHIP ₵
SHIP PITCH ANGLE −1.5° ROLL ANGLE 0°
GLIDE ANGLE 4°
TOUCHDOWN 150' FWD OF DECK AFT EDGE
WING 6' ABOVE DECK

$V_{VX} = \dfrac{PROJECT}{}$

$V_{VZ} = \dfrac{PROJECT}{}$

D = DIST
H = DIST

V_{VX}

D·1030' H·78'

D·1310' H·97.5'

D·1875' H·137'

ROJECTION OF VELOCITY VECTOR IN AXIAL PLANE
               AVERAGE VELOCITY

ROJECTION OF VELOCITY VECTOR IN VERTICAL PLANE
               AVERAGE VELOCITY

· DISTANCE AFT OF TOUCHDOWN POINT

· DISTANCE ABOVE TOUCHDOWN POINT

FIGURE 22

assumes different pitch attitudes. It should be remembered that
the evidence from high speed movies and strobotac observations
is very strong that dynamic motions of the carrier introduce
stronger variations in the velocity vector magnitudes than are
indicated with fixed "steady state" measurements. Thus the
aircraft in all probability will encounter velocity vector
variations of a larger magnitude than those indicated here.

For conditions of zero and -1.5° pitch angle, the
velocity vector component distribution about a 4° glide path to
a carrier in a fixed orientation is such than an aircraft would
experience an upward velocity on the port wing and a downward
velocity on the starboard wing. The forces resulting from this
velocity distribution increase in magnitude rather rapidly and
become quite severe as the plane approaches an area within 500
feet of touchdown. Added to these forces, which tend to cause
the plane to roll, are forces acting on the wings in an axial or
longitudinal direction. Here the port wing encounters a velocity
defect relative to the starboard wing, this defect also increasing
in intensity as touchdown is approached.

For conditions of +1.5° pitch angle of the carrier
deck, the velocity vectors tend to be downward on both wings, but
the strength of the downward component on the port wing is con-
siderably stronger than that on the starboard wing. These forces
would tend to roll the aircraft in the opposite direction from
that experienced with the deck angle at a zero or -1.5° pitch

angle. For this fixed carrier orientation, the velocity
variations again become significantly stronger as an area within
500 feet of touchdown is traversed. For this case of carrier
orientation, the velocity variations along the span of the wing
are also in evidence although they are somewhat milder than
those indicated with the deck at a zero degree or -1.5° pitch
angle.

Figure -23- shows velocity component variations about a
4° glide path when the wind is from dead ahead and the deck pitch
angle is zero. For this case there is little evidence of velocity
variations in the flow vector components until the aircraft is
within perhaps 300 feet of touchdown, and even then the forces
which an aircraft would encounter are of considerably smaller
magnitude than when the wind is 9° from port (or approximately
over the angled landing deck).

Figure -24- illustrates the flow conditions about the
glide path with the wind 13° from port and with a deck pitch
angle of zero. For this wind direction and carrier orientation,
the velocity vector components in the axial and vertical directions
are considerably stronger than those in evidence with the other
cases investigated. These variations in the flow velocities
associated with the wake are noticeable even 1300 feet aft of the
touchdown point.

From the investigations described above, which are
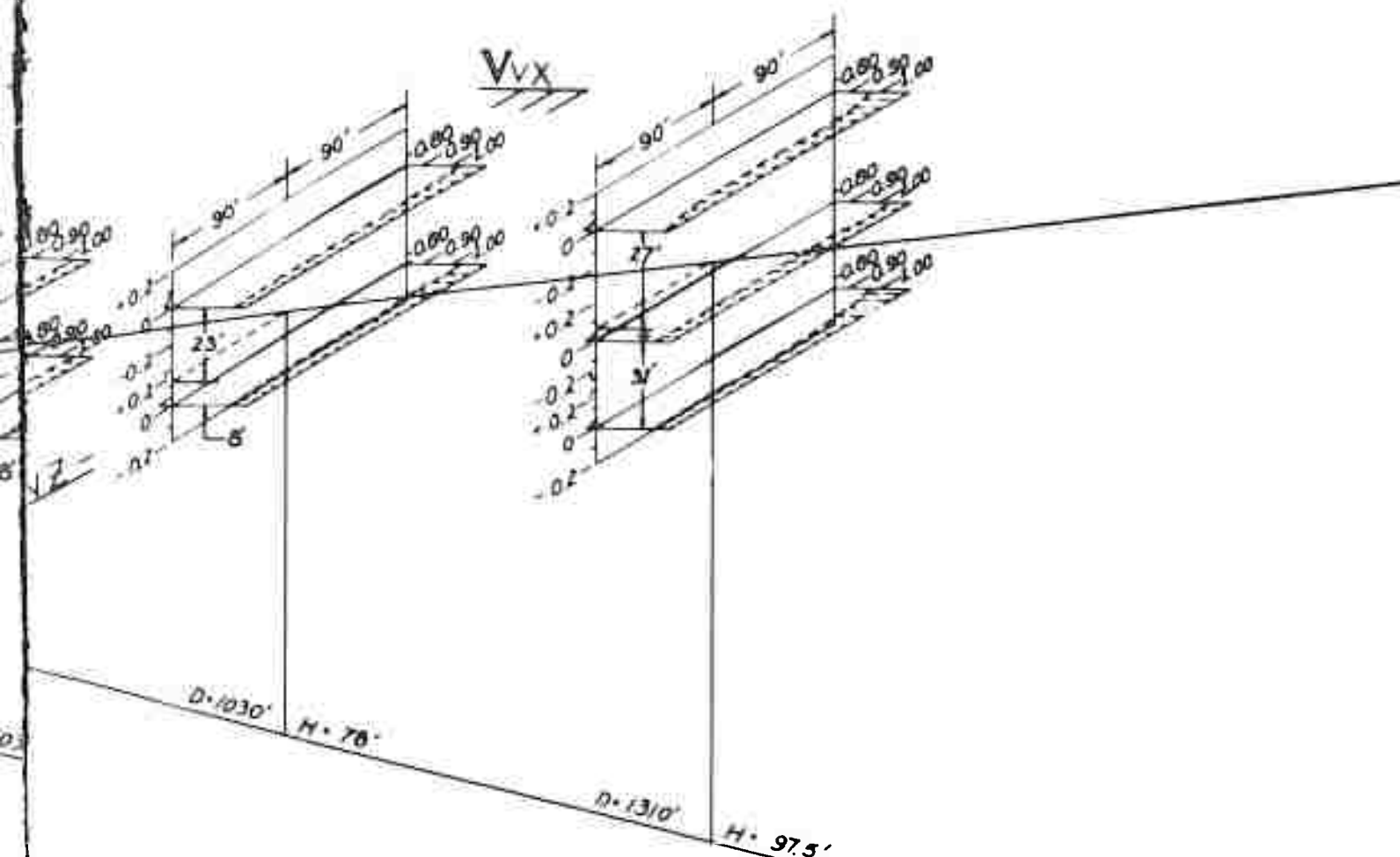artificial in the sense that the carrier maintains a fixed
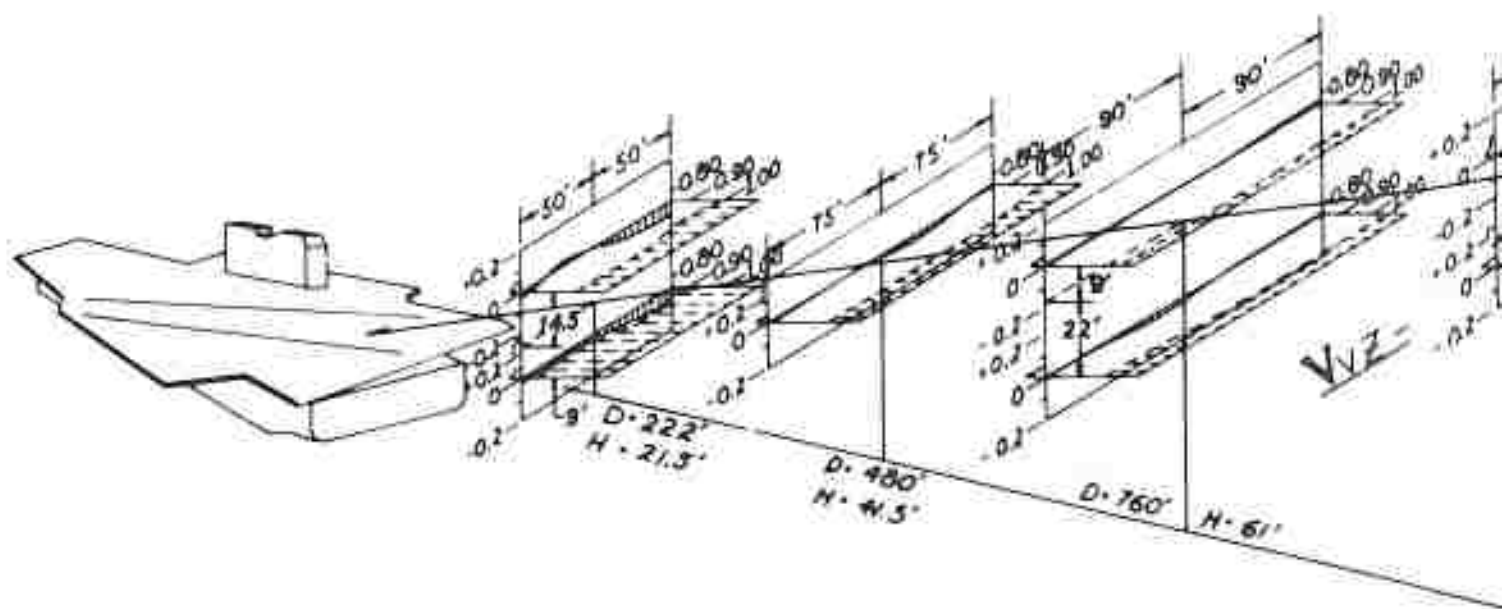
CONDITIONS

WIND 35 KTS; FROM DEAD AHEAD
SHIP PITCH ANGLE 0° ROLL ANGLE 0°
GLIDE ANGLE 4°
TOUCHDOWN 150' FWD OF DECK AFT EDGE
WING 6' ABOVE DECK

$V_{VX} = \underline{PROJECT}$

$V_{VZ} = \underline{PROJECT}$

D = DIST

H = DISTA

PROJECTION OF VELOCITY VECTOR IN AXIAL PLANE
AVERAGE VELOCITY
PROJECTION OF VELOCITY VECTOR IN VERTICAL PLANE
AVERAGE VELOCITY
D· DISTANCE AFT OF TOUCHDOWN POINT
H· DISTANCE ABOVE TOUCHDOWN POINT

FIGURE 23.

CONDITIONS

WIND 35 KTS; 13° PORT OF SHIP ⊄
SHIP PITCH ANGLE 0° ROLL ANGLE 0°
GLIDE ANGLE 4°
TOUCHDOWN 150' FWD OF DECK AFT EDGE
WING 6' ABOVE DECK

$V_{VX} = \underline{PROJECTION}$

$V_{VZ} = \underline{PROJECTION}$

D· DISTANCE

H· DISTANCE
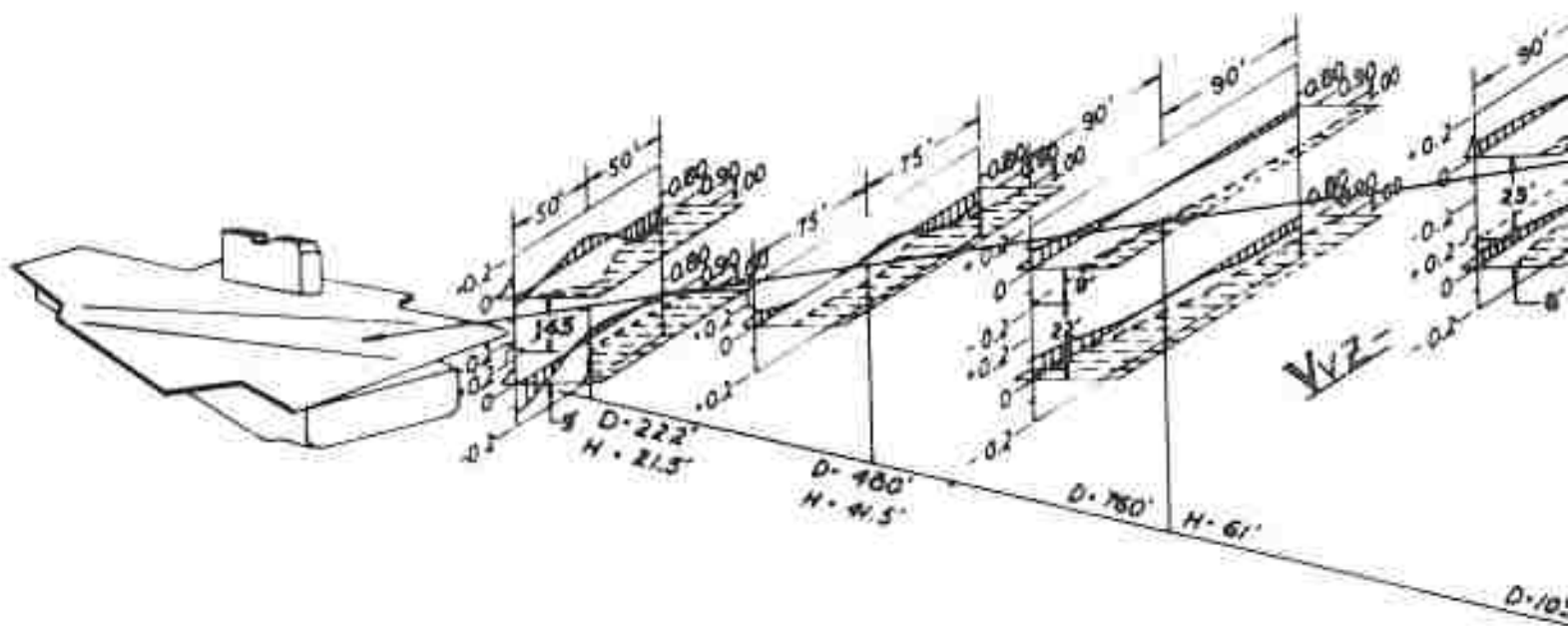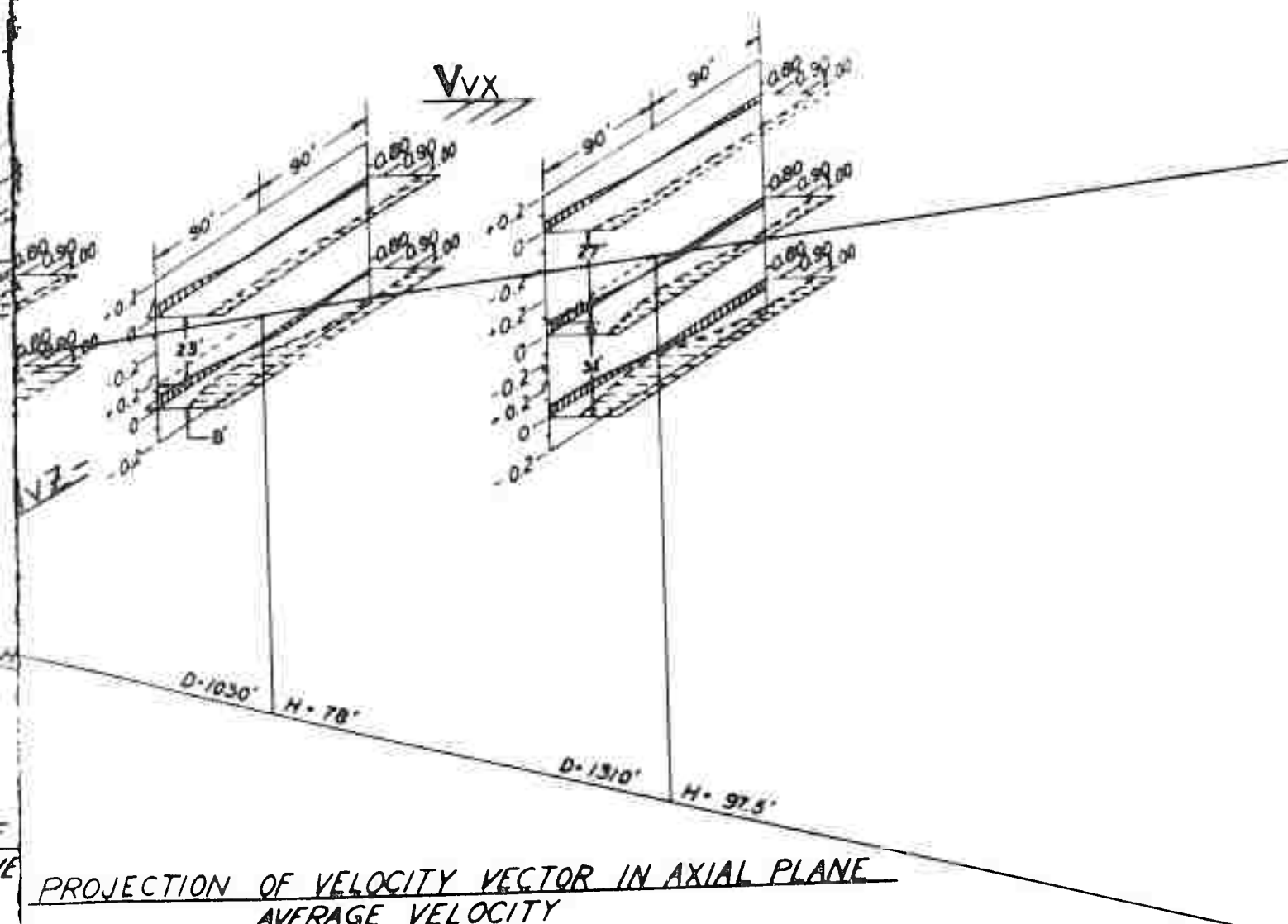
V_{vx}

V_Z

D·1030' H·78'

D·1310' H·97.5'

PROJECTION OF VELOCITY VECTOR IN AXIAL PLANE
AVERAGE VELOCITY

PROJECTION OF VELOCITY VECTOR IN VERTICAL PLANE
AVERAGE VELOCITY

D· DISTANCE AFT OF TOUCHDOWN POINT

H· DISTANCE ABOVE TOUCHDOWN POINT

FIGURE 24

orientation in space, it is possible to conclude the following:

1. The flow disturbances occurring primarily from the deck and those occurring from the island tend to merge into a single major disturbance in the general region of some 500 feet aft of the carrier. (This conclusion is reinforced by the steady state and dynamic cavitation observations and also by material presented in [3]).

2. There is a strong variation in the flow velocity component values with a change in height above the touchdown point. (This conclusion is also reinforced from flow observations using the cavitation technique and the total dynamic head variations as presented in [3]).

3. As an aircraft approaches the touchdown point, the disturbances encountered become more severe. This holds for all conditions investigated. With the wind from dead ahead, the flow disturbances appear to be minimized.

4. The flow disturbance velocity variations tend to increase as the wind goes from dead ahead (along the ship center-line) to port.

5. With the wind coming from port, it can be generally stated that a drop below and/or to the port of the glide path will place an aircraft into an area of more severe flow disturbances than would an approach on the 4° glide path.

6. The strong axial and vertical velocity disturbance components generally showed a large increase in the degree of variation

in an area within 500 or so feet of the touchdown point.
This would indicate the need for considerable control
activity on the part of the pilot. This conclusion coincides
with the actual happenings as presented in [1], where the
results of an instrumented aircraft show a major increase in
control surface activity during the last 5 seconds before
touchdown.

It has been pointed out several times in this report
that there is little doubt that dynamic conditions produce flow
conditions considerably different from those displayed by a model
in a fixed orientation. The flow observations using the cavitation
technique permitted qualitative interpretation of the differences.
These steady state measurements reinforce the basic conclusion
and permit at least an indication of the actual variation of
flow disturbances with carrier motion. In discussing Figures -20-,
-21-, and -22-, which apply for conditions of the wind approximately
over the angled landing deck and carrier pitch angles of zero and
$\pm 1.5°$, it was pointed out that for the zero and -1.5° deck angles
the velocity vectors' vertical components tended to roll the air-
craft in a clockwise direction, while the flow conditions with a
deck angle of +1.5° tended to roll the aircraft in a counter-
clockwise direction. Even without considering the effects of the
motion of the aircraft itself as it approaches the deck for a
landing, it can be readily concluded from these flow measurements
that with a carrier undergoing positive and negative deck angles,

the flow disturbance conditions in the glide path are going to contain components associated with both positive and negative deck angles. Therefore, the aircraft would encounter flow regimes tending to roll it first in one direction and then the other. The above illustration is oversimplified, but it does present irrefutable evidence that changes in deck orientation will change the downstream flow pattern and that these flow patterns will produce conditions in direct opposition to one another.

CONCLUSIONS

These investigations have permitted obtaining a considerably enlightened viewpoint of the disturbances encountered during landing operations by carrier-based aircraft. These studies encompassed what is believed to be the first investigations of flow disturbances created by dynamic carrier motions, augmented by a fairly extensive study of the flow magnitude and direction of the downstream flow field with fixed carrier orientation. The individual sections discussing both phases of the investigation presented in considerable detail conclusions which can be drawn from these studies. Therefore, only the more pertinent are included here.

1. The use of the cavitation technique and high speed photography permits three-dimensional observation and qualitative analysis

of the downstream dynamic flow field and the portions of
the carrier responsible for such disturbances.

2. The dynamic disturbed flow field is markedly different from
the flow field created with the carrier models in a fixed
orientation, but studies of the steady state conditions do
permit some estimate of the dynamic disturbance magnitudes.

3. With carrier motions the flow disturbances are periodic in
nature. This periodicity is directly associated with carrier
pitch and heave motions - one disturbance per cycle.

4. The two major causes of flow disturbances are the deck and
the island, with the disturbance from the island being much
weaker and essentially merging with the deck disturbances
generally within 500 feet aft of the carrier. The dynamic
disturbances then tend to form single discretely spaced flow
masses downstream of the carrier. The flow disturbances
rotate in a clockwise direction looking in the direction of
ship travel.

5. The disturbed wake is minimized when the flow is from dead
ahead. The disturbances increase as the wind shifts to port.

6. For the conditions tested (and ignoring periodicity), aircraft
will always encounter some disturbance. The strength of the
disturbance becomes of significant magnitude usually when
the aircraft is within 500 feet from touchdown, but under
certain conditions of carrier-wind orientation the disturbances
will extend aft to 1300 feet. For an example of the magnitude

of the disturbances, the difference in the vertical velocity component acting on the port and starboard wing can approach a value equal to one quarter of the oncoming flow velocity about 200 feet from touchdown, with this magnitude increasing as touchdown is approached!

7. For the conditions tested, it appears as if an approach below and/or to the port of the glide path will place the aircraft in a position encountering flow disturbances of greater magnitude than one following the proper glide path. In general it appears as if a slightly steeper glide angle would be advantageous in that disturbances some distance downstream would then be below the glide path.

ACKNOWLEDGEMENTS

REFERENCES

1. Oldmixon, Lt. W. J.: "The Acquisition, Reduction, and Analysis of Turbulence Data Associated with PA Configuration Approaches to Carrier Landings," Department of Aeronautical Engineering, Princeton University, Report No. 653, July 1963.

2. Lehman, August F.: "Some Cavitation Observation Techniques for Water Tunnels and a Description of the Oceanics Tunnel," in Symposium on Cavitation Research Facilities and Techniques, May 18-20, 1964, edited by J. William Holl and Glenn M. Wood, The American Society of Mechanical Engineers, 1964.

3. White, Herbert E.: "Wind-Tunnel Tests to Determine the Air-Flow Characteristics in the Wakes of Three Aircraft Carrier Models. Part II: Tests of the Attack Carrier CVA 62," Aerodynamics Laboratory, David Taylor Model Basin, Report C-1073, Aero Report 955, June 1959. (Classification Changed to Unclassified 6 March 1964).

4. Durand, T. S.: "Synopsis of the Carrier Approach and Landing Problem," Systems Technology, Inc. Working Paper No. 137-3, presented at Office of Naval Research Meeting, Washington D. C., March 6, 1964.

APPENDIX

GRAPHS SHOWING THE FLOW DISTRIBUTION
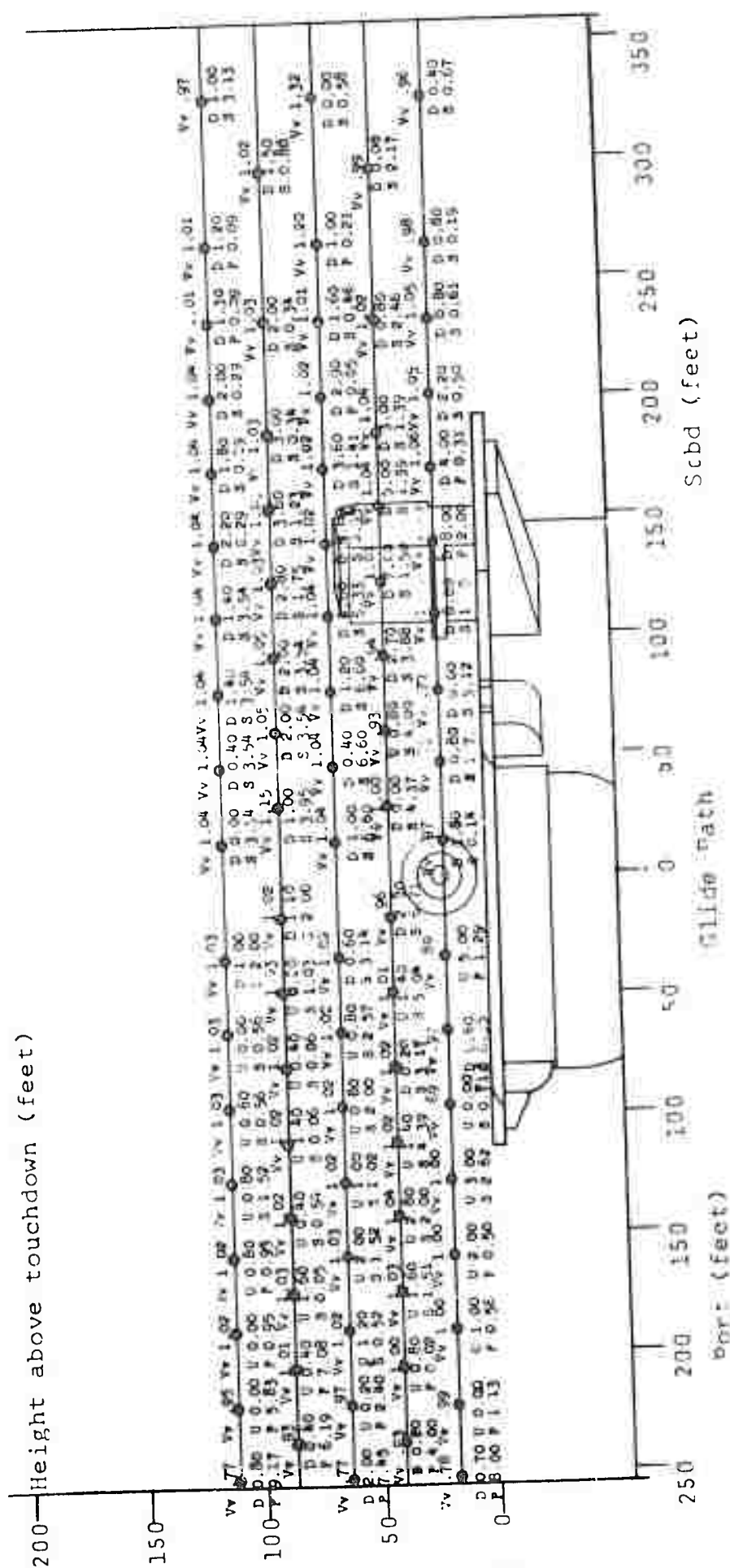
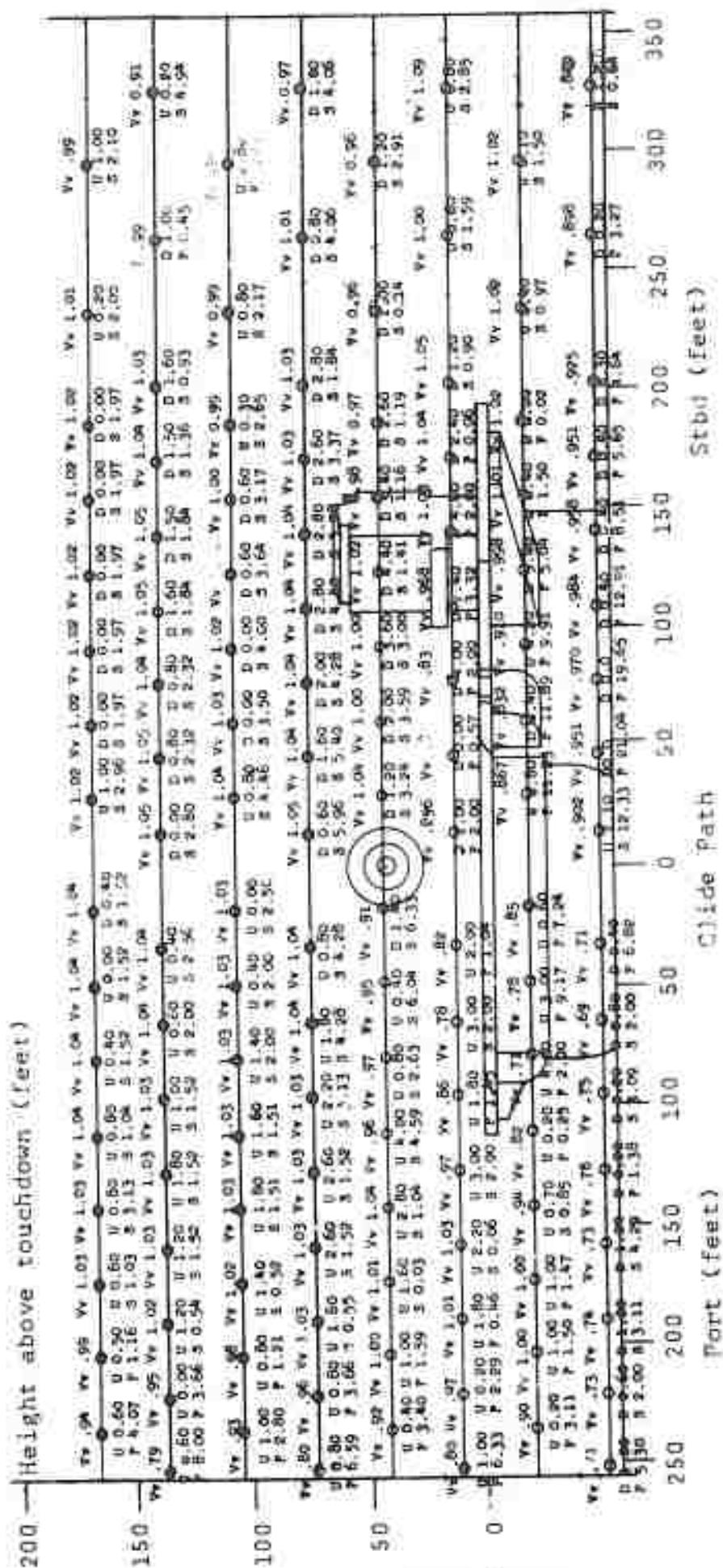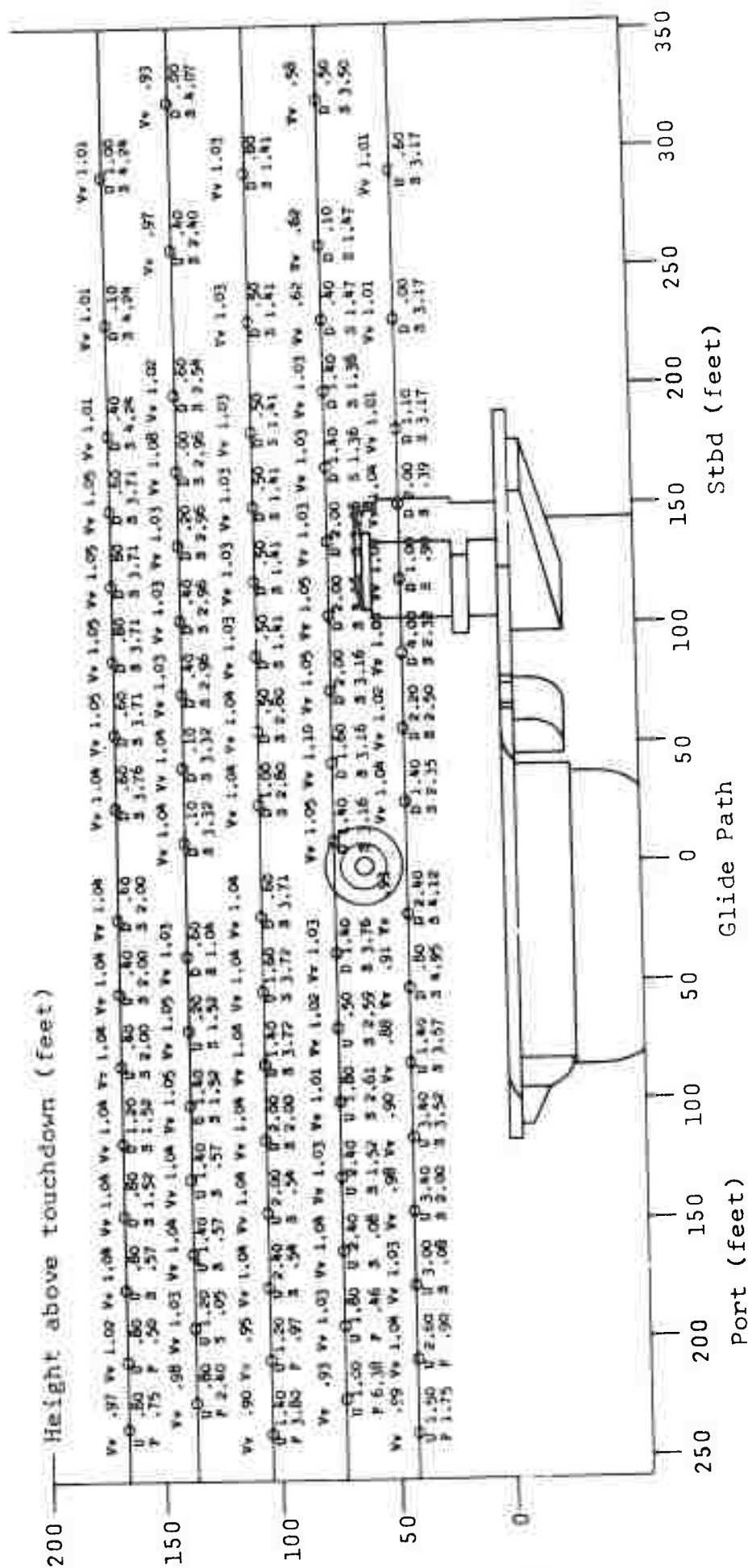AT VARIOUS POSITIONS DOWNSTREAM OF THE MODEL CARRIER

Conditions:
Wind 35 knots; 9° port of ship center-line;
Carrier pitch angle 0°; Roll 0°; Measurement
222 feet aft of touchdown
Target marks position of 4° glide path

Vv = Local velocity vector divided by
     average velocity in section
D = Degrees flow is down from horizontal
U = Degrees flow is up from horizontal
P. = Degrees flow is from port of
     average wind direction
S = Degrees flow is from starboard of
     average wind direction

Figure A-1

A-2

Height above touchdown (Feet)

Port (Feet) Glide Path Stbd (Feet)

Conditions:
Wind 35 knots; 9° port of ship center-line;
Carrier pitch angle 0°; Roll 0°; Measurement
480 feet aft of touchdown
Target marks position of 4° glide path

Vv = Local velocity vector divided by
     average velocity in section
D = Degrees flow is down from horizontal
U = Degrees flow is up from horizontal
P = Degrees flow is from port of
    average wind direction
S = Degrees flow is from starboard of
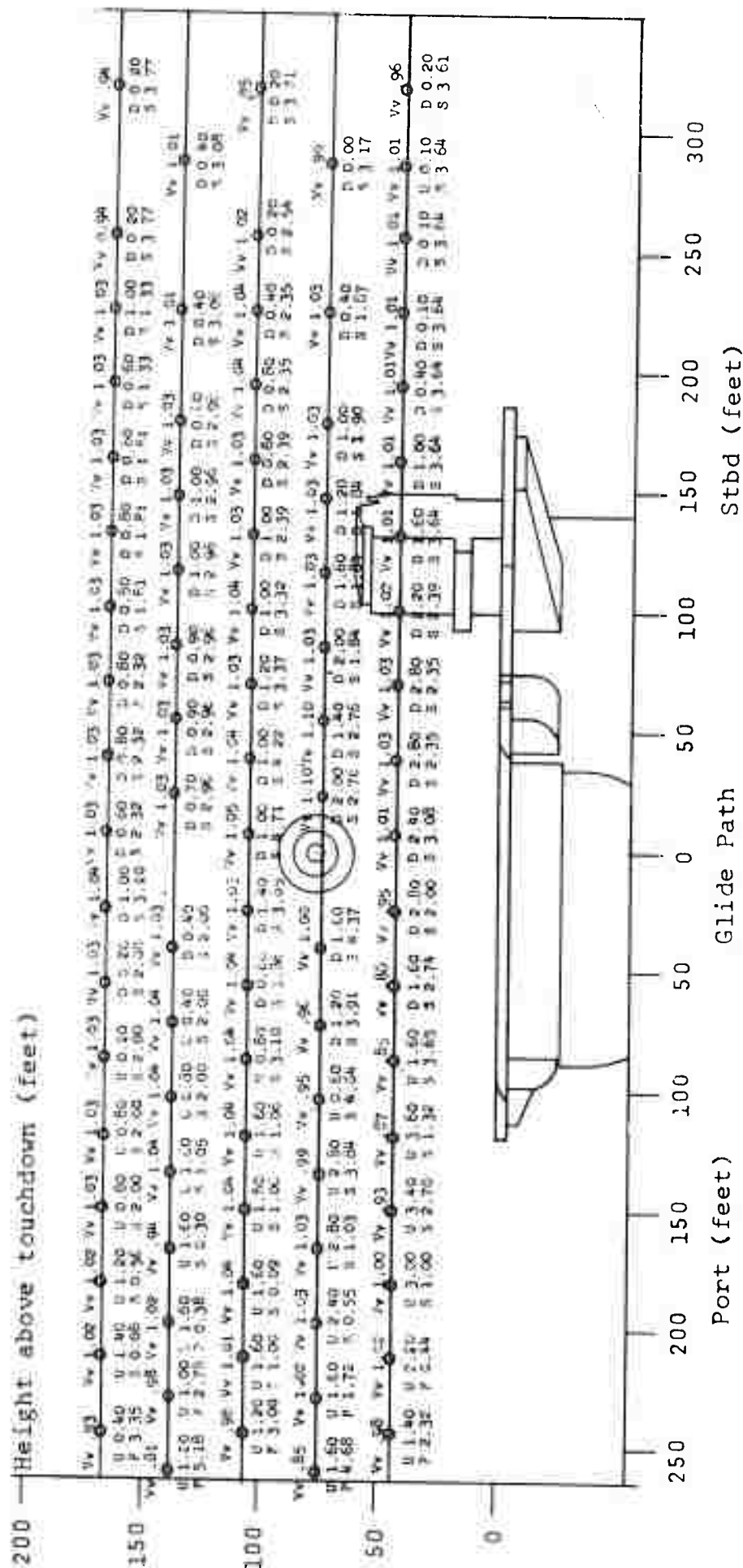   average wind direction

Figure A-2

OCEANICS INC.

Conditions:
Wind 35 knots; 9° port of ship center-line;
Carrier pitch angle 0°; Roll 0°; Measurement
760 feet aft of touchdown
Target marks position of 4° glide path

Vv = Local velocity vector divided by
     average velocity in section
D = Degrees flow is down from horizontal
U = Degrees flow is up from horizontal
P = Degrees flow is from port of
     average wind direction
S = Degrees flow is from starboard of
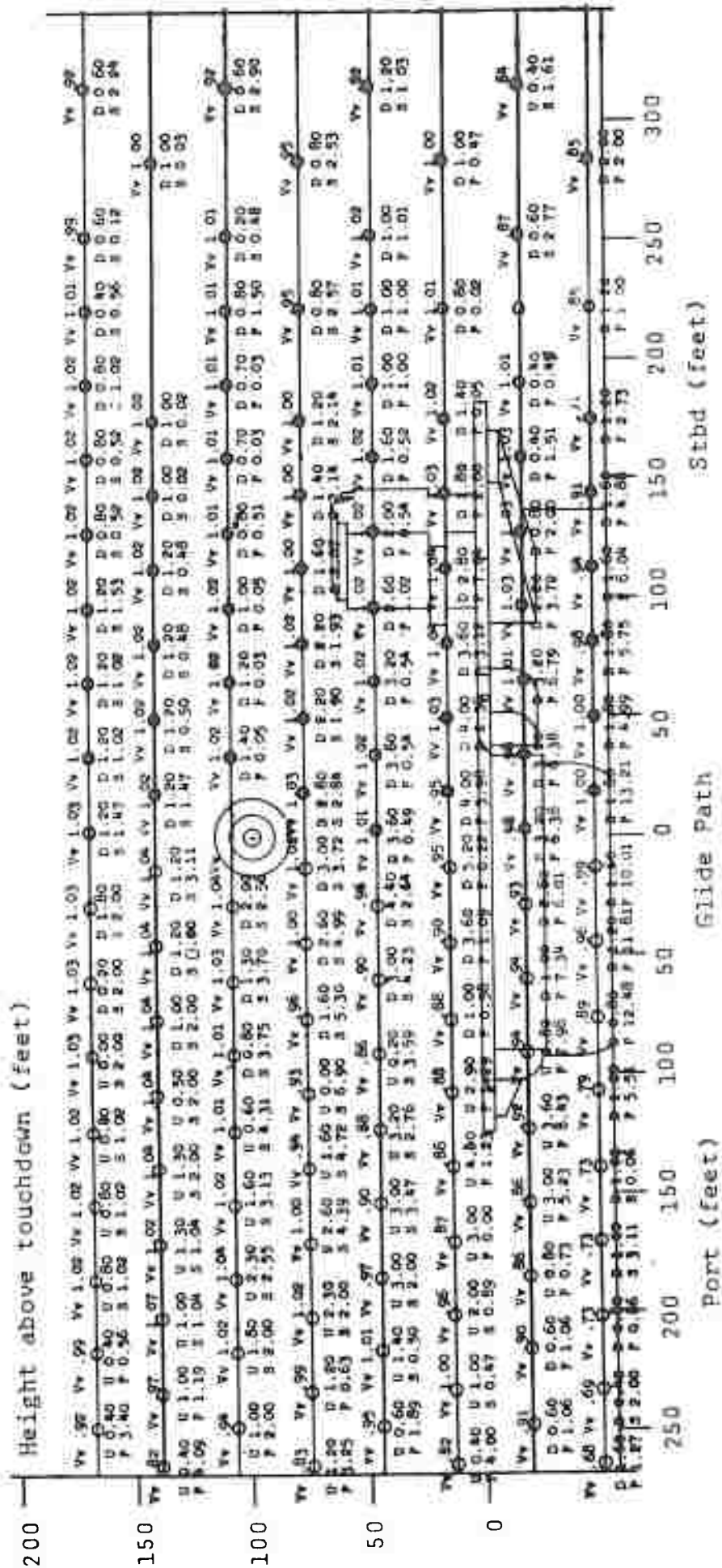   average wind direction

Figure A-3

Height above touchdown (feet)

200

150

100

50

0

250   200   150   100   50   0   50   100   150

Port (feet)   Glide Path   Stbd (feet)

250   200   150   100   50   0   50   100   150   200   250   300

~OCEANICS~ INC.

Conditions:
Wind 35 knots; 9° port of ship center-line;
Carrier pitch angle 0°; Roll 0°; Measurement
1030 feet aft of touchdown
Target marks position of 4° glide path

Vv = Local velocity vector divided by
     average velocity in section
D = Degrees flow is down from horizontal
U = Degrees flow is up from horizontal
P = Degrees flow is from port of
     average wind direction
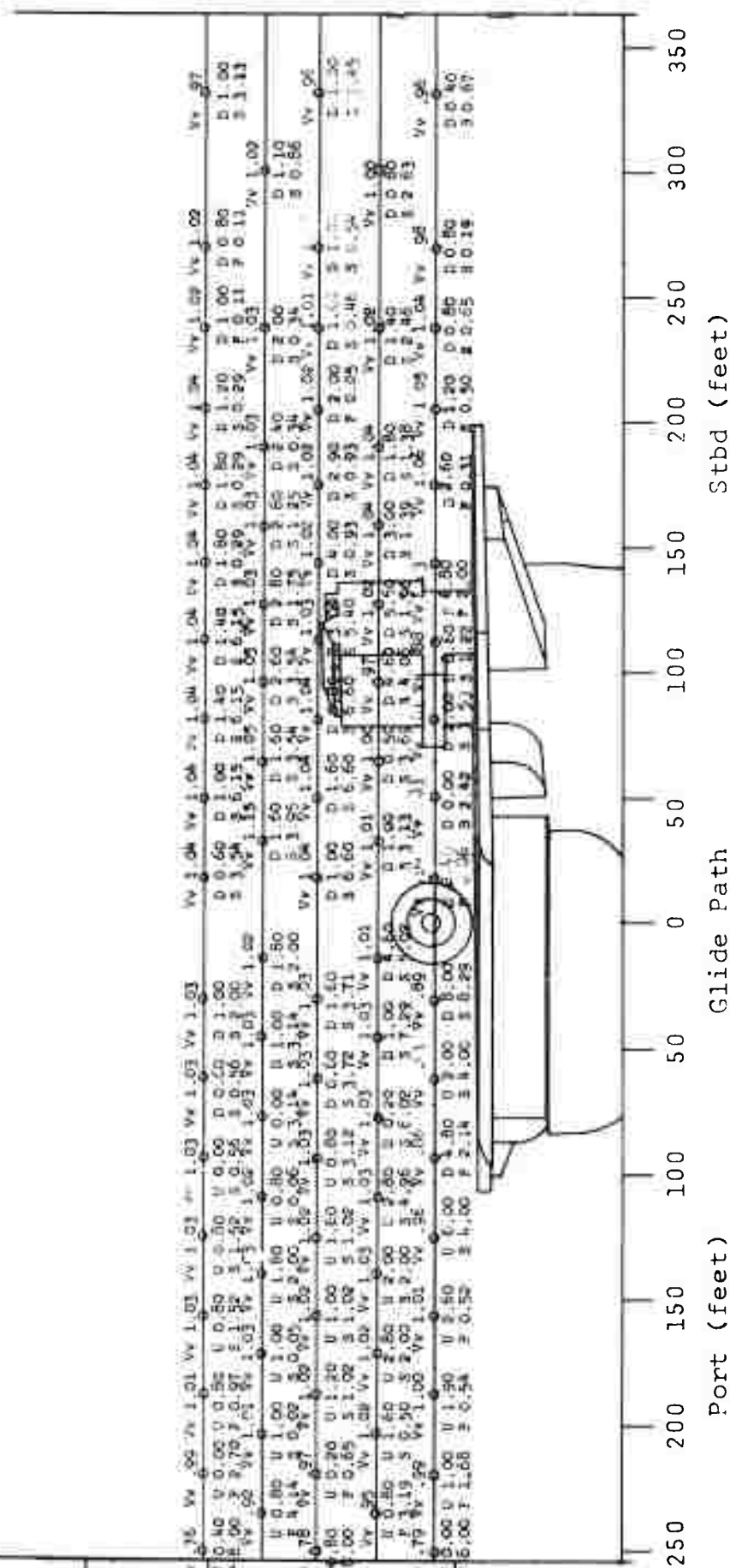S = Degrees flow is from starboard of
     average wind direction

Figure A-4

Height above touchdown (Feet)

Port (Feet)   Glide Path   Stbd (Feet)

OCEANICS INC.

Vv = Local velocity vector divided by
     average velocity in section
D = Degrees flow is down from horizontal
U = Degrees flow is up from horizontal
P = Degrees flow is from port of
     average wind direction
S = Degrees flow is from starboard of
     average wind direction

Conditions:

Wind 35 knots; 9° port of ship center-line;
Carrier pitch angle 0°; Roll 0°; Measurement
1310 feet aft of touchdown
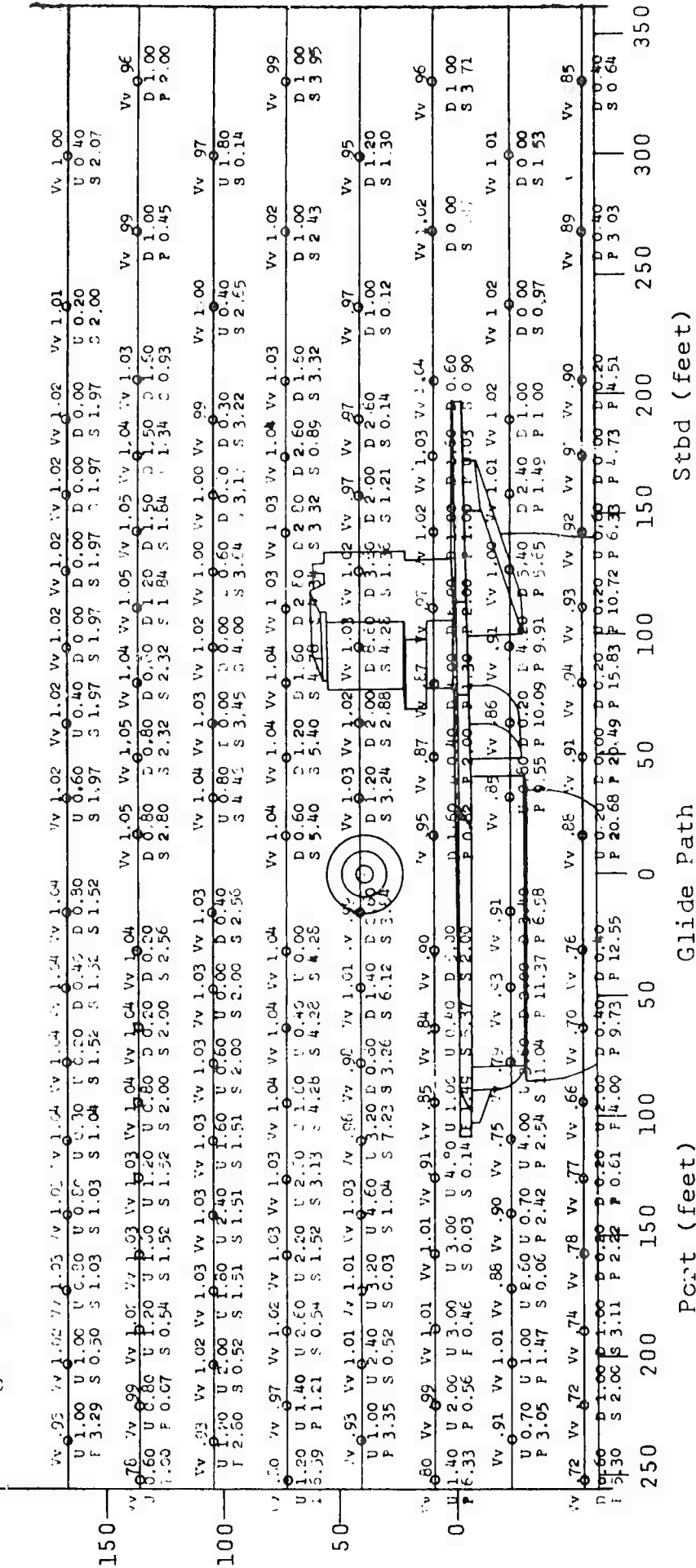Target marks position of 4° glide path

Figure A-5

Figure A-6

Conditions:
Wind 35 knots; 9° port of ship center-line;
Carrier pitch angle +1.5°; Roll 0°; Measurement
222 feet aft of touchdown
Target marks position of 4° glide path

Vv = Local velocity vector divided by
     average velocity in section
D = Degrees flow is down from horizontal
U = Degrees flow is up from horizontal
P = Degrees flow is from port of
    average wind direction
S = Degrees flow is from starboard of
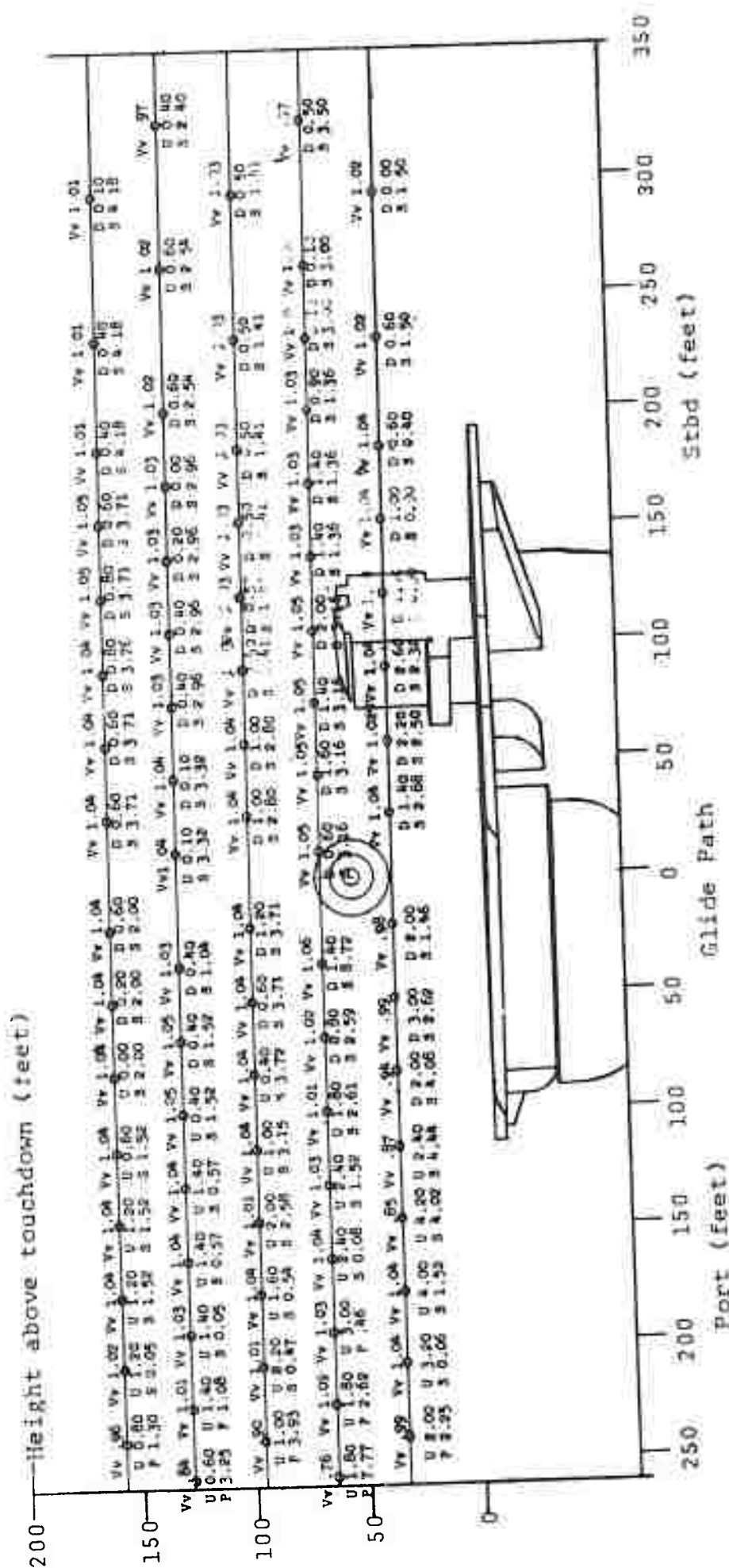   average wind direction

Figure A-7

Conditions:
Wind 35 knots; 9° port of ship center-line;
Carrier pitch angle +1.5°; Roll 0°; Measurement
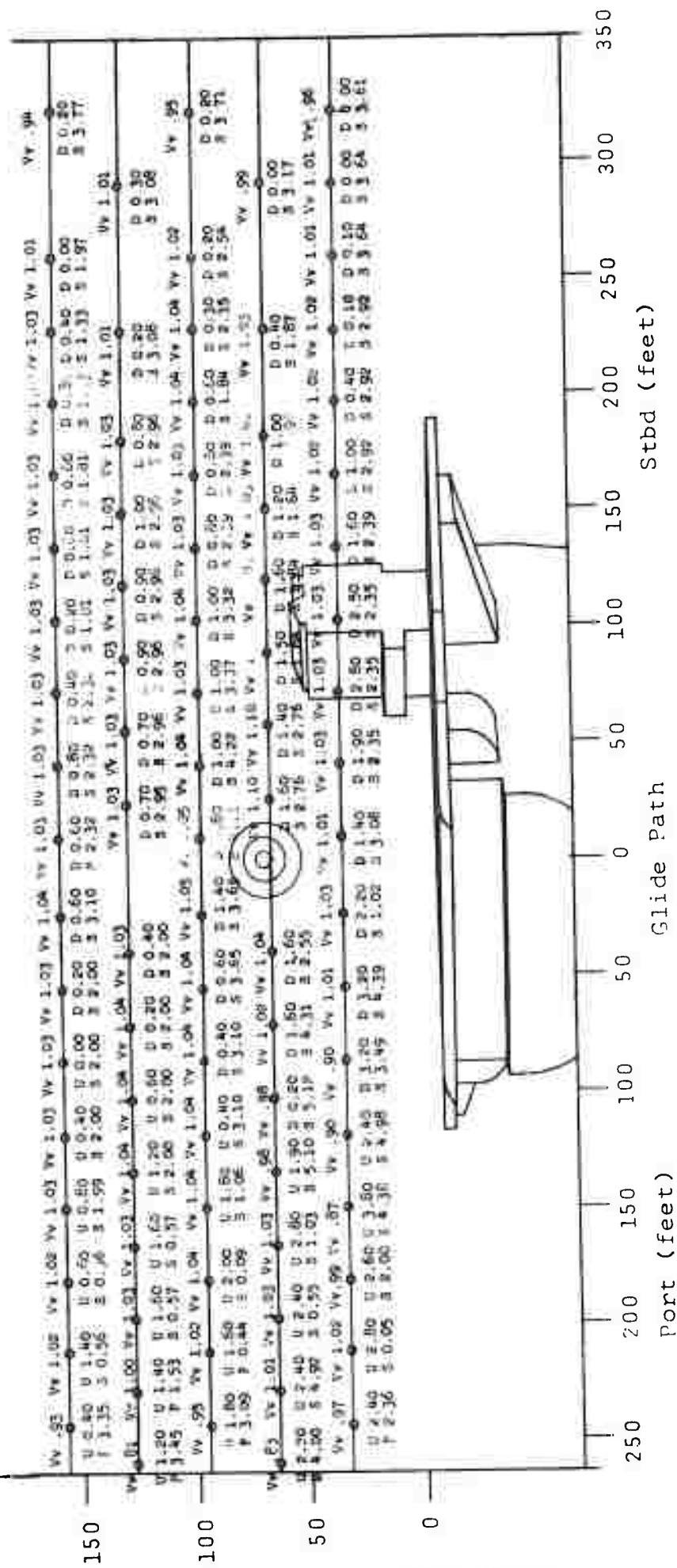480 feet aft of touchdown
Target marks position of 4° glide path

Vv = Local velocity vector divided by
     average velocity in section
D = Degrees flow is down from horizontal
U = Degrees flow is up from horizontal
P = Degrees flow is from port of
     average wind direction
S = Degrees flow is from starboard of
     average wind direction

Figure A-8

Conditions:
Wind 35 knots; 9° port of ship center-line;
Carrier pitch angle +1.5°; Roll 0°; Measurement
760 feet aft of touchdown
Target marks position of 4° glide path

Vv = Local velocity vector divided by
       average velocity in section
D = Degrees flow is down from horizontal
U = Degrees flow is up from horizontal
P = Degrees flow is from port of
       average wind direction
S = Degrees flow is from starboard of
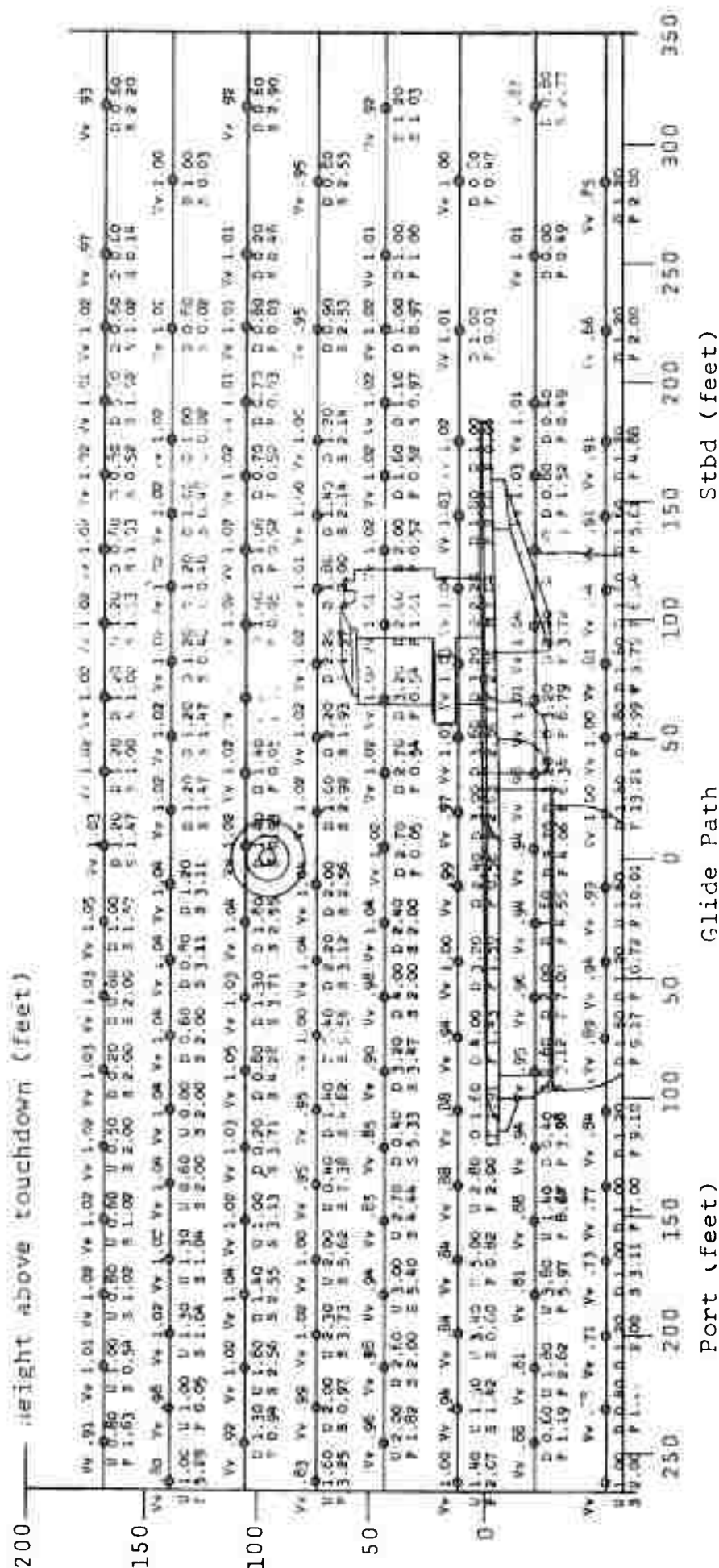   average wind direction

OCEANICS INC.

Figure A-9

Conditions:
Wind 35 knots; 9° port of ship center-line;
Carrier pitch angle +1.5°; Roll 0°; Measurement
1030 feet aft of touchdown
Target marks position of 4° glide path

Vv = Local velocity vector divided by
average velocity in section
D = Degrees flow is down from horizontal
U = Degrees flow is up from horizontal
P = Degrees flow is from port of
average wind direction
S = Degrees flow is from starboard of
average wind direction

OCEANICS INC.

A-10

Height above touchdown (feet)

Port (feet) Glide Path Stbd (feet)

Conditions:
Wind 35 knots; 9° port of ship center-line;
Carrier pitch angle +1.5°; Roll 0°; Measurement
1310 feet aft of touchdown
Target marks position of 4° glide path

Vv = Local velocity vector divided by
     average velocity in section
D = Degrees flow is down from horizontal
U = Degrees flow is up from horizontal
P = Degrees flow is from port of
    average wind direction
S = Degrees flow is from starboard of
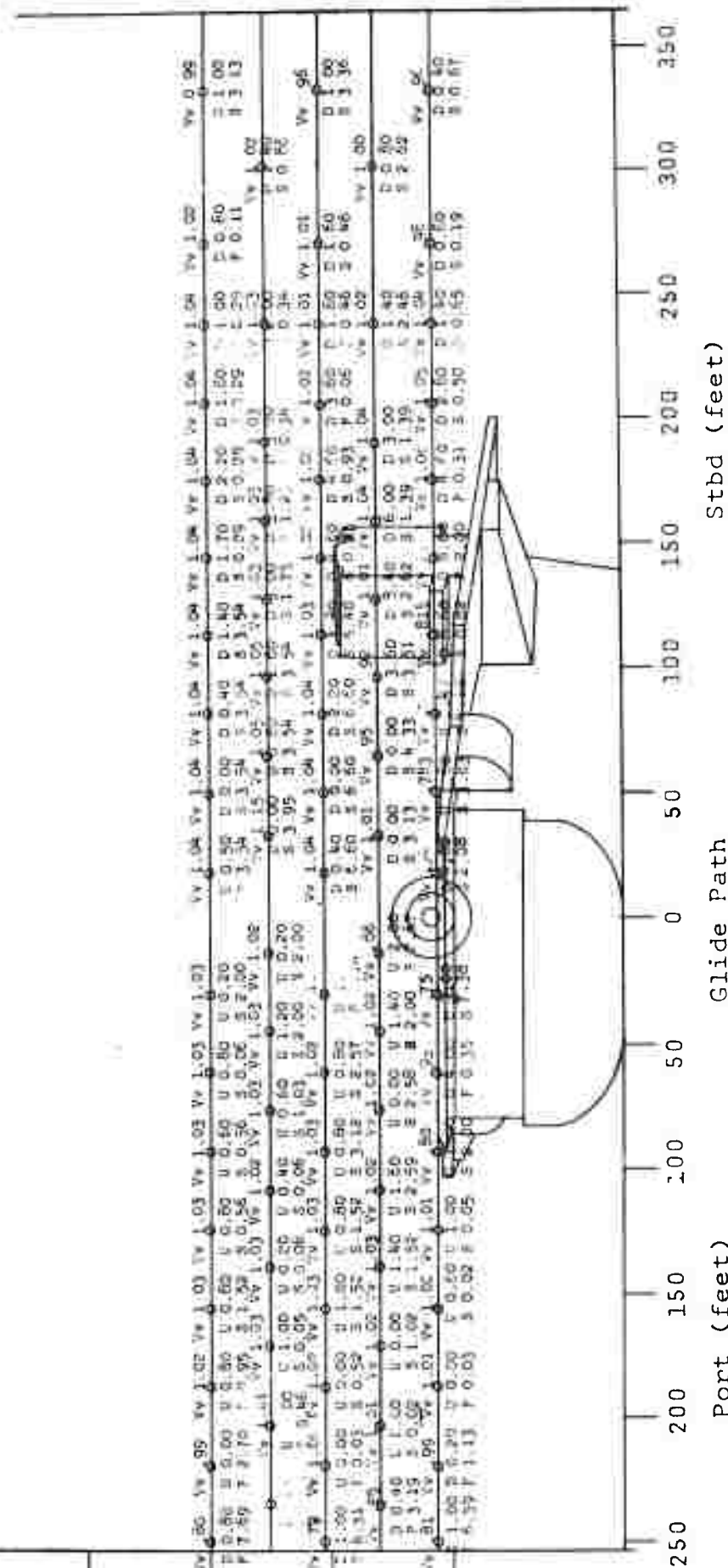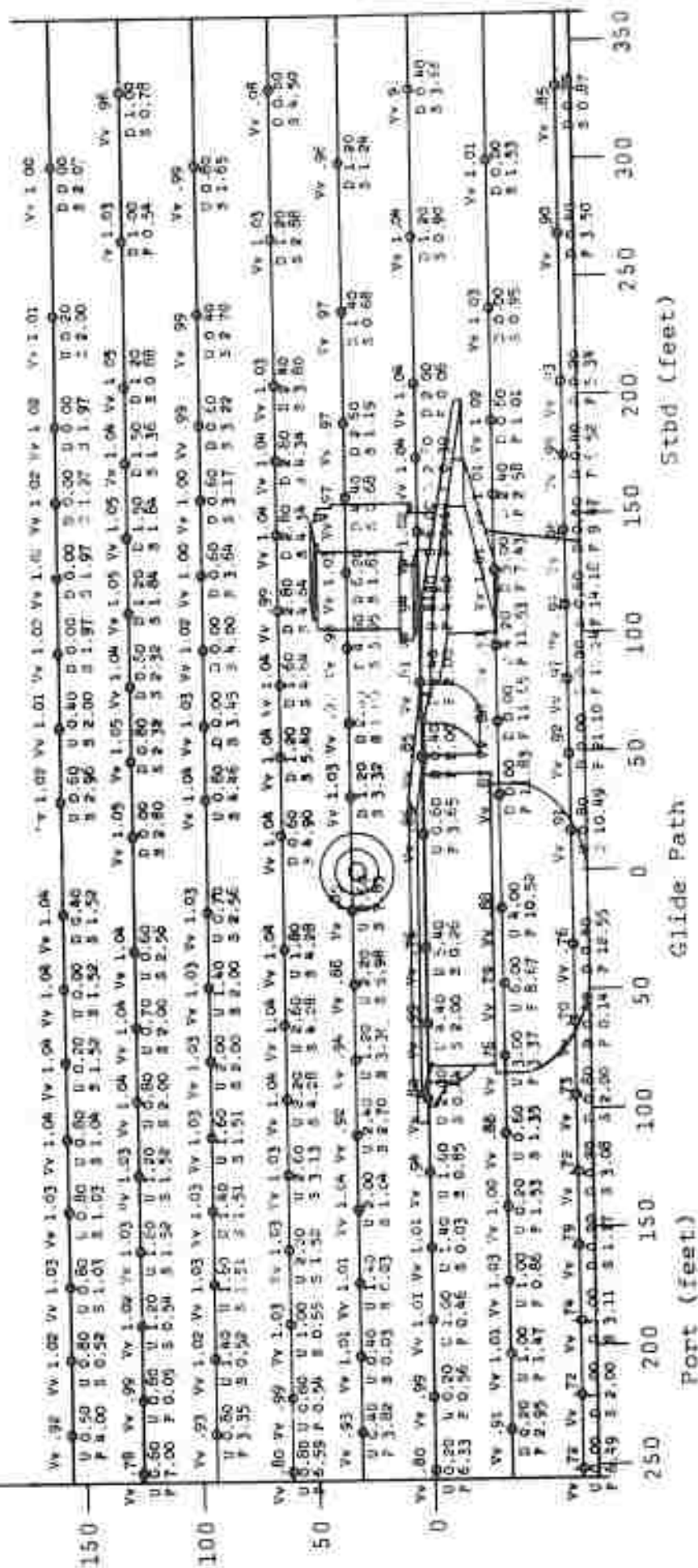   average wind direction

Figure A-10

OCEANICS INC.

Figure A-11

Conditions:
Wind 35 knots; 9° port of ship center-line;
Carrier pitch angle -1.5°; Roll 0°; Measurement
222 feet aft of touchdown
Target marks position of 4° glide path

Vv = Local velocity vector divided by
     average velocity in section
D = Degrees flow is down from horizontal
U = Degrees flow is up from horizontal
P = Degrees flow is from port of
     average wind direction
S = Degrees flow is from starboard of
     average wind direction

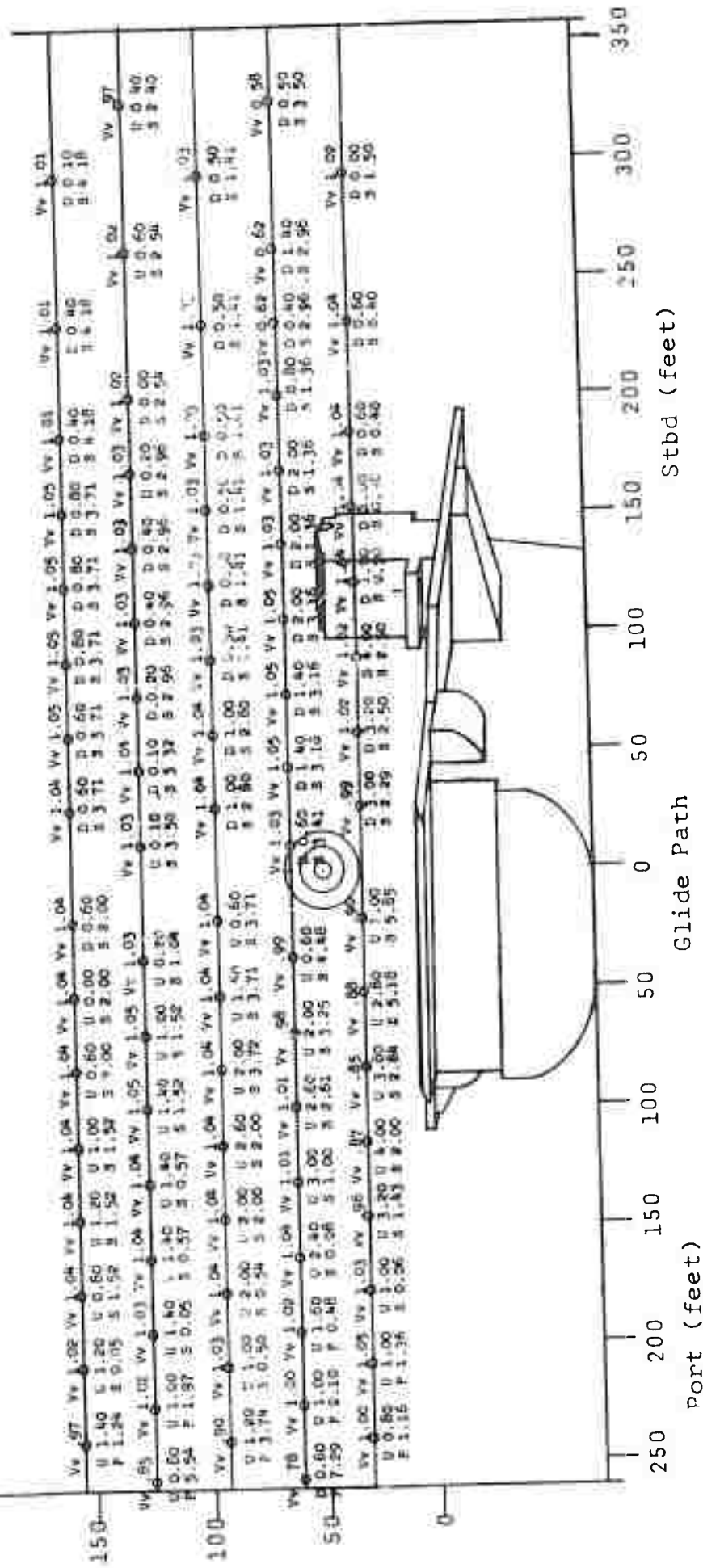Port (feet)   Glide Path   Stbd (feet)

Conditions:
Wind 35 knots; 9° port of ship center-line;
Carrier pitch angle -1.5°; Roll 0°; Measurement
480 feet aft of touchdown
Target marks position of 4° glide path

Vv = Local velocity vector divided by
     average velocity in section
D = Degrees flow is down from horizontal
U = Degrees flow is up from horizontal
P = Degrees flow is from port of
    average wind direction
S = Degrees flow is from starboard of
    average wind direction
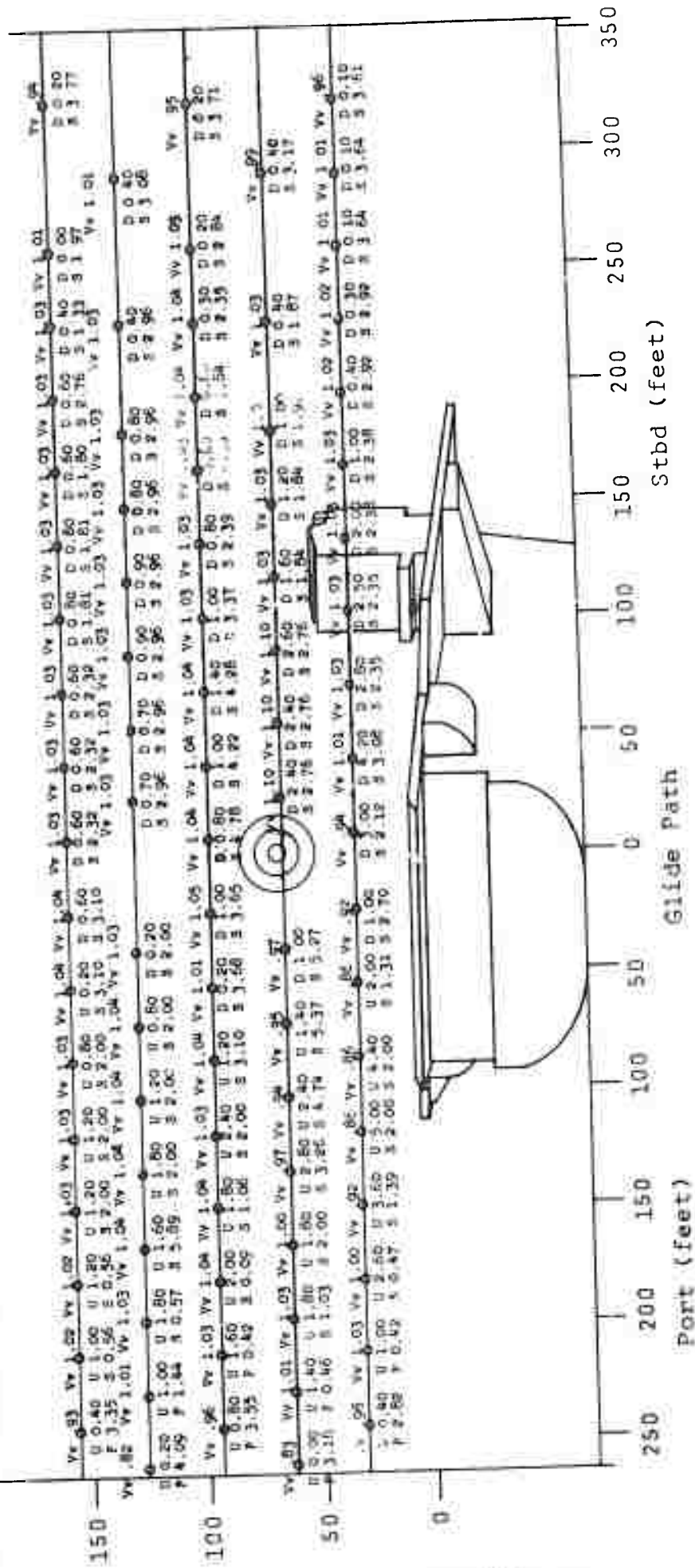
Figure A-12

OCEANICS inc.

Figure A-13

Conditions:
Wind 35 knots; 9° port of ship center-line;
Carrier pitch angle -1.5°; Roll 0°; Measurement
760 feet aft of touchdown
Target marks position of 4° glide path

Vv = Local velocity vector divided by
     average velocity in section
D = Degrees flow is down from horizontal
U = Degrees flow is up from horizontal
P = Degrees flow is from port of
     average wind direction
S = Degrees flow is from starboard of
     average wind direction

Height above touchdown (feet)

Port (feet)   Glide Path   Stbd (feet)

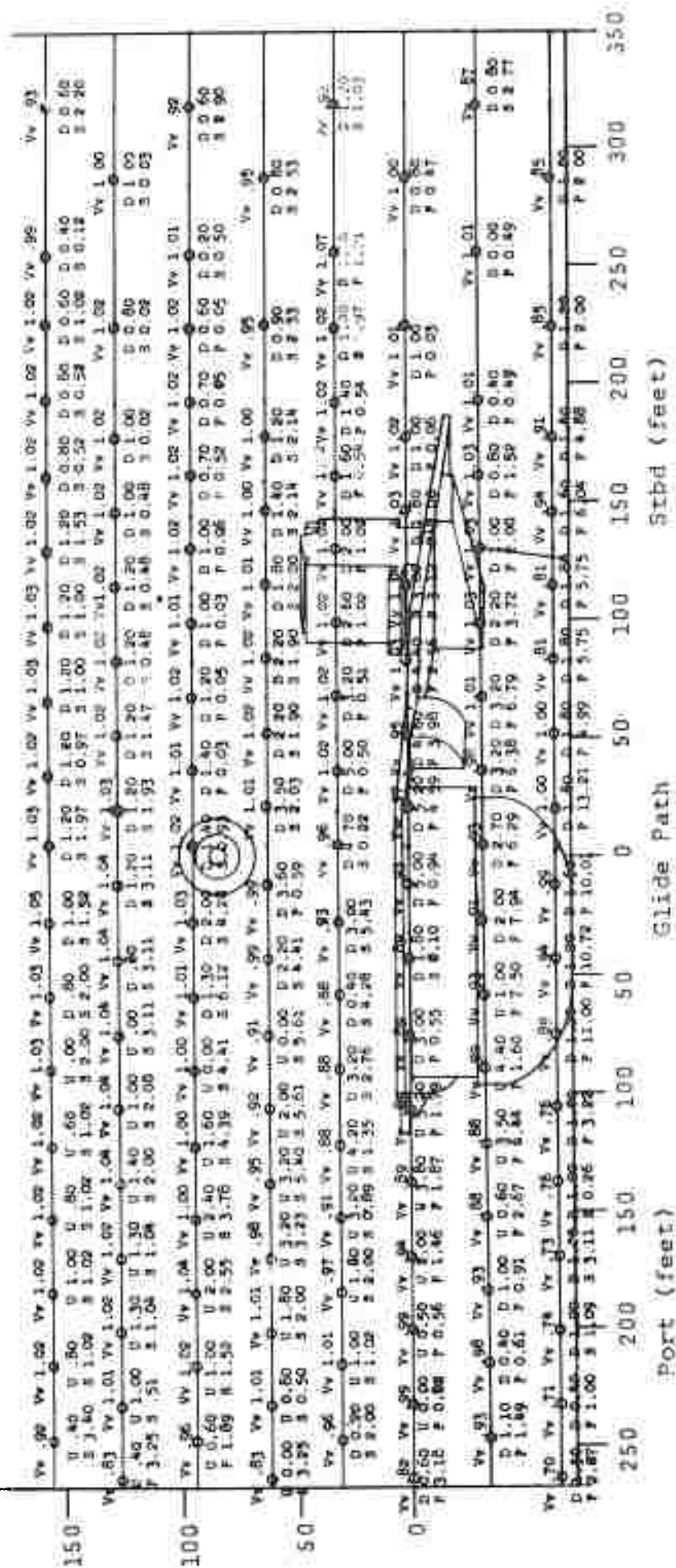OCEANICS INC.

Figure A-14

A-14

Conditions:
   Wind 35 knots; 9° port of ship center-line;
   Carrier pitch angle -1.5°; Roll 0°; Measurement
   1030 feet aft of touchdown
   Target marks position of 4° glide path

Vv = Local velocity vector divided by
     average velocity in section
D = Degrees flow is down from horizontal
U = Degrees flow is up from horizontal
P = Degrees flow is from port of
     average wind direction
S = Degrees flow is from starboard of
     average wind direction

Height above touchdown (feet)

Stbd (feet)

Port (feet)

Glide Path

Height above touchdown (feet)

Stbd (feet)

Glide Path

Port (feet)

Vv = Local velocity vector divided by
    average velocity in section
D = Degrees flow is down from horizontal
U = Degrees flow is up from horizontal
P = Degrees flow is from port of
    average wind direction
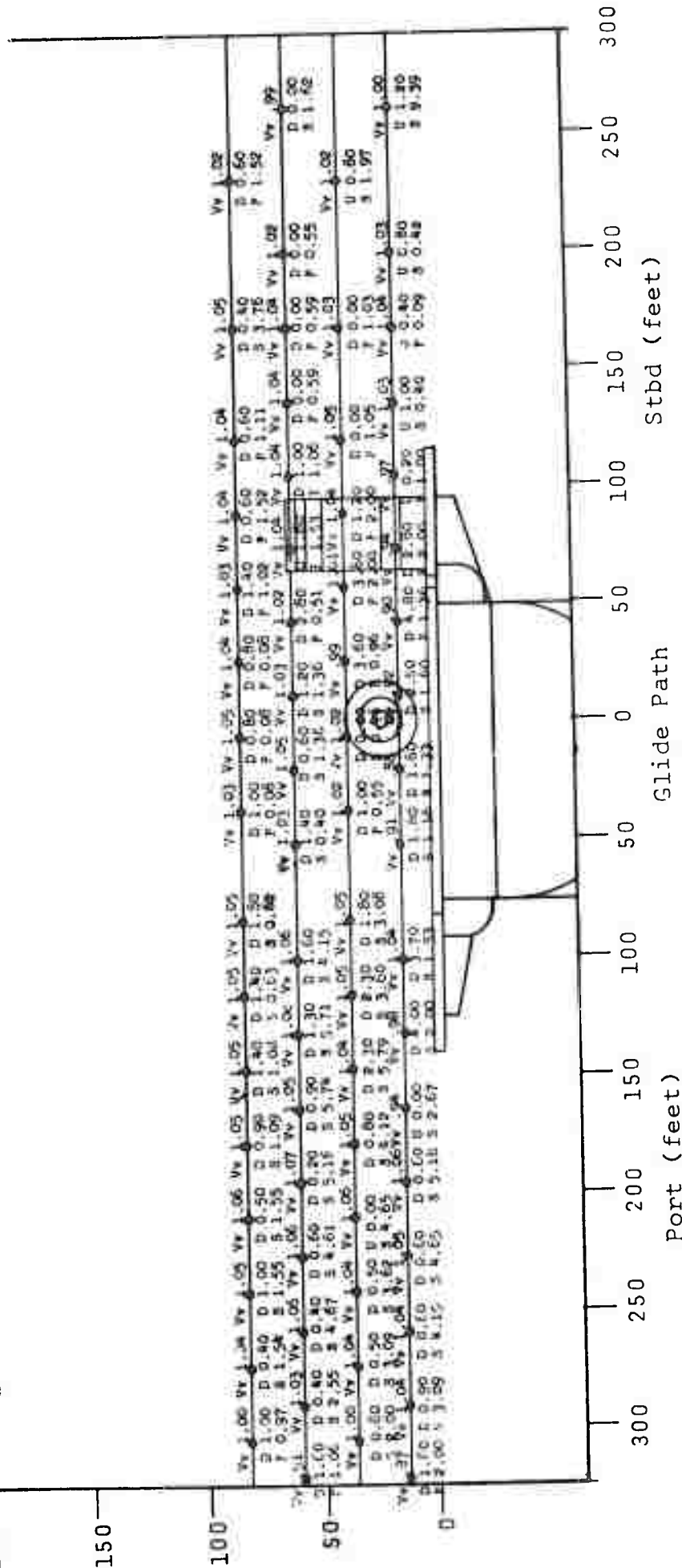S = Degrees flow is from starboard of
    average wind direction

Conditions:
Wind 35 knots; 9° port of ship center-line;
Carrier pitch angle -1.5°; Roll 0°; Measurement
1310 feet aft of touchdown
Target marks position of 4° glide path

Figure A-15

OCEANICS INC.

Figure A-16

Conditions:
Wind 35 knots; Dead ahead of ship center-line;
Carrier pitch angle 0°; Roll 0°; Measurement
222 feet aft of touchdown
Target marks position of 4° glide path

Vv = Local velocity vector divided
by average velocity in section
D = Degrees flow is down from horizontal
U = Degrees flow is up from horizontal
P = Degrees flow is from port of
average wind direction
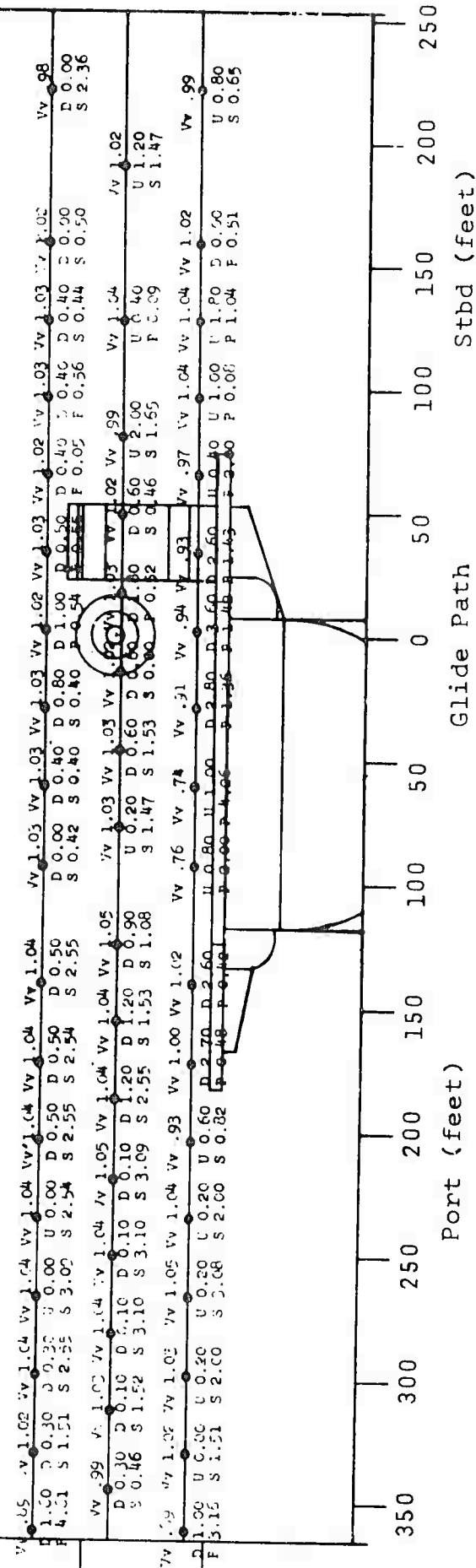S = Degrees flow is from starboard of
average wind direction

Height above touchdown (feet)

Stbd (feet)

Glide Path

Port (feet)

OCEANICS INC.

200 — Height above touchdown (feet)

150

100

50

0

350   300   250   200   150   100   50   0   50   100   150   200   250

Port (feet)   Glide Path   Stbd (feet)

Vv = Local velocity vector divided
     by average velocity in section
D = Degrees flow is down from horizontal
U = Degrees flow is up from horizontal
P = Degrees flow is from port of
     average wind direction
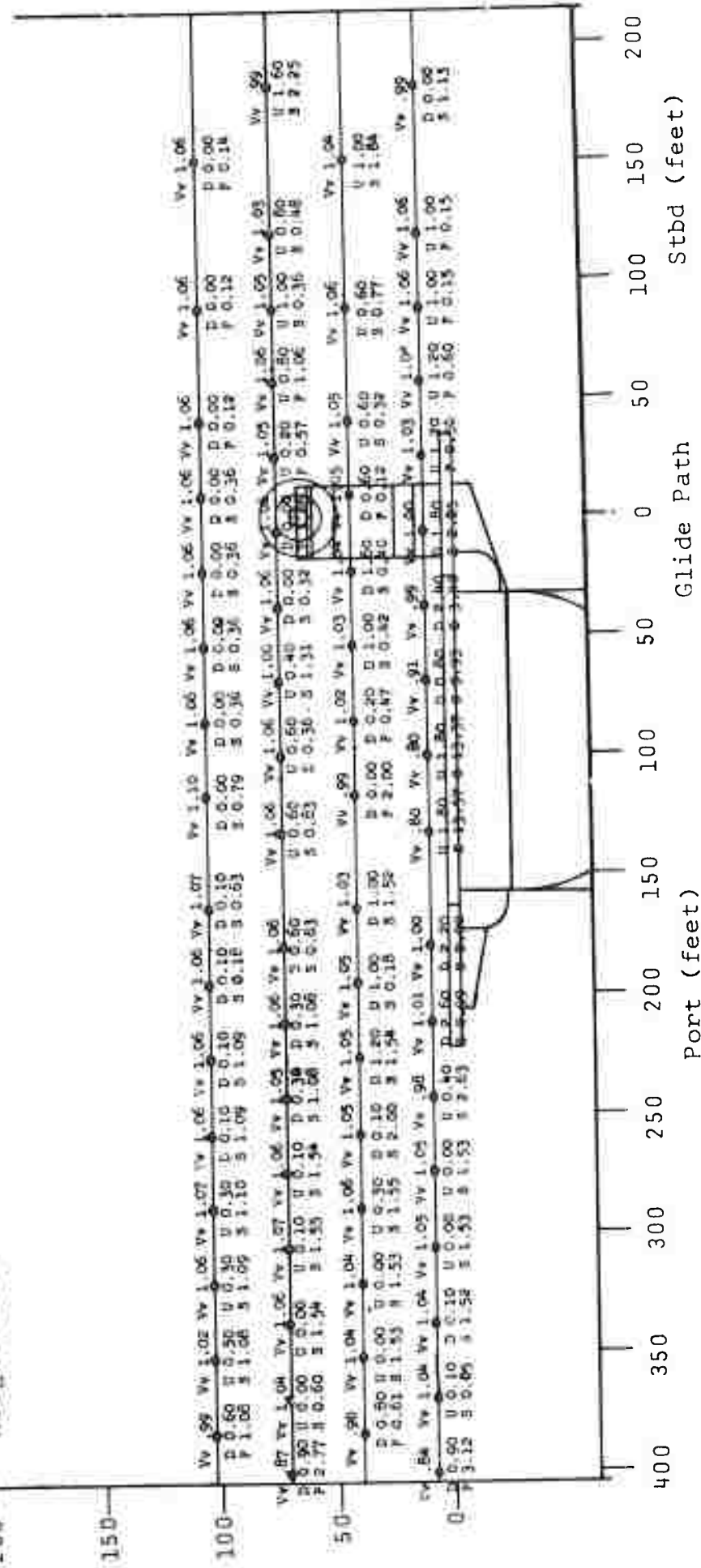S = Degrees flow is from starboard of
     average wind direction

Conditions:
Wind 35 knots; Dead ahead of ship center-line;
Carrier pitch angle 0°; Roll 0°; Measurement
480 feet aft of touchdown
Target marks position of 4° glide path

Figure A-17

OCEANICS INC.

Figure A-18

A-18

Height above touchdown (feet)

200

150

100

50

0

Stbd (feet)

Glide Path

Port (feet)

150   100   50   0   50   100   150   200   250   300   350   400
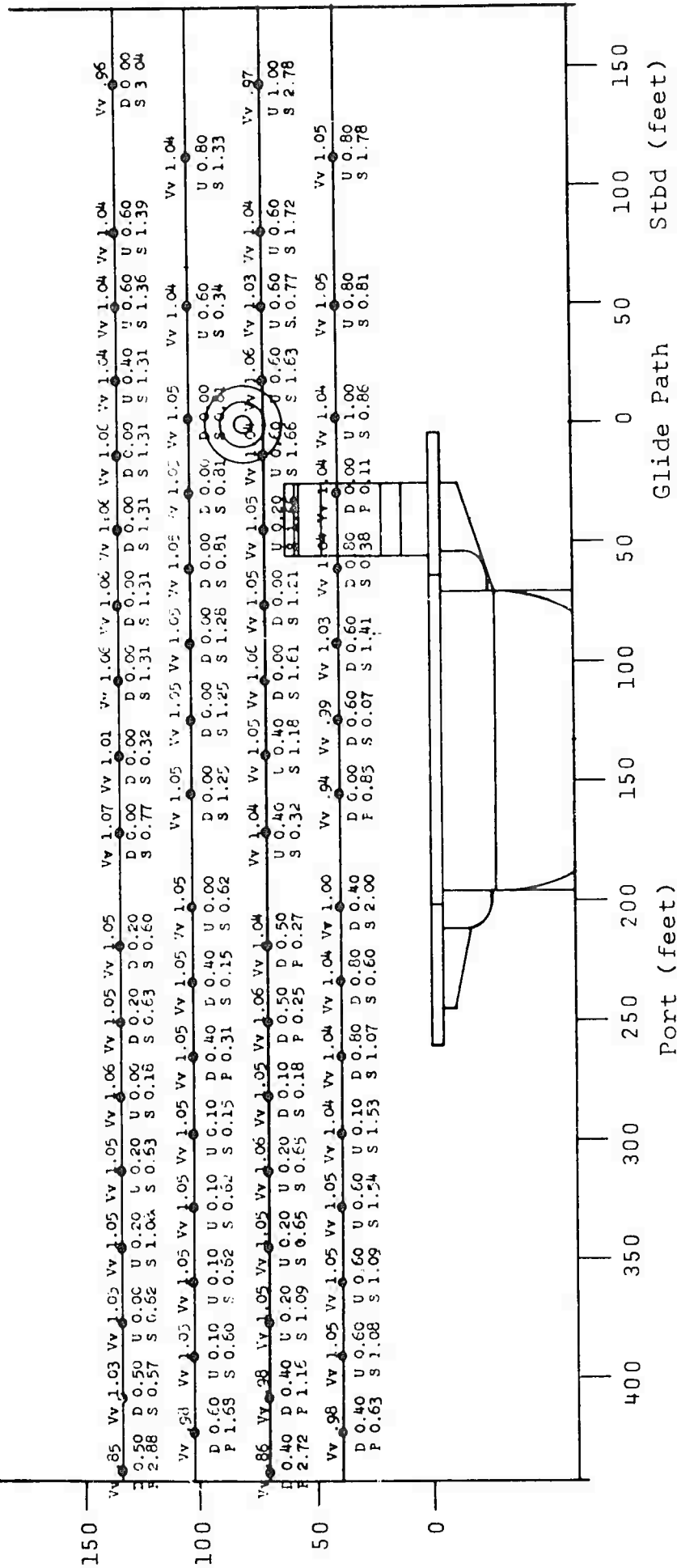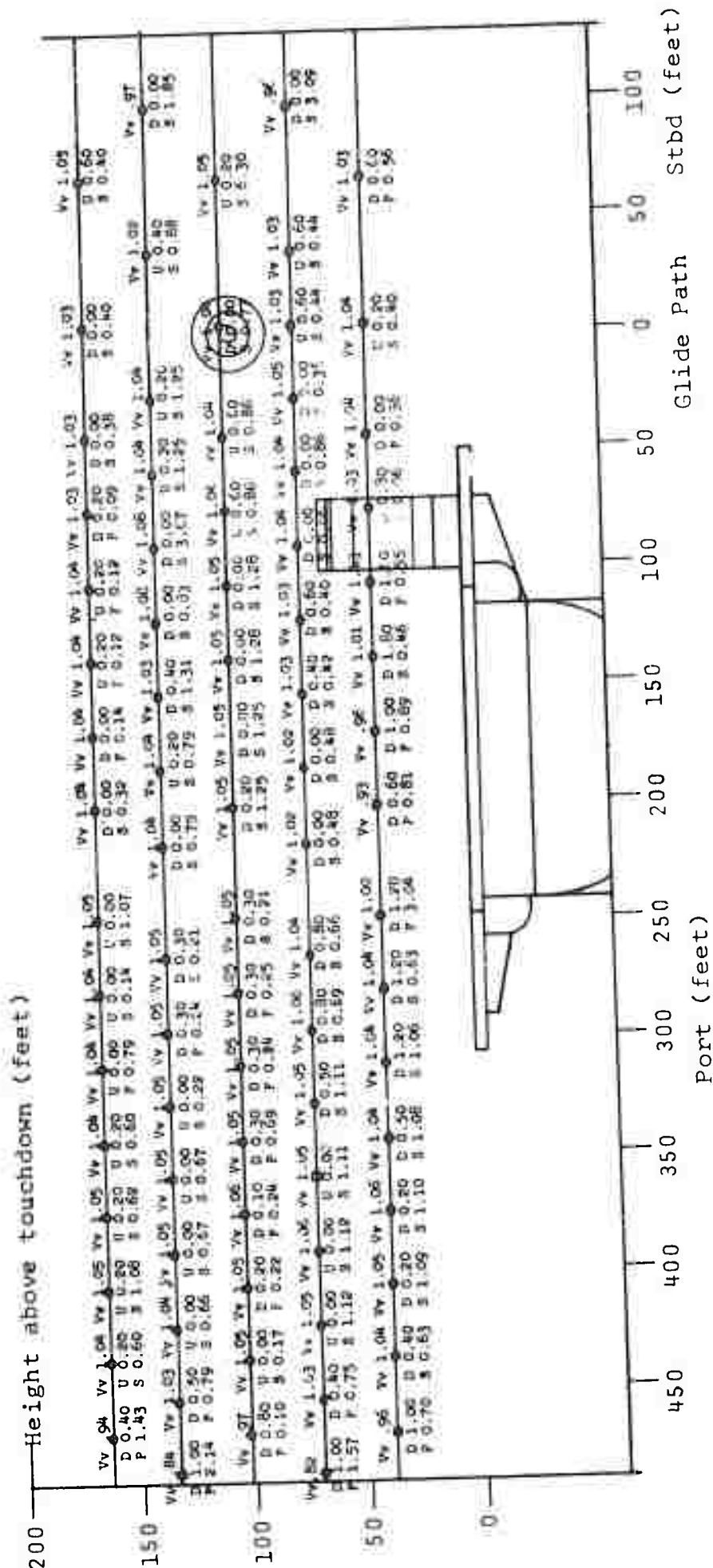
OCEANICS INC.

Conditions:
Wind 35 knots; Dead ahead of ship center-line;
Carrier pitch angle 0°; Roll 0°; Measurement
1030 feet aft of touchdown
Target marks position of 4° glide path

Vv = Local velocity vector divided
     by average velocity in section
D = Degrees flow is down from horizontal
U = Degrees flow is up from horizontal
P = Degrees flow is from port of
    average wind direction
S = Degrees flow is from starboard of
    average wind direction

Figure A-19

Conditions: Dead ahead of ship center-line;
Wind 35 knots; Roll 0°; Measurement
Carrier pitch angle 0°; Roll 0°; Measurement
1310 feet aft of touchdown
Target marks position of 4° glide path

Vv = Local velocity vector divided
     by average velocity in section
D = Degrees flow is down from horizontal
U = Degrees flow is up from horizontal
P = Degrees flow is from port of
     average wind direction
S = Degrees flow is from starboard of
     average wind direction

Figure A-20

OCEANICS INC.

Conditions:
Wind 35 knots; 13° port of ship center-line;
Carrier pitch angle 0°; Roll 0°; Measurement
222 feet aft of touchdown
Target marks position of 4° glide path

Vv = Local velocity vector divided
     by average velocity in section
D = Degrees flow is down from horizontal
U = Degrees flow is up from horizontal
P = Degrees flow is from port of
     average wind direction
S = Degrees flow is from starboard of
     average wind direction

Figure A-21

A-21

OCEANICS inc.

Figure A-22

Height above touchdown (feet)

Port (feet) Glide Path Stbd (feet)

Conditions:
Wind 35 knots; 13° port of ship center-line;
Carrier pitch angle 0°; Roll 0°; Measurement
760 feet aft of touchdown
Target marks position of 4° glide path

Vv = Local velocity vector divided
     by average velocity in section
D = Degrees flow is down from horizontal
U = Degrees flow is up from horizontal
P. = Degrees flow is from port of
     average wind direction
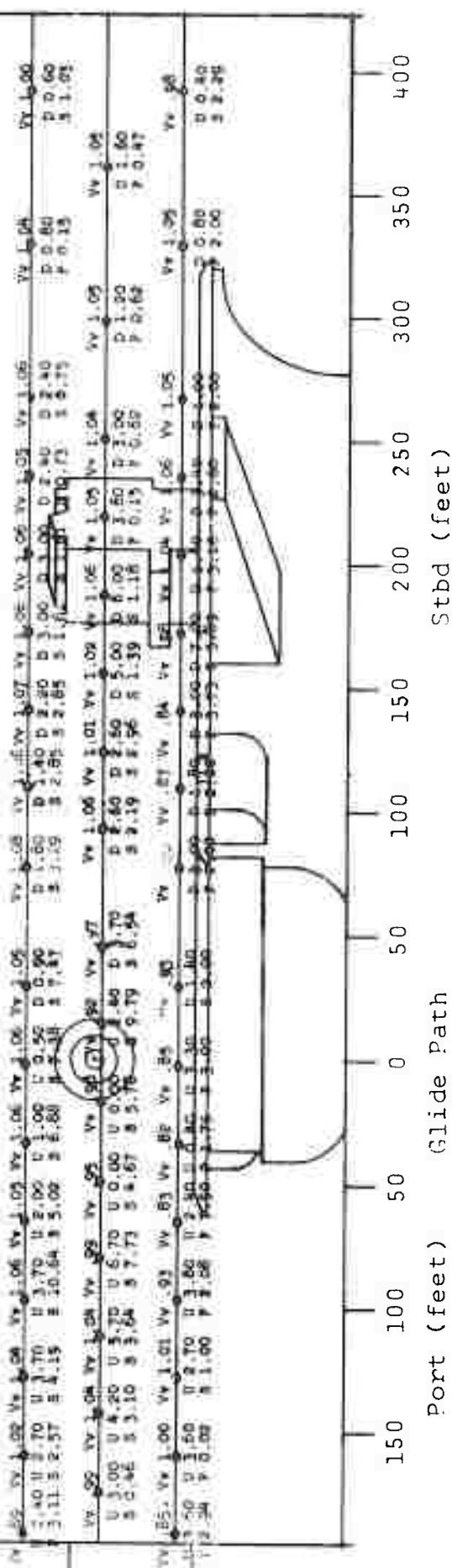S = Degrees flow is from starboard of
     average wind direction

Figure A-23

OCEANICS INC.

Figure A-24

A-24

Conditions:
Wind 35 knots; 13° port of ship center-line;
Carrier pitch angle 0°; Roll 0°; Measurement
1030 feet aft of touchdown
Target marks position of 4° glide path

Vv = Local velocity vector divided
     by average velocity in section
D = Degrees flow is down from horizontal
U = Degrees flow is up from horizontal
P = Degrees flow is from port of
     average wind direction
S = Degrees flow is from starboard of
     average wind direction

Height above touchdown (feet)

200 —

150 —

100 —

50 —

0 —

150   100   50   0   50   100   150   200   250   300   350   400   450
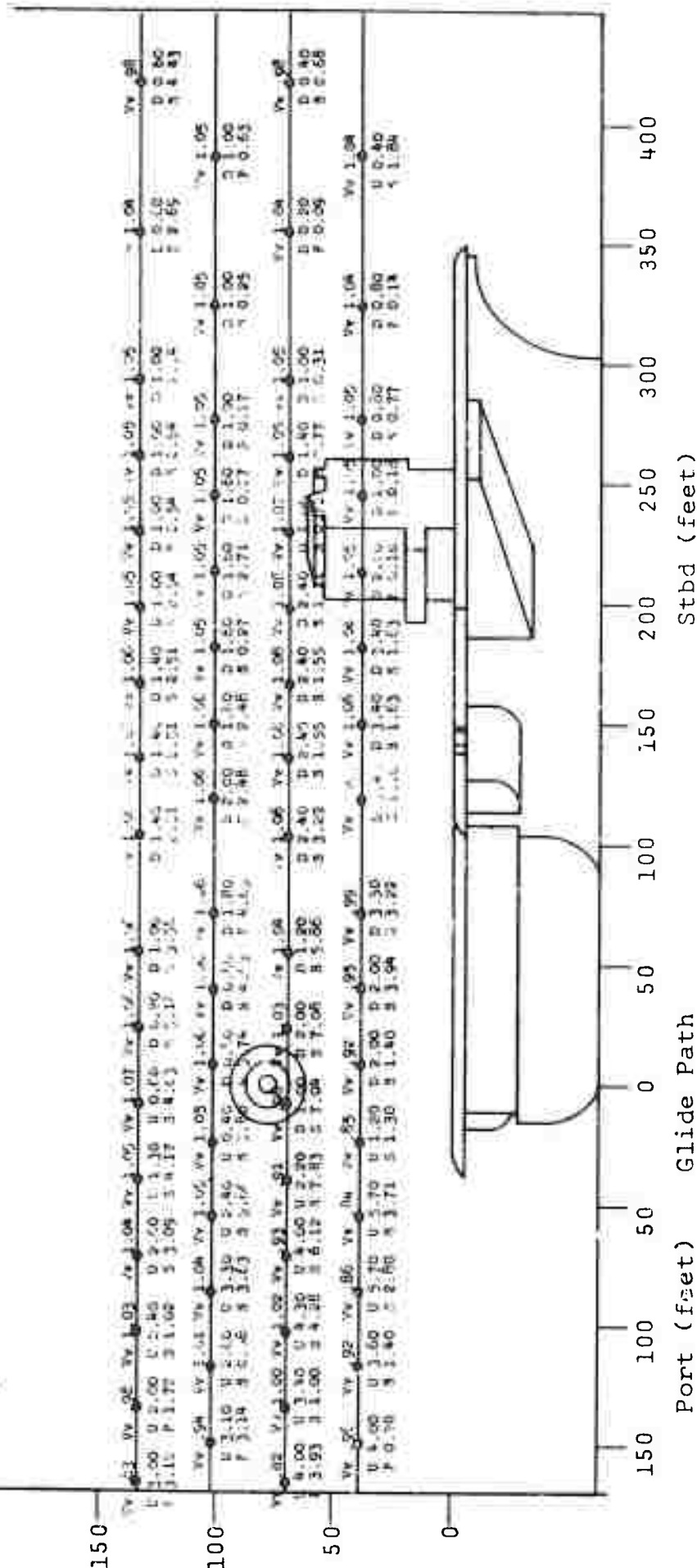
Port (feet)   Glide Path   Stbd (feet)

Conditions:
Wind 35 knots; 13° port of ship center-line;
Carrier pitch angle 0°; Roll 0°; Measurement
1310 feet aft of touchdown
Target marks position of 4° glide path

Vv = Local velocity vector divided
     by average velocity in section
D = Degrees flow is down from horizontal
U = Degrees flow is up from horizontal
P = Degrees flow is from port of
     average wind direction
S = Degrees flow is from starboard of
     average wind direction

Figure A-25

OCEANICS INC.

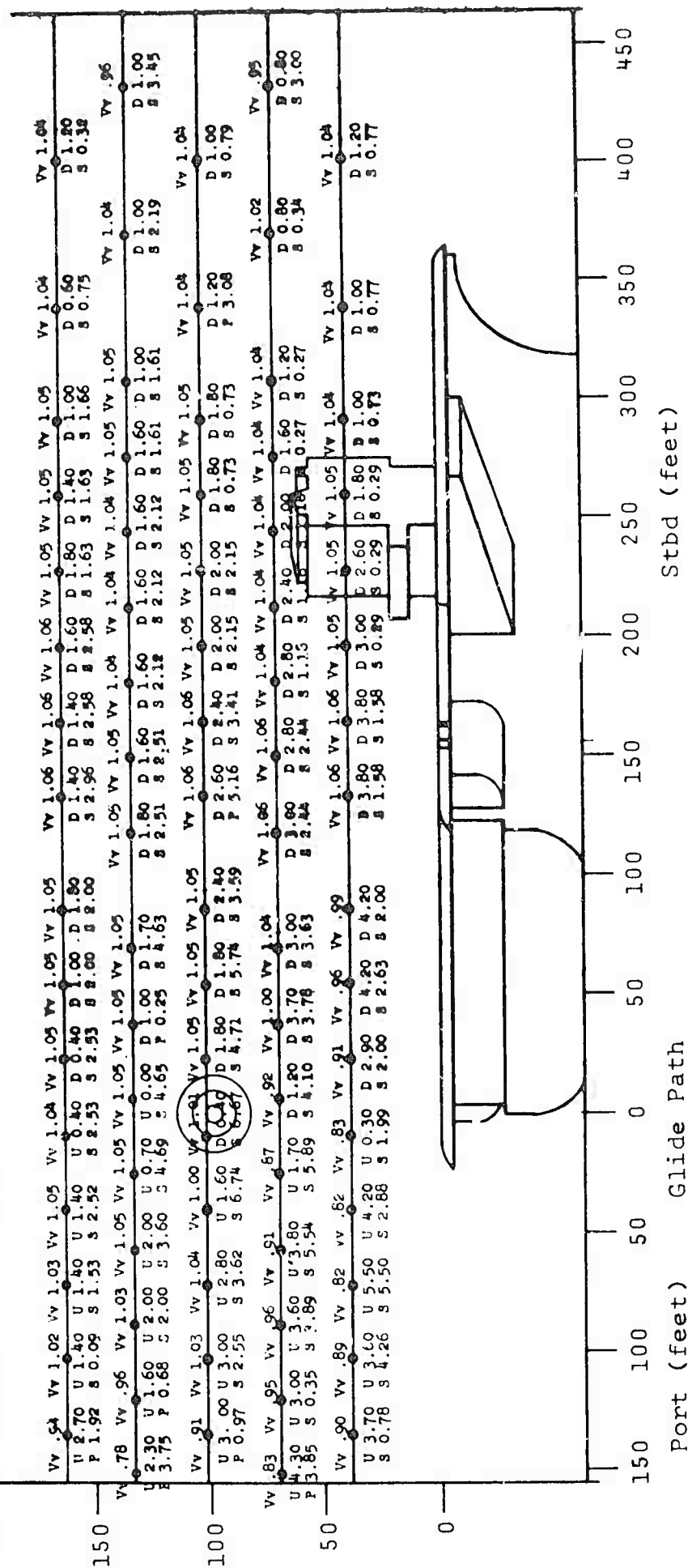Height above touchdown (feet)

Port (feet)   Glide Path   Stbd (feet)

Conditions:
Wind 35 knots; 9° port of ship center-line;
Carrier pitch angle 0°; Roll 0°; Measurement
600 feet aft of touchdown
Target marks position of 4° glide path

Vv = Local velocity vector divided
     by average velocity in section
D = Degrees flow is down from horizontal
U = Degrees flow is up from horizontal
P = Degrees flow is from port of
     average wind direction
S = Degrees flow is from starboard of
     average wind direction

Figure A-26

OCEANICS INC.

Height above touchdown (feet)

250

200

150

100

50

0

300 250 200 150 100 50 0 50 100 150 200 250 300 350 400
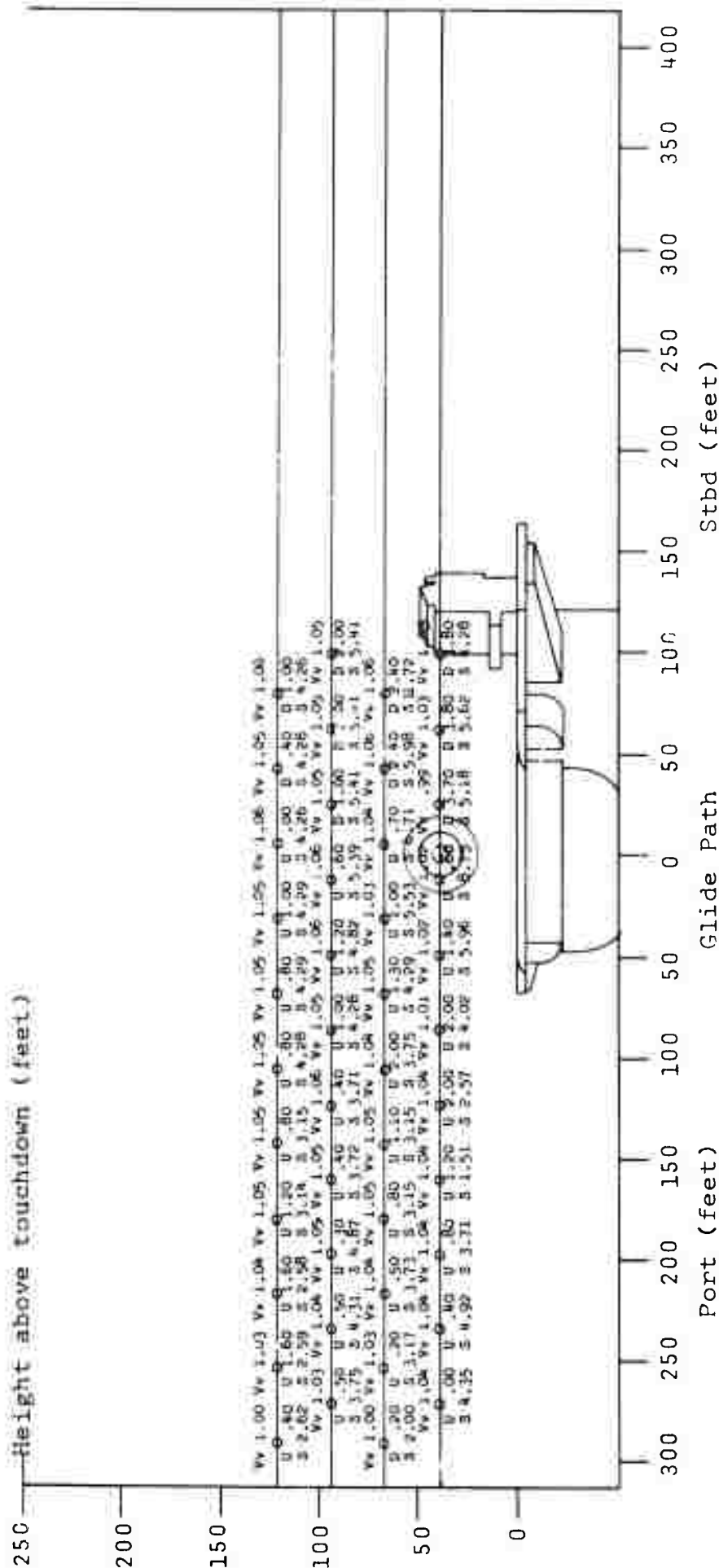
Port (feet)   Glide Path   Stbd (feet)

Conditions:
Wind 35 knots; 9° port of ship center-line;
Carrier pitch angle 0°; Roll 0°; Measurement
1875 feet aft of touchdown
Target marks position of 4° glide path

Vv = Local velocity vector divided
    by average velocity in section
D = Degrees flow is down from horizontal
U = Degrees flow is up from horizontal
P = Degrees flow is from port of
    average wind direction
S = Degrees flow is from starboard of
    average wind direction

Figure A-27

OCEANICS INC.

Figure A-28

Conditions:
Wind 35 knots; 9° port of ship center-line;
Carrier pitch angle +1.5°; Roll 0°; Measurement
600 feet aft of touchdown
Target marks position of 4° glide path

Vv = Local velocity vector divided
     by average velocity in section
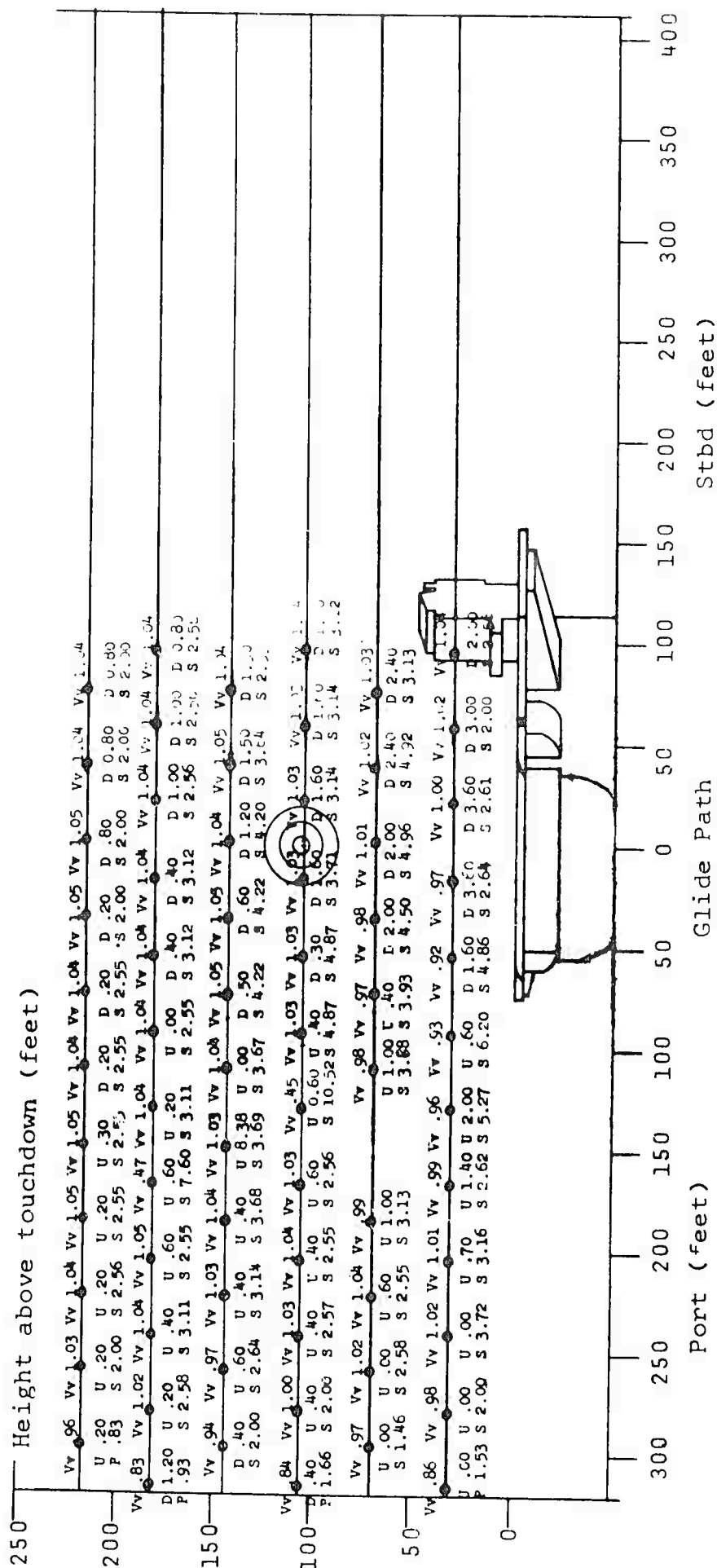D = Degrees flow is down from horizontal
U = Degrees flow is up from horizontal
P = Degrees flow is from port of
    average wind direction
S = Degrees flow is from starboard of
    average wind direction

Height above touchdown (feet)

Port (feet)   Glide Path   Stbd (feet)

Conditions:
Wind 35 knots; 9° port of ship center-line;
Carrier pitch angle +1.5°; Roll 0°; Measurement
1875 feet aft of touchdown
Target marks position of 4° glide path

Vv = Local velocity vector divided
     by average velocity in section
D = Degrees flow is down from horizontal
U = Degrees flow is up from horizontal
P = Degrees flow is from port of
     average wind direction
S = Degrees flow is from starboard of
     average wind direction

Figure A-29
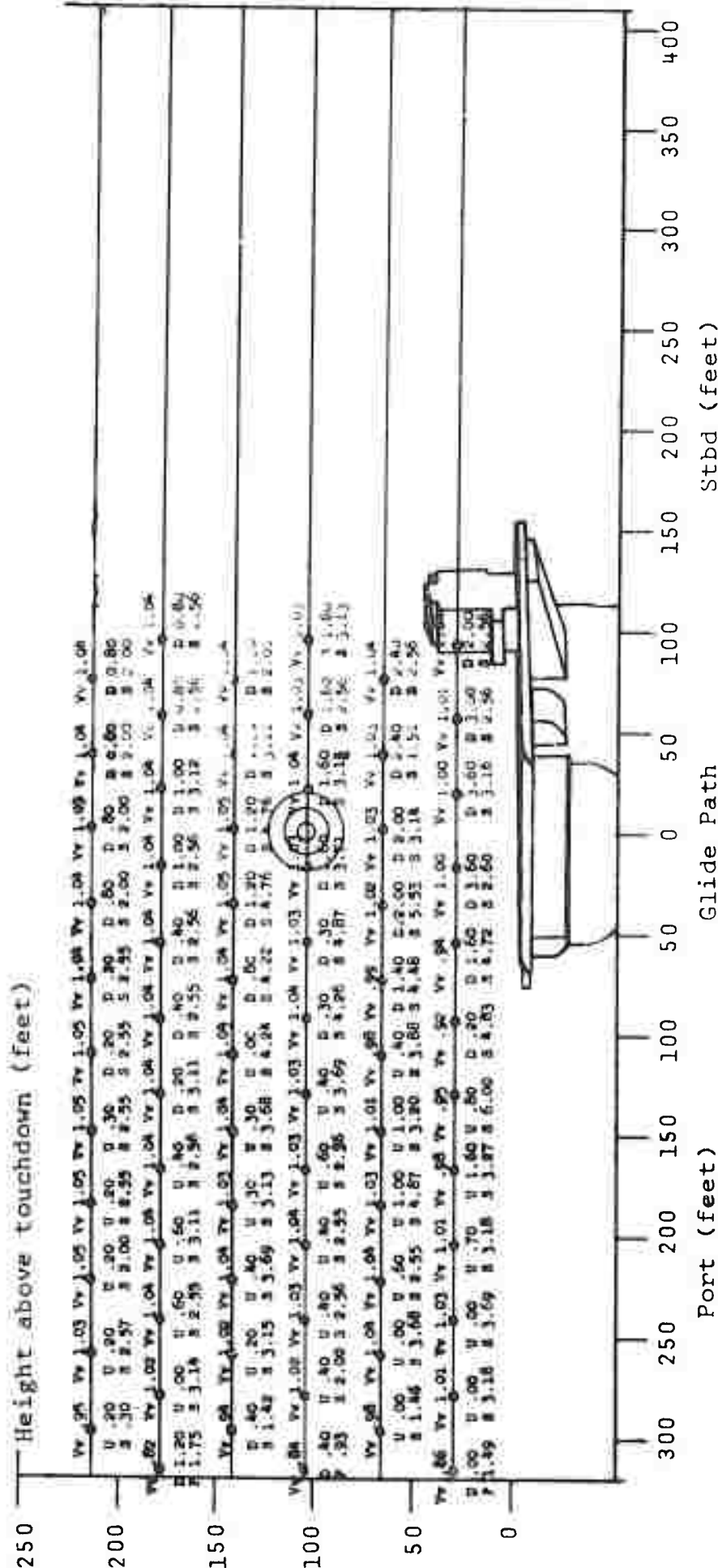
OCEANICS INC.

Figure A-30

Conditions:
Wind 35 knots; 9° port of ship center-line;
Carrier pitch angle -1.5°; Roll 0°; Measurement
600 feet aft of touchdown
Target marks position of 4° glide path

Vv = Local velocity vector divided
     by average velocity in section
D = Degrees flow is down from horizontal
U = Degrees flow is up from horizontal
P = Degrees flow is from port of
     average wind direction
S = Degrees flow is from starboard of
     average wind direction

Height above touchdown (feet)

Port (feet)   Glide Path   Stbd (feet)
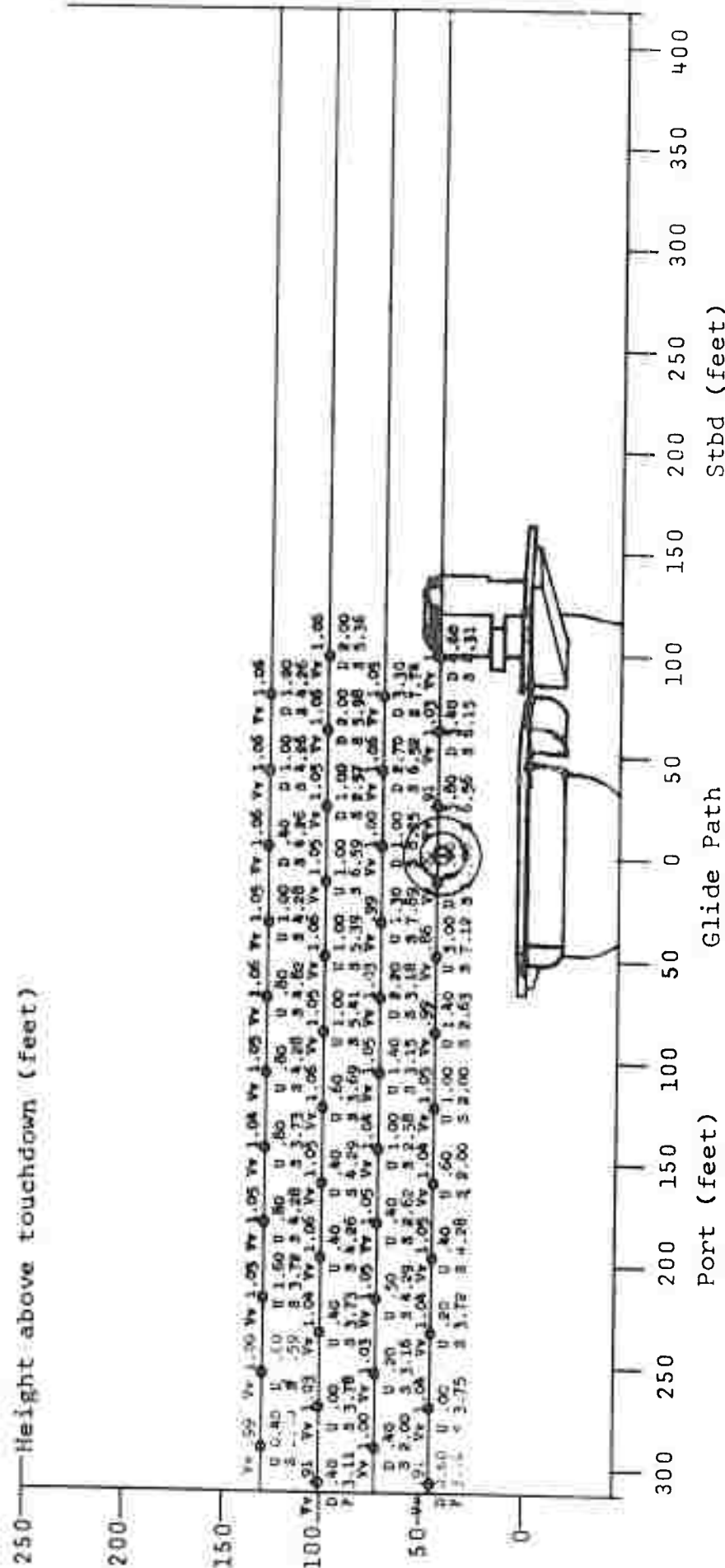
OCEANICS INC.

Figure A-31

Conditions:
Wind 35 knots; 9° port of ship center-line;
Carrier pitch angle -1.5°; Roll 0°; Measurement
1875 feet aft of touchdown
Target marks position of 4° glide path

Vv = Local velocity vector divided
     by average velocity in section
D = Degrees flow is down from horizontal
U = Degrees flow is up from horizontal
P = Degrees flow is from port of
     average wind direction
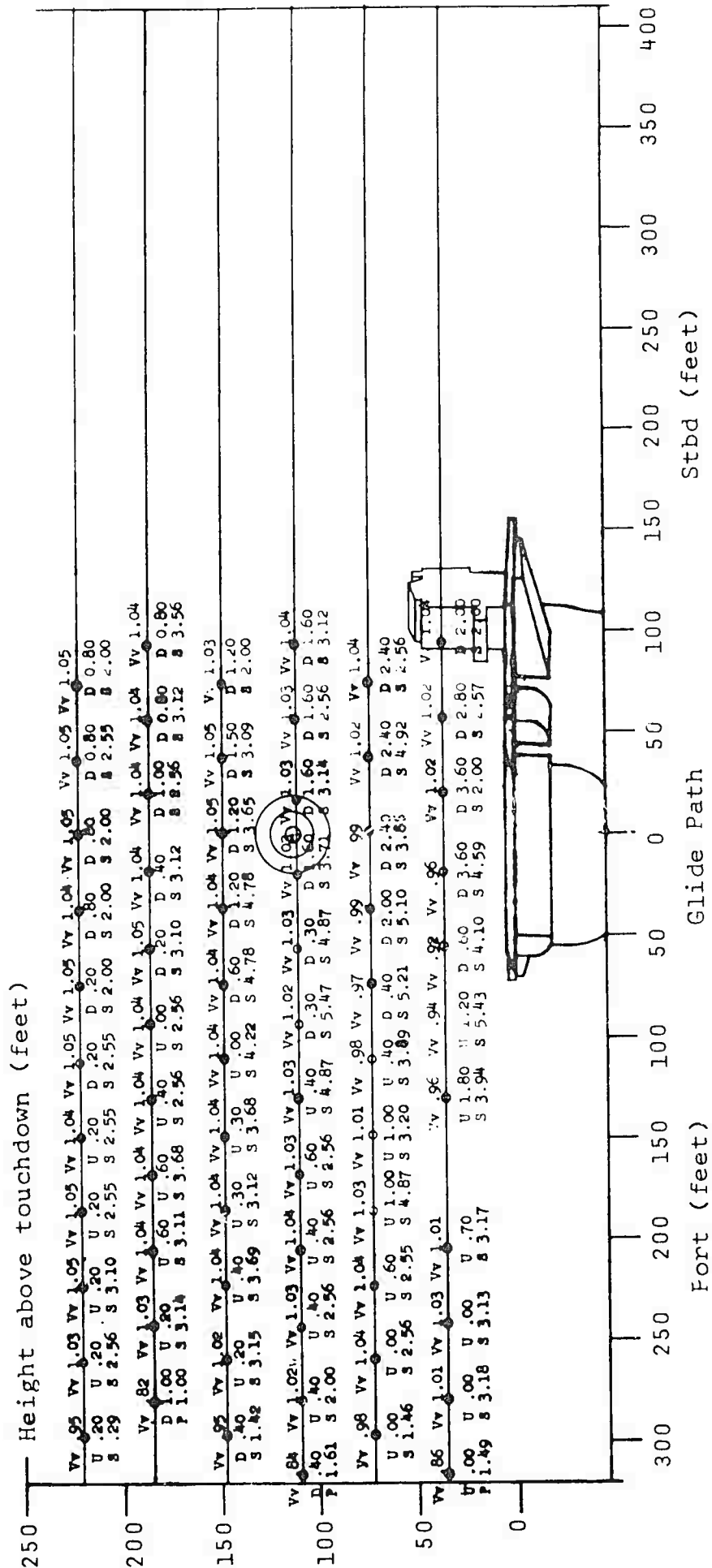S = Degrees flow is from starboard of
     average wind direction

DISTRIBUTION LIST

Contract No. Nonr-4186(00)

Chief,   (2)
Bureau of Naval Weapons (DLI-3)
Navy Department
Washington, D. C. 20360

Defense Documentation Center   (20)
Cameron Station
Alexandria, Virginia

Chief,   (5)
Bureau of Naval Weapons (RSSH-5)
Navy Department
Washington, D. C. 20360
    RAAV-92   (1)
    RAAD-3   (1)
    RAAD-223   (1)
    RAAD-321   (1)

Chief of Naval Research   (6)
Navy Department
Washington, D. C. 20360

Commanding Officer   (4)
David Taylor Model Basin
Carderock, Maryland

Chief, Bureau of Ships   (1)
Navy Department
Washington 25, D. C.
    Code 685B   (1)
    Code 442   (1)

Commanding Officer   (2)
U. S. Naval Oceanographic Office
Suitland, Maryland
    Code 330   (1)

Bell Aerosystems Company   (1)
Buffalo 5, New York
Attn: Mr. Fred Powell

⸺OCEANICS⸺

DISTRIBUTION LIST

Contract No. Nonr-4186(00)

Director   (2)
National Bureau of Standards
U. S. Department of Commerce
Washington, D. C.
Attention: Mr. C. A. Douglas

Director   (2)
U. S. Naval Research Laboratory
Washington, D. C. 20390
    Code 5120   (1)
    Code 5263   (1)

Commanding Officer   (10)
Naval Air Engineering Center
Attn: Director,
        Naval Air Engineering Laboratory (SI)
        Philadelphia, Pennsylvania 19112

Commander   (3)
U. S. Naval Aviation Safety Center
U. S. Naval Air Station
Norfolk, Virginia 23511

Chief of Naval Operations   (5)
Navy Department
Washington, D. C. 20350
    Op-03EG   (1)
    Op-725C   (1)

Commander Naval Air Force   (5)
U. S. Atlantic Fleet
U. S. Naval Air Station
Norfolk, Virginia 23511

Commander Naval Air Force   (5)
U. S. Pacific Fleet
Box 1210
U. S. Naval Air Station
North Island
San Diego, California 92135

Commander   (5)
U. S. Naval Air Test Center
Patuxent River, Maryland 20670

OCEANICS INC.